PONTIFICIA UNIVERSIDAD CATOLICA DE CHILE

ESCUELA DE INGENIERIA

NATURAL AND MIXED CONVECTIVE HEAT TRANSFER THROUGH HORIZONTAL OPENINGS IN BUILDINGS

MARÍA MAGDALENA CORTÉS SAAVEDRA

Thesis submitted to the Office of Research and Graduate Studies in partial fulfillment of the requirements for the Degree of Master of Science in Engineering

Advisor:

SERGIO VERA ARAYA

Santiago de Chile, (July, 2013)

PONTIFICIA UNIVERSIDAD CATOLICA DE CHILE
ESCUELA DE INGENIERIA

NATURAL AND MIXED CONVECTIVE HEAT TRANSFER THROUGH HORIZONTAL OPENINGS IN BUILDINGS

MARÍA MAGDALENA CORTÉS SAAVEDRA

Members of the Committee:

SERGIO VERA ARAYA

CLAUDIO MOURGUES ALVAREZ

WALDO BUSTAMANTE GÓMEZ

IGNACIO LIRA CANGUILHEM

Thesis submitted to the Office of Research and Graduate Studies in partial fulfillment of the requirements for the Degree of Master of Science in Engineering

Santiago de Chile, (July, 2013)

To my family

ACKNOWLEDGEMENTS

This work was supported by the National Commission for Science and Technology (CONICYT) under the research projects FONDECYT 11100120 and CONICYT/FONDAP 15110020. This work was partially developed during my stay at Concordia University (Montreal, Canada) supported by the Canadian Government via the Canada-Chile Leadership Exchange Scholarship.

I would like to thank my advisor Dr. Sergio Vera for support and guidance over this time, which has lead me to get interested in research and the study of new topics. His knowledge and research experience has helped me to develop journal papers, to get two scholarships for research abroad, and to participate in conferences to present our work.

My special thanks Dr. Fazio, Dr. Rao and Dr. Wang and students who, during my stay at Concordia University, showed me hospitality and assisted me help in computational topics that played a fundamental role in my research.

I would also like to thank Dr. Claudio Gelmi for his help in topics of fluid mechanics that guided me for developing the final stage of my research. I would like to thank all my colleagues in the Department of Construction Engineering and Management for their collaboration and friendship.

I want to thank my family for their patience and support, especially my parents for instilling the importance of working with dedication and responsibility and the devotion to freely pursue my interests and what makes me happy.

TABLE OF CONTENTS

LIST OF TABLES

LIST OF FIGURES

ABSTRACT

Building design has the objective to achieve a comfortable and healthy indoor environment for the occupants with high energy efficiency. Both, indoor environment conditions and energy consumption could be significantly influenced by heat and mass exchange through building zones.

Multizone airflow mainly occurs through large vertical and horizontal openings, such as windows or staircases openings respectively. The research developed in this thesis allows contributing to the understanding of the heat exchange through horizontal opening.

Although a wide variety of building energy simulation tools (which provide users with building performance indicators) have been developed, they do not consider airflow exchange through horizontal openings in general. One way to enhance the study of airflow through large openings has been the incorporation of Computational Fluid Dynamics (CFD) technique in building design.

In this thesis, correlations that describe the heat flow through a horizontal opening in a two-story test-hut were developed. Theses correlations are based on dimensionless fluid numbers (Nu, Gr, Re, Pr) and are applicable for different air conditions such as; temperature difference between the lower and upper room, ventilation strategies (natural and mixed convection) and opening aspect ratios.

The thesis suggests that reliable and robust CFD results require users' skills on CFD modeling even for basics indoor airflows. Also, indoor environments under natural convection regimes can be predicted by k-ε standard model while indoor environments under mixed convection regimes can be predicted by k-ε realizable model. Finally, based on CFD results, empirical equation representing upward heat transfer through the horizontal opening were developed for natural and mixed convection.

RESUMEN

El objetivo del diseño de edificios es crear ambientes confortables y saludables para los ocupantes considerando eficiencia energética. Las condiciones interiores del edificio y su consumo de energía son afectados por el intercambio de calor y aire a través de las zonas del edificio.

El flujo de aire a través de las zonas de un edificio sucede principalmente por aberturas horizontales y verticales tales como aberturas de escaleras y ventanas respectivamente. Esta tesis contribuye al conocimiento sobre el intercambio de calor a través de aberturas horizontales.

A pesar de que existe una gran variedad de herramientas de simulación para determinar consumos y datos de energía para edificios, los que proveen a los usuarios con indicadores sobre su comportamiento, en general estos consideran de manera muy básica el intercambio de flujos de aire a través de aberturas horizontales. Una forma de complementar el estudio de flujos a través de aberturas ha sido la incorporación de la técnica de Dinámica de Fluidos Computacional (CFD) en el diseño de edificios.

En esta tesis se desarrollaron correlaciones para describir el flujo de calor a través de una abertura horizontal en una casa de dos pisos usando CFD. Estas correlaciones se basan en números adimensionales del fluido (Nu, Gr, Re, Pr) y son aplicables para diferentes condiciones del aire tales como: diferencias de temperatura entre las habitaciones, estrategias de ventilación (convección natural y mixta) y dimensiones de la abertura.

La tesis revela que, para obtener resultados confiables y robustos al usar CFD en la modelación de ambientes interiores, es necesario adquirir habilidades previas, incluso para casos básicos. Además, el modelo *k-ε standard* es el más preciso para modelar ambientes interiores bajo régimen de convección natural mientras que el modelo *k-ε realizable* es el más preciso para convección mixta. Finalmente, se desarrollaron correlaciones empíricas basadas en resultados de CFD para representar el flujo ascendente de calor a través de una abertura horizontal para convección natural y mixta.

1. Introduction

1.1. Background information

Building design objective is to achieve a comfortable and healthy indoor environment for the occupants with high energy efficiency. As example of design specifications, the indoor temperature recommended for houses, apartments, offices, school rooms, hotels and restaurants for healthy adults and kids is 23-24 °C with a maximum indoor operative temperature change allowed in a 15 min period of 1.1 °C (ASHRAE, 2004). Also, minimum ventilation is required to eliminate contaminants and odors concentrated in closed spaces. For livings and rooms with 5 persons per 100 m^2 the recommended ventilation rate per person is 3.3- 4.7 x 10^{-3} m^3/s (ASHRAE, 1977). Also, there are requirements associated to the air velocity, for example the mean air velocity in a single office or kindergarten during the winter season may not exceed 0.10 m/s (ISO 7730, 2005). When these considerations are not taken into account in the building design, may cause negatives effects on occupant for example the sick building syndrome (SBS). The SBS describes a situation in which the occupants of a building experience a health- or comfort-related effect that are linked to the time they stay in the building. This problem increases sickness absenteeism and decreases productivity. Some symptoms are headache, dizziness, nausea, eye, nose or throat irritation, flu-like symptoms, increased incidence of asthma attacks and personality changes (Sumedha M, 2008). On the other hand, a building design without energy efficiency consideration may cause extra costs in the energy used for building operation such heating or cooling, lighting etc. For example, in Chile 22% of the total energy consumed is for residential use and 60% of this electricity consumption is used only in lighting and refrigeration (CNE, 2008).

Since the past 50 years, a wide variety of building energy simulation tools have been developed, which provide users with key building performance indicators such as heater and cooling energy demand, indoor conditions (temperature, humidity) and costs, with the objective to achieve more comfortable buildings for occupants considering energy

efficiency. The tools have modeling features and capabilities in different categories as zone loads, infiltrations, building envelope, daylighting, ventilation and multizone airflow, renewable energy systems, HVAC systems, etc.

In particular, consideration of ventilation and multizone airflows are important aspects in building design because they allow the mass and energy transport inside multi-zone building and between the indoor and outdoor environments. The heat and mass exchange influences the indoor environment perceived by occupants and the energy requirements for the building operation. An important way in which mass and energy may be transported inside multi-zone building is through large vertical and horizontal openings. Figure 1 shows the typical vertical and horizontal openings in a multi-zone building in which airflow exchange happens.

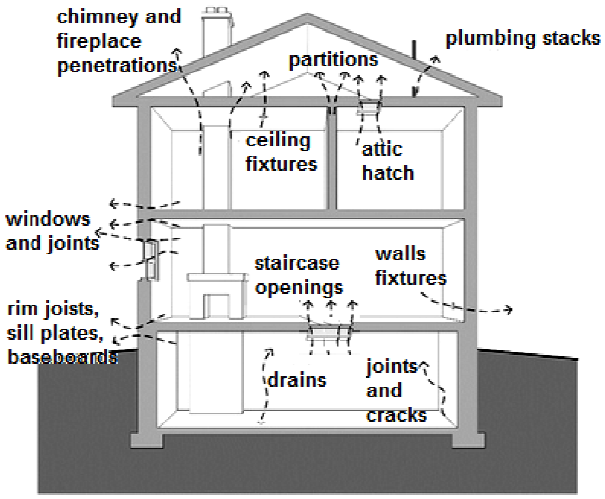

Figure 1: Airflow through horizontal and vertical openings in a house (Straube, 2008).

Some energy simulation tools are TRNSYS, SUNREL, eQUEST, EnergyPlus, ECOTECT, ESP-r, Energy-10, BSim among others. All this programs can simulate single zone infiltration common in any building, in contrast only few software can take into account multizone airflow via pressure network model (Crawley et al., 2005). Moreover, these multizone airflow models only considerer airflow exchange through

vertical opening as windows or doors while, they consider the airflow exchange through horizontal opening as staircases opening in a basic form. One exception is Energy Plus software which in the last version includes horizontal trench ground heat exchanger object (EnergyPlus, 2013) but it does not consider airflow exchange through horizontal openings in general.

Mass and heat flow through the different building zones is caused by convection due to diverse air conditions in each zone. Convection is the heat and mass transfer mode comprised by both diffusion (energy transfer due to random individual particles motion) and advection (energy transfer due macroscopic motion of currents in the fluid). Convection heat transfer may be classified according to the nature of the flow as natural, forced or mixed convection. Pure forced convection is present when the flow is caused by external sources such as fans, pumps or wind induced pressure, whereas a pure natural convection is present when the flow is induced by buoyancy forces caused by density differences due to temperature variations in the fluid. A mixed convection exists when a combination of forced and natural convections is present. The flow is determined simultaneously by both an external forcing system and a inner not uniform density distribution of the fluid medium (Incropera et al., 2006).

Interzone energy and mass transport in a building can have important implications in indoor temperature variations, thermal comfort, pollutants distributions, spread of smoke and energy consumption. Consequently, empirical equations representing the airflow through horizontal openings are essential for an appropriate buildings design.

Little work has been done about energy and mass transfer between different zones in buildings. Particularly, few authors have studied airflow through horizontal openings and most of them only considered pure buoyancy- driven flows. Also, limited experimental data is available. Thus there is a lack of studies and validated empirical correlations of natural convective and mixed convective heat transfer through horizontal opening.

1.2. Objective

Develop correlations capable to describe the heat flow through a horizontal opening separating two rooms via Computational Fluid Dynamics (CFD) technique. The correlations will be based on dimensionless numbers (Nu, Gr, Re, Pr) that describe the fluid, and the opening dimensions.

It is expected to develop a correlation applicable to different air conditions such as temperature difference between the lower and upper room, ventilation strategies (natural and mixed convection), as well as the opening aspect ratios, which are all independent variables.

1.3. Hypothesis

The temperature difference between two rooms connected by a horizontal opening will cause a bidirectional flow of air through the opening, depending on the temperature difference between the spaces and opening dimensions. The CFD simulated datasets would allow obtaining correlations to describe the interzonal airflow under different conditions.

1.4. Methodology

This thesis is a numerical work with the aim to obtain empirical correlations to describe the upward heat flux through a horizontal opening. Figure 2 shows the flowchart of the thesis work consisting in three stages:

1. Acquire basic skills in CFD technique: CFD will be used to study the upward heat flow through a horizontal opening. The software used is FLUENT 14.0, a component of Ansys software. The CFD technique requires that the modeler acquire basics skill to obtain accurate and robust solutions. Three cases of natural, forced and mixed convections found in literature will be modeled. An analysis of the influence of modeler experience on the simulation results will be performed.

2. Evaluation of two- eddy turbulence models: A two-story test-hut with available experimental data (Vera et al., 2010) will be modeled using CFD technique. Five two-eddy turbulence models will be evaluated for predicting indoor air distribution and the upward mass flow through the horizontal opening. Six cases will be modeled, which present variations on the ventilation strategy and temperature differences between the upper and the lower room. A turbulence model will be selected as the most accurate model to predict natural convection and mixed convection by separate.

3. Determination of correlations to describe heat flow through a horizontal opening: Thirty two cases will be modeled to extend experimental data available (Vera et al., 2010) of the airflow distribution in a two-story test-hut. The cases will be model using CFD technique using the turbulence models previously found. The cases are modeled to study the interzonal airflow through the horizontal opening for different combinations of opening dimensions, temperature difference between the upper and lower room and ventilation strategies. A correlation for the heat transfer through the horizontal opening which considers the opening dimensions will be found for natural convection and for mixed convection.

1.5. Thesis structure

The following thesis consists of seven chapters which start by presenting the problem and a literature review of the state of the art about airflow and heat exchange through large verticals and horizontals openings and the use of CFD technique for indoor environment modeling. Chapter 3 corresponds to a journal article that describes the CFD technique and the necessary user skills to properly model indoor environments and obtains reliable and robust CFD simulations results. Three basics convection cases found

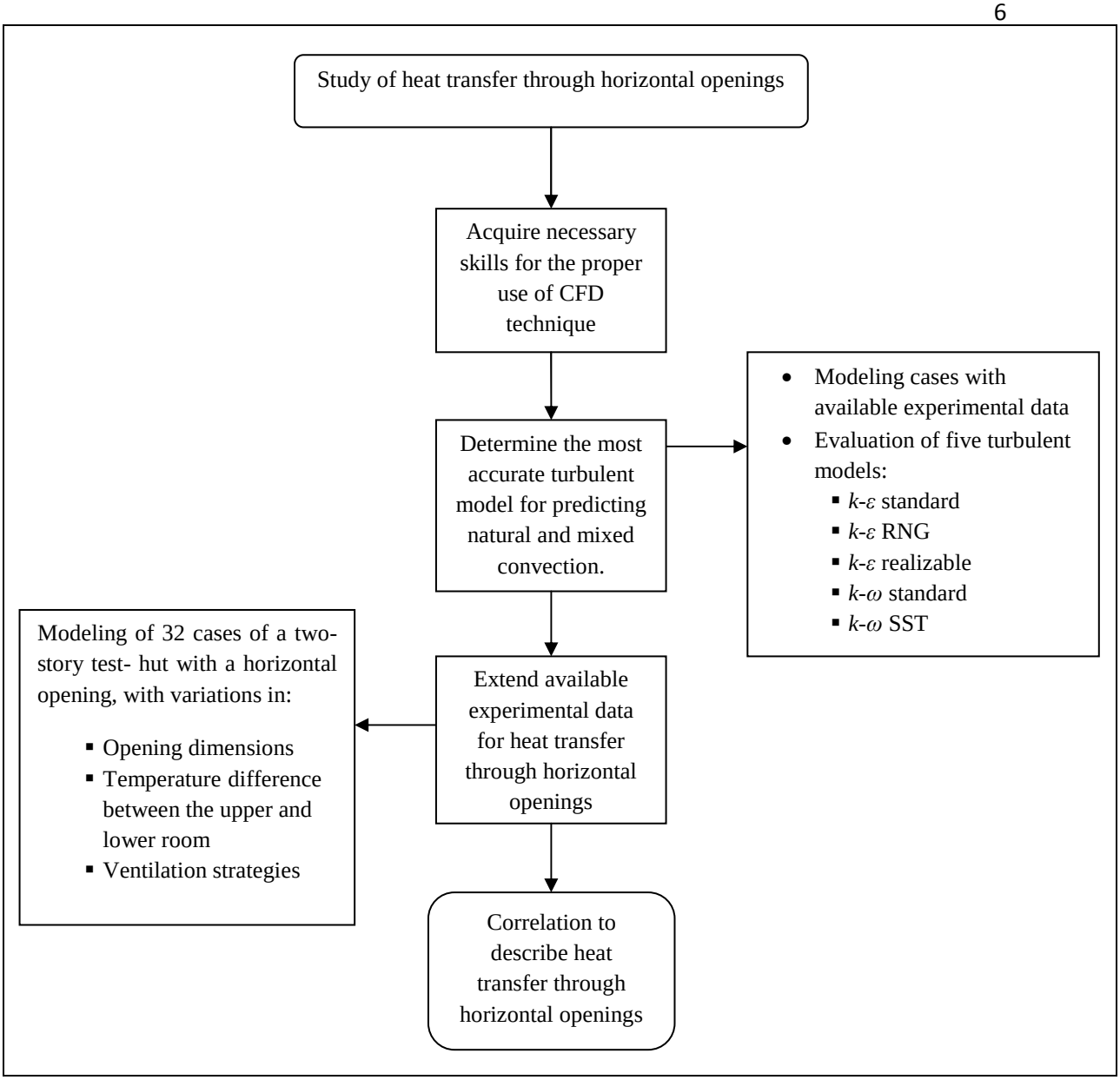

Figure 2: Flowchart of the thesis work.

in literature with available experimental data were used to acquire basics skills in CFD technique. Chapter 4 presents another journal article in which a two- story test-hut with available experimental data (Vera et al., 2010) is modeled to study the airflow exchange through a horizontal opening connecting two rooms with a specific size of the opening but different initial conditions of the rooms. This chapter aims to evaluate five two-eddy viscosity turbulence models to predict the indoor environment and the airflow exchange through a horizontal opening in a two-story full-scale test-hut. Chapter 5 shows CFD results of a variety of natural and mixed convection cases. The cases describe a two-

story test-hut with four different opening aspect ratios. These simulations are performed using the turbulence models evaluated in chapter 4. This chapter concludes with two correlations that represent the upward heat flow through the horizontal opening for natural and mixed regimes. Finally chapter 6 shows the main conclusions of this thesis work and chapter 7 presents the contribution of this research and suggests future researches.

2. Literature Review

Indoor air distribution in buildings has significant impacts on thermal comfort, indoor air quality and energy efficiency. Important indoor air parameters are distribution of air velocity, temperature and relative humidity, indoor pollutants concentration such as carbon dioxide (CO2) and volatile organic compounds (VOC), indoor surface temperatures and air turbulence intensity (Zhaiet et al., 2007). Otherwise, indoor airflow in multi-zone buildings can be driven by different forces such as wind, thermal buoyancy, and/or mechanical ventilation causing natural, forced or mixed complex airflows.

Important paths through which mass and energy are transported in multi-zone buildings are large vertical and horizontal openings such as doors and stairwell opening respectively. There are different investigations describing the airflow through vertical opening. In this case a relatively stable velocity distribution or flow pattern at the opening is observed. This results in a stable pressure distribution between the zones that is greater at the top and bottom of the opening and weaker at the centre. On the other hand, horizontal opening have not been profoundly studied. The transient and unstable pattern across this opening for natural convection cases and the lack of experimental data are the main reasons for the limited knowledge we have of the airflow through horizontal openings.

2.1. Experimental studies of airflow through openings.

2.1.1. Experimental studies of airflow through vertical openings.

The first solution to estimate the airflow through vertical openings for natural convection was proposed by Brown and Solvason (1962). The authors assume that airflows through the vertical opening are driven by density fields on both sides of the opening. Since an incompressible and inviscid flow in steady condition is considered, it is possible to use Bernoulli's equation to determine the horizontal velocity along the streamline as equation (1), then the mass flow below the neutral plane (ZN) is given by equation (2) (see Figure 3). The discharge coefficient C_d is assumed to be a characteristic of the whole opening and it is constant. ρ_0 and ρ_i, T_0 and T_i are the densities and temperatures at each side of the opening respectively. W is the width of the opening in meters, g is the acceleration due to gravity in meters per second squared and z is the high level of the opening in meters. In the case of an existing supply of air in one zone, or of different thermal gradients on both sides of the opening, a solution can also be reached using numerical tools.

$$V_Z = \left[2\left(\frac{\rho_0-\rho_i}{\bar{\rho}}\right)gz\right]^{1/2} \quad (1)$$

$$m'_{0,ZN} = C_d \int_{z=0}^{z=ZN} \rho_0 V_Z W dz \quad (2)$$

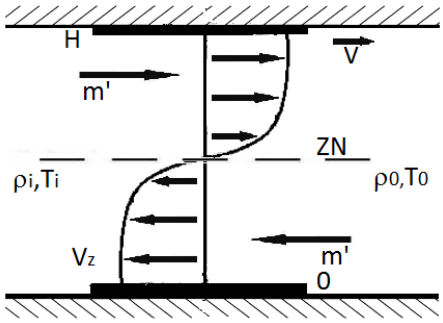

Figure 3: Velocity distribution through vertical opening for natural convection

Several studies (Allard and Utsumi, 1992; Santamouri et al.,1995; Woloszyn and Rusaouën, 1999; Favarolo and Manz, 2005; Tanny et al., 2008; Özcan et al., 2009; Ravikumar and Prakash, 2009; Nitatwichita et al., 2008; Cheung and Liu, 2011; Allocca et al., 2003) have been carried out in order to develop general solutions to predict airflow through large vertical openings with extensive experimental data available.

2.1.2. Experimental studies of airflow through horizontal openings.

The stable distribution of the driving force found in vertical openings is not present in the case of horizontal openings especially under pure buoyancy driven flows. Figure 4 shows a horizontal opening for natural convection. At the horizontal plane separates the air of two zones, the pressure is constant and the pressure difference across the plane at any point is zero therefore, there is theoretically no driving force at all. However, in the case of greater density in the upper room the flow pattern is highly transient and an unstable equilibrium occurs across the horizontal opening in which a minor disturbance breaks the equilibrium and causes that warm air moves upward and cold air moves downward. There is no force to stabilize or regulate this exchange. This scenario of instability has made to researchers more difficult the study of airflows through horizontal opening.

The first study in considered mass transport through horizontal opening was carried out by Brown (1962) about natural convection across horizontal partitions for heavier fluid above the partition using air as the fluid. In this situation an unstable condition across the opening and an exchange of lighter and heavier fluid is observed.

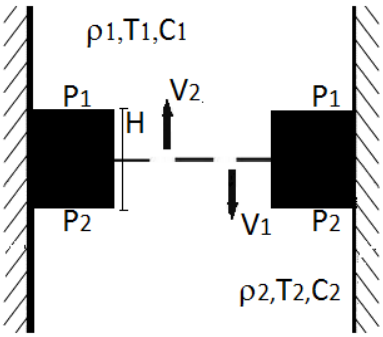

Figure 4: Natural convection through horizontal opening

The experimental tests were carried out in a large wall-panel test consisting in two boxes. One box produces the warm side and the other box produces the cold side. Three singles square were used to try different openings sizes: 15.24x15.24 cm, 22.86x22.86 cm and 30.48x30.48 cm, with air difference temperature across the opening ranging about 20 to 90°C.

Although an experimental study was carried out, it was necessary to take into account theoretical considerations in order to derive a correlation for convective heat transfer through a square opening. Figure 4 shows the theory of two cavities containing fluid at densities ρ_1 and ρ_2 $(\rho_1 > \rho_2)$ connected by a horizontal opening of thickness H. It is not possible to assume a steady distribution due the inherently unstable condition mentioned before. Using Bernoulli's equation, for the lighter fluid flowing upward and the heavier fluid flowing downward, density difference can be described by equation (3)

$$(\rho_1 - \rho_2)gH = \rho_1 \frac{V_1^2}{2} + \rho_2 \frac{V_2^2}{2} + (l_1 + l_2) \qquad (3)$$

where g is the acceleration due to gravity in meters per second squared and l_1, l_2 are pressure losses due to entrance into the opening and fluid friction. After manipulating the equations, Brown obtained an expression for velocity, heat and mass transfer as described by equation (4), (5) and (6) respectively.

$$V = \frac{C_2\left(\frac{\Delta\rho}{\bar{\rho}}gH\right)^{1/(2+bd)}}{\left(\frac{H}{L}\right)^{ad/(2+bd)}\left(\frac{L}{\nu}\right)^{bd/(2+bd)}} \quad (4)$$

$$\dot{q} = \bar{\rho}C_p\frac{L^2}{2}(T_2 - T_1)V \quad (5)$$

$$\dot{m} = \bar{\rho}\frac{L^2}{2}(C_2 - C_1)V \quad (6)$$

Where exponent *bd* lies between 0 and -1 and exponent *ad* lies between 0 and 1; ν is the kinematic viscosity in kilograms per second×meters, L is length of the side of the square opening in meters, C_1 and C_2 are constants and C_p is the specific heat of air.

The result showed that the heat and mass transfer rate increase with increasing partition thickness. Then, introducing the heat transfer coefficient h_T and the mass transfer coefficient h_m, Brown obtained dimensionless relationship for heat transfer through a horizontal square opening based on experimental data represented by equation (7).

$$Nu_H = 0.0546Gr_H^{0.55}\,Pr(L/H)^{1/3} \quad (7)$$

where L is length of the side of the square partition, Nu_H is the Nusselt number based on partition thickness, Gr_H is Grashof number based on partition thickness and Pr is Prandtl number.

Epstein (1998) carried out an experimental study of buoyancy-driven flows through horizontal opening using brine above the partition as a higher density fluid, and fresh water below the partition. Flows measurements were made with a single round opening varying the L/D ratio between 0.01 to 10, where L is the thickness opening in the direction normal to the partition, and D is the diameter of the opening. The density difference makes that the heavier fluid moves downward from the upper compartment into the lower compartment while mass conservation makes the lighter fluid moves upward causing a countercurrent exchange flow across the opening. The results of the experiments suggested that there exists an influence of the density ratio, $\Delta\rho/\bar{\rho}$, on the

Froude number where at lower L/D the flows rate decrease and appears to be tending toward a constant value as $L/D -> 0$. Whereas, at higher L/D the flow rate decreases with increasing L/D. Thus, Epstein recognizes four different flow regimes as L/D is increased as shown in Figure 5: (I) an oscillatory exchange flow regime, (II) a countercurrent Bernoulli flow regime, (III) a regime of combined turbulent binary diffusion and Bernoulli flow, and (IV) a region of pure turbulent binary diffusion. In the first regime, at very small L/D the thickness of the partition is reduced and the pressure at the level of the opening is essentially the same in both bodies of fluid. Visual observations revealed upward and downward plumes in both bodies of fluid, periodically breaking through the opening. In the second regime, the exchange flow data adjusts with air exchange flow reported by Brown (1962). An expression for the exchange flow was given by equation 8:

$$\dot{m} = 0.23(D^5 g\, \Delta\rho/\bar{\rho})^{1/2}(L/D)^{1/2} \qquad (8)$$

In regime (IV) the progress of each liquid into the other was observed to be much slower in vertical tubes with large L/D than in the other three regimes. The $\dot{m} \sim (L/D)^{-3/2}$ behavior is determinate for this regime but it is not apply if L/D decreased so it is necessary to link Bernoulli and turbulent diffusion approaches in regime (III).

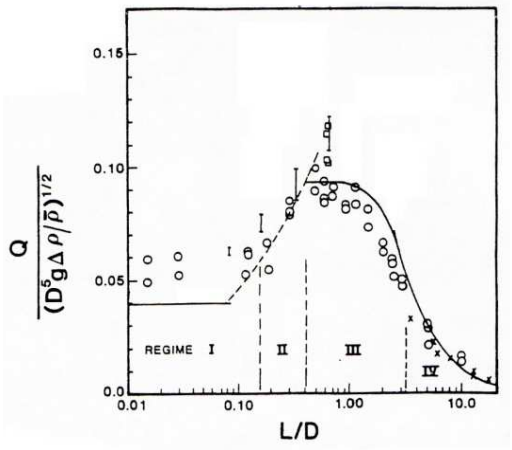

Figure 5: Experimental results for countercurrent exchange flow through a single opening (Epstein, 1998).

Heiselberg and Li (2007) analyzed the same case than Epstein in a full-scale experimental setup. They measured airflow rate through a horizontal opening using constant injection tracer gas technique. The smoke visualization confirms a bi-directional airflow through the opening which is highly transient, unstable and complex. Figure 6 shows a comparison between the measured airflow rates as a function of temperature difference with predicted airflow rate calculated with Epstein (1998) formula. The results show a good agreement for all regimes except in regime (III) because in this study the regime (III) and regime (IV) could not be distinguished.

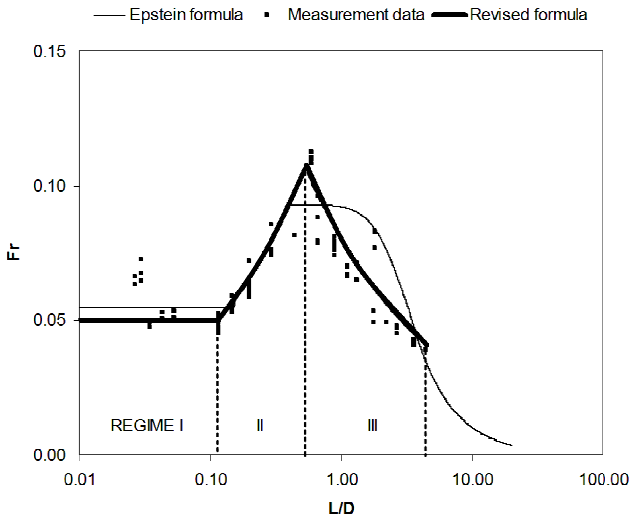

Figure 6: Comparison of the relation between the dimensionless number Fr and L/D ratio developed by Heiselberg and Li and the relations developed by Epstein (1998).

A similar unstable situation was observed by Zohrabian et al. (1989) in an experimental study of buoyancy-driven flows of mass and energy in a half-scale model of a stairwell. The circulation of air was maintained by the operation of a heater in the lower floor. The study was focused in the throat area of the stairwell showing a tridimensional and unsteady flow with considerable temporal variations. In this area, it is possible to identify two layers of fluid one above the other consistent of an upward fluid of warm air and a downward fluid of cold air moving in opposite directions causing the heat and

mass exchange. There were also detected a number of separations, reattachment and circulation zones which contributed to the complex flow situation as shown in Figure 7.

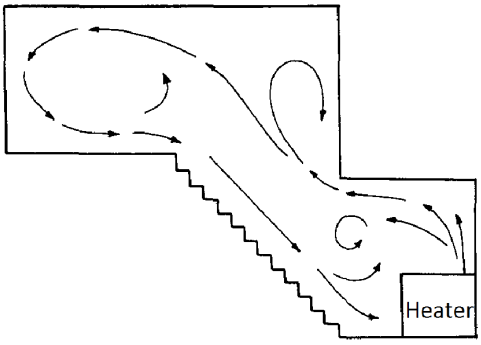

Figure 7: View of the flow pattern in the stairwell (Zohrabianet al., 1989).

Previous studies include only buoyancy driven flows. A study of forced convection was carried out by Cooper (1994). He presented a study of available experimental data of a combined buoyancy and pressure (i.e., forced) driven flow through a horizontal vent where the higher density fluid is above the opening and the lower density fluid is below the opening. The analysis of experimental data shows that for relatively large cross vent pressure difference Δp, the flow through the vent is unidirectional, from the space with higher pressure to space with lower pressure, while for relatively small to moderate Δp the flow through the vent is bidirectional and the standard model, which use Bernoulli´s equations with constant discharge coefficient C_d, does not predict the expected behavior. The study suggests an algorithm to predict the rates flow through shallow, horizontal, circular vents under high Grashof number conditions and for an arbitrary specified fluid pressure in each space.

Vera et al., (2010) carried out an experimental study about interzonal air and moisture transport through a horizontal opening in a full scale two-story test-hut. The study extended the cases with buoyancy driven flows to cases with combined buoyancy airflows and mechanical ventilation and cases with warmer upper room than the lower rooms. Interzonal airflows were calculated based on tracer gas technique using water vapor as a single tracer gas. The results show that interzonal air and moisture exchange

through the horizontal opening are strongly linked to the temperature difference between the two rooms where higher upward mass airflows occurred when the upper room was much colder, while much smaller upward mass airflow were found when ΔT was near 0°C. Upward interzonal mass airflow existed also when the upper room was warmer; however, it is not evident why upward mass airflow occurred under this condition. The mechanical ventilation significantly restricts the horizontal airflows in comparison with cases without mechanical ventilation.

2.2. Studies of airflow through horizontal openings by means of CFD technique.

2.2.1. Computational Fluid Dynamics technique.

One way to enhance the study of airflow and heat exchanges through large openings has been the incorporation of Computational Fluid Dynamic (CFD) technique in the design of buildings.

2.2.1.1. What is CFD?

CFD is a technique used to study fluid in motion and how the fluid behavior influences processes that may include heat and mass transfer and chemical reactions. The physical characteristics of the fluid motion can usually be described through three fundamental mathematical equations: continuity, momentum and energy equations (Tu et al., 2008). In their general form, these equations are an integral equation or partial differential equation. The CFD technique is to solve these equations computationally through numerical simulations. This is done by replacing the integrals or partial derivates in the fundamental equations by discretized algebraic forms. These discretized forms are solved to obtain numbers for the flow field values at discrete points in time and/or space (Anderson, 1995).

CFD is a well suited tool for research and design because it might save time and effort (Hajdukiewicz et al., 2013). For this reason CFD computational tools have had

significant advances, thus CFD software are more accessible with user interfaces that facilitates students, researchers and engineers to perform CFD simulations in different areas. In building design it can be used to model temperature distribution and air movement within spaces that allows designers to know the building performance under different configurations before they are built and select the most effective solutions. Figure 8 shows examples of CFD applications in different industries such as chemical processing, biomedical sciences, civil engineering, automotive engineering, building design and sports where fluid flows play an important role. CFD is a useful tool to predict and have a full picture about how the fluid will flow in a studied zone, and allows localizing regions or process with deficient performance depending on the industry objective. This technique provides a complete description of the three-dimensional flow in the entire domain in terms of velocity field and pressure distribution.

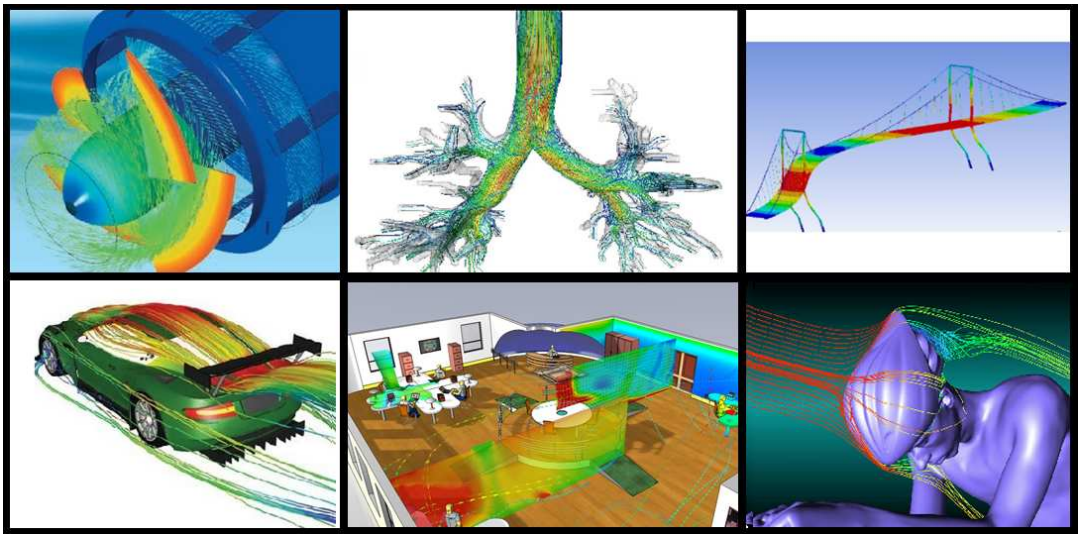

Figure 8: CFD uses in chemical processing, biomedical sciences, civil engineering, automotive engineering, building design and sports.

2.2.1.2. Fundamentals of fluid dynamics

Next section describes the CFD technique based on Tu et al. (2008) description.

CFD technique is based on the conservation laws of physics expressed as equations. Thus, the objective is to solve the governing equations of fluid dynamics. These are: continuity, momentum and energy equations, described as follow.

- Continuity equation: mass conservation

The law of conservation of mass states that the mass of a system must remain constant over the time, which implies that matter can neither be created nor destroyed. Considering Figure 9 at a control volume, the mass conservation requires that the rate of change of mass within a control volume is equivalent to the mass flux outside the control volume. This can be expressed as:

$$\frac{dm}{dt} = \sum_{in} \dot{m} - \sum_{out} \dot{m} \quad (9)$$

Applying Gauss's divergence theorem and considering the scenario of a fluid flowing between two stationary parallel plates, mass conservation equation can be expressed as

$$\frac{\partial \rho}{\partial t} = \nabla \cdot (\rho \mathbf{V}) = 0 \quad (10)$$

Where V is the fluid velocity, and $\nabla \cdot (\rho \mathbf{V}) \equiv \mathbf{div}\ \rho \mathbf{V}$

And in cartesian coordinate system

$$\frac{\partial \rho}{\partial t} + \frac{\partial (\rho u)}{\partial x} + \frac{\partial (\rho v)}{\partial y} + \frac{\partial (\rho w)}{\partial z} = 0 \quad (11)$$

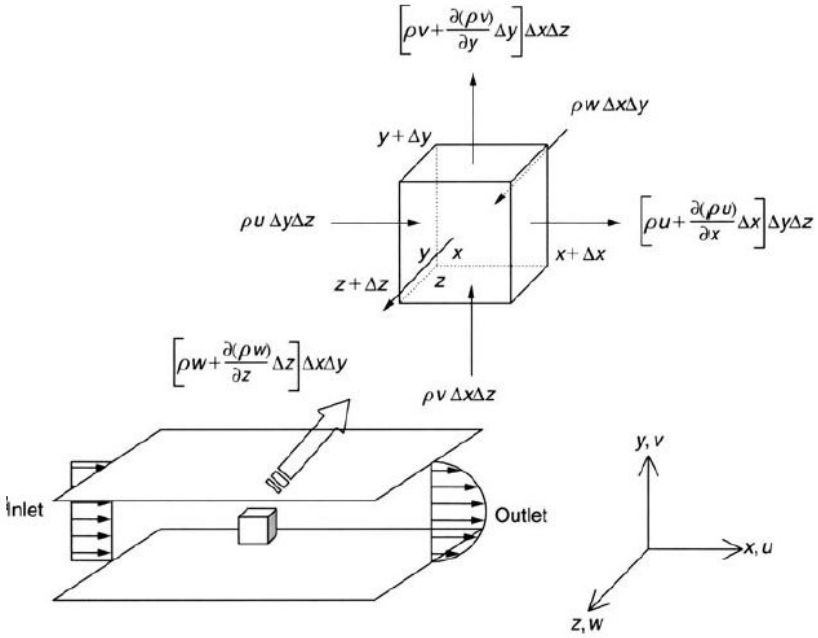

Figure 9: Conservation of mass in an infinitesimal control volume (Tu et al., 2008).

- Momentum equation: force balance

Newton's second law of motion describes the relationship between a body, the forces acting upon it, and its motion in response to those forces. The law states that the acceleration of a body is directly proportional to, and in the same direction as, the net force acting on the fluid element, and inversely proportional to its mass. Considering Figure 10, the Newton second law can de expressed as $\sum F_x = ma_x$

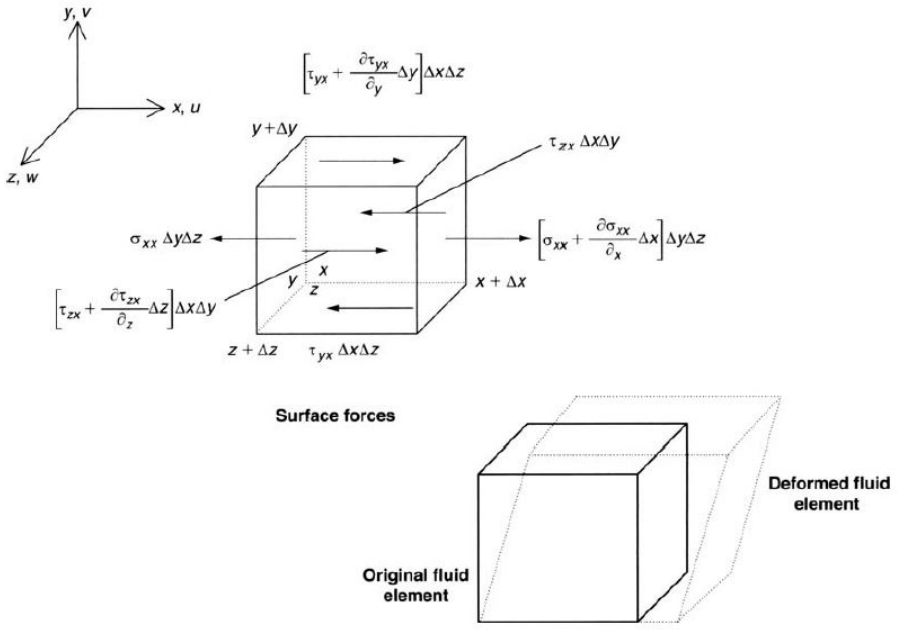

Figure 10: Surfaces forces acting on the control volume for the velocity component *u*. Deformed fluid element due to the action of the surface forces (Tu et al., 2008).

There are two sources of forces that the moving fluid element experiences, body forces and surface forces. The body forces are the forces distributed over the entire mass or volume of the element that influence on the rate of change of the fluid momentum as gravity, centrifugal or electromagnetic forces. The surface forces are the forces exerted on the surface of the fluid element by its surroundings, as normal stress and tangential stress. By citing the continuity equation, the momentum equations with the inclusion of stress-strain relationships can be reduced to equation (12) and equation (13) also known as Navier-Stokes equations.

$$\frac{\partial u}{\partial t} + u\frac{\partial u}{\partial x} + v\frac{\partial u}{\partial y} = -\frac{1}{\rho}\frac{\partial p}{\partial x} + \nu\frac{\partial^2 u}{\partial x^2} + \nu\frac{\partial^2 u}{\partial y^2} \tag{12}$$

$$\frac{\partial v}{\partial t} + u\frac{\partial v}{\partial x} + v\frac{\partial v}{\partial y} = -\frac{1}{\rho}\frac{\partial p}{\partial y} + \nu\frac{\partial^2 v}{\partial x^2} + \nu\frac{\partial^2 v}{\partial y^2} \tag{13}$$

where v is the kinematic viscosity $v = \mu/\rho$ with μ the dynamic viscosity.

- Energy equation: energy conservation

The equation of the conservation of energy said that the total energy has to be conserved over time and is derived from the first law of thermodynamics. This law can be expressed as

$$\Delta U = Q - W \tag{14}$$

where U is the internal energy of the system Q is the net of heat supplied to the system and W is the work done by the system. Figure 11 show the first law of thermodynamics over a finite element.

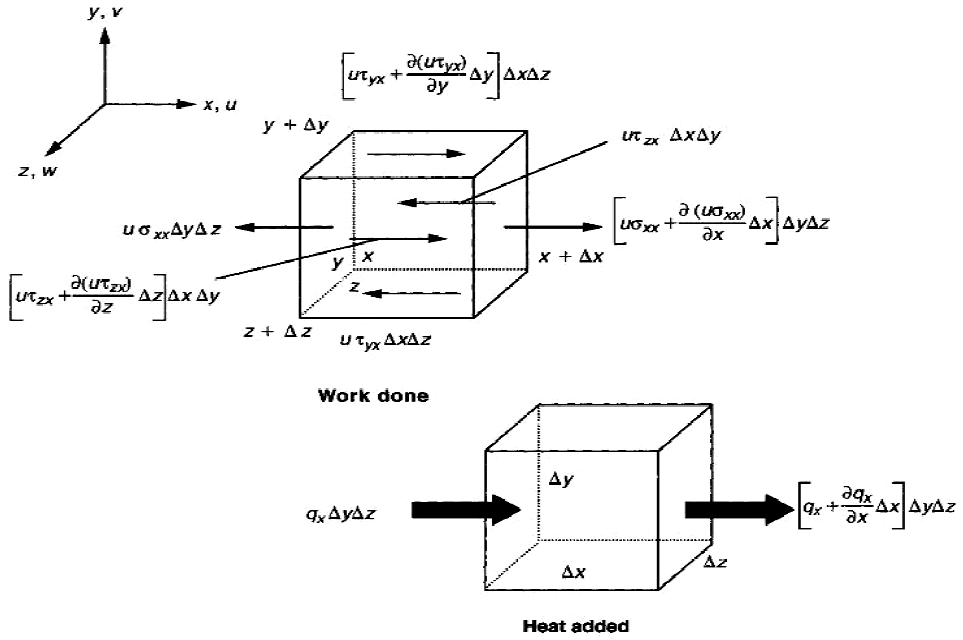

Figure 11: Work done by surfaces forces on the fluid and heat added to the fluid within the control volume. Only the fluxes in the *x* direction are shown (Tu et al., 2008).

Combining all contributions of the surface forces in the x, y and z direction and applying Fourier's law of heat conduction that relates the heat flux to the local temperature gradient, energy equation can be expressed as

$$\rho C_p \frac{DT}{Dt} = \frac{\partial}{\partial x}\left[k\frac{\partial T}{\partial x}\right] + \frac{\partial}{\partial y}\left[k\frac{\partial T}{\partial y}\right] + \frac{\partial}{\partial z}\left[k\frac{\partial T}{\partial z}\right] \tag{15}$$

Finally, since there are similar commonalities between continuity, momentum and energy equations, it is possible to introduce a general variable ψ and formulate a unique general transport equation as follow:

$$\frac{\partial \Psi}{\partial t} + (u\nabla)\Psi = \delta\nabla^2\Psi + \dot{\Psi}_G \qquad (16)$$

where ψ can be any fluid property and u is the velocity vector which is function of space and time, $u(x, y, z, t)$. In words, eq. 16 describes in the left side the rate of change of Ψ term and the net flux due to convection and in the right hand the net flux due the diffusion term (δ= difussion coefficient) and the generation term of Ψ respectively.

2.2.1.3. Two- eddy viscosity turbulence models

Most of the engineering problems are related with turbulent flows. These flows are complex cases and need a numerical solution through CFD technique unlike laminar flows which can be easily described by continuity and momentum equations. The turbulence condition is produced when small disturbances in the flow are amplified and lead a chaotic and random state of motion. In these cases, the fluid becomes unstable and flow properties varying in a random way.

Considering a flow property as velocity u, the governing equations have to be applied for an instantaneous velocity which is impossible to predict under a constant fluctuating. Then, the velocity can be decomposed as $u(t) = \bar{u} + u'(t)$ with a steady mean value $\bar{u}$ and a fluctuating component $u'(t)$. Visualizations of turbulent flows has revealed the presence of turbulent eddies which are rotational flow structures with different lengths and velocities.

To solve the Navier- Stoke equations for turbulent flows in a direct numerical solution (DNS), extremely high computational efforts are required. Then CFD technique has the ability to supply adequate information about turbulent processes but avoiding the prediction of effect associated with insignificant eddies. Then, the solution is focus in

the mean quantities. This process that produces the time- averaged governing equations is commonly known as Reynolds- Averaged Navier- Stokes (RANS) equations which contain means values of the steady component ($\bar{u}$) and mean values of the turbulent fluctuations (u'). Then, the governing equation can be written as follow

$$\frac{\partial \bar{u}}{\partial x} + \frac{\partial \bar{v}}{\partial y} = 0 \tag{17}$$

$$\frac{\partial \bar{u}}{\partial t} + \frac{\partial (\overline{u}\overline{u})}{\partial x} + \frac{\partial (\overline{v}\overline{u})}{\partial y} = -\frac{1}{\rho}\frac{\partial \bar{p}}{\partial x} + \frac{\partial}{\partial x}\left(\nu \frac{\partial \bar{u}}{\partial x}\right) + \frac{\partial}{\partial y}\left(\nu \frac{\partial \bar{u}}{\partial y}\right) + \frac{\partial}{\partial x}\left[\nu \frac{\partial \bar{u}}{\partial x}\right] + \frac{\partial}{\partial y}\left[\nu \frac{\partial \bar{v}}{\partial x}\right] - \left[\frac{\partial \overline{u'u'}}{\partial x} + \frac{\partial \overline{u'v'}}{\partial y}\right] \tag{18}$$

$$\frac{\partial \bar{v}}{\partial t} + \frac{\partial (\overline{u}\overline{v})}{\partial x} + \frac{\partial (\overline{v}\overline{v})}{\partial y} = -\frac{1}{\rho}\frac{\partial \bar{p}}{\partial y} + \frac{\partial}{\partial x}\left(\nu \frac{\partial \bar{v}}{\partial x}\right) + \frac{\partial}{\partial y}\left(\nu \frac{\partial \bar{v}}{\partial y}\right) + \frac{\partial}{\partial x}\left[\nu \frac{\partial \bar{u}}{\partial y}\right] + \frac{\partial}{\partial y}\left[\nu \frac{\partial \bar{v}}{\partial y}\right] - \left[\frac{\partial \overline{u'v'}}{\partial x} + \frac{\partial \overline{v'v'}}{\partial y}\right] \tag{19}$$

$$\frac{\partial \bar{T}}{\partial t} + \frac{\partial (\overline{u}\overline{T})}{\partial x} + \frac{\partial (\overline{v}\overline{T})}{\partial y} = \frac{\partial}{\partial x}\left(\frac{k}{\rho C_p}\frac{\partial \bar{T}}{\partial x}\right) + \frac{\partial}{\partial y}\left(\frac{k}{\rho C_p}\frac{\partial \bar{T}}{\partial y}\right) - \left[\frac{\partial \overline{u'T'}}{\partial x} + \frac{\partial \overline{v'T'}}{\partial y}\right]$$

Since the equations above introduce the term $\overline{a'b'}$, knows as Reynolds stress, three additional unknowns variables are introduced, thus it is necessary to add additional equations to solve the system.

Many turbulence model have been developed in order to introduce relationships to solve the govern equations system. The eddy-viscosity models are classified according to the number of transport equations used. The two- equations eddy-viscosity models includes two extra transport equations to represent the turbulent properties of the flow.

The most popular turbulence model is the *k-ε* standard model. This model was developed by Launder and Spalding (1974) and is used for high Reynolds numbers flows. The model proposes that the turbulent viscosity μ_T, which includes the effects of turbulence, can be calculated as $\mu_T = C_\mu \frac{k^2}{\varepsilon}$ where ε is the dissipation rate of turbulence energy and C_μ is an empirical constant. It is a popular model for indoor

airflow simulations due the simple format, robust on solutions and wide validations (Zhai et al., 2007).

The *k*-*ε* standard model calculates the turbulent effect for a single turbulence length scale, thus a modified model had to be developed to calculating the turbulent diffusion for different scales of motion. The *k*-*ε* RNG model was developed by Yakhot and Orszag (1986) using Re-Normalization Group (RNG) method. This model has also been widely used to predict indoor airflows. Other variation in the *k*-*ε* models family is the *k*-*ε* realizable model. This model was developed by Shih (1995) and is recommendable for high Reynolds number flows. This model provides good predictions for swirling flows and flows involving separations.

The *k*-*ε* models usually fail in the treatment of the near wall zone due that the dissipation of the turbulence in this region is not well considered. Thus, *k*-*ω* models family was developed.

The *k*-*ω* standard model was developed by Wilcox (1988) introducing the term *ω* as the ratio of *ε* over *k* which represent the scale of the turbulence. This model is superior to *k*-*ε* models in predicting low Reynolds number flows. Thus, one advantage of *k*-*ω* models is the easy formulation to the near wall zone treatment and flow separations. However *k*-*ω* model is less robust than *k*-*ε* models in predicting far wall regions and free-shear flows. In this way, a new model was developed by Menter (1994) to integrate the advantages of *k*-*ε* and *k*-*ω* models. The shear stress transport (SST) *k*-*ω* model works as a *k*-*ω* model in the near wall zones and as a transformed *k*-*ε* models in free-shear zones. The *k*-*ω* models present a potential for modeling indoor environment with good accuracy and numerical stability. Some advantages of *k*-*ω* models are the accurate prediction for low Reynolds number flows and heat transfer with a simple and robust formulation (Zhai et al., 2007).

All these models have been extensively validated for indoor airflow simulation (Zhai et al., 2007) and an evaluation of their ability on the prediction of airflow in a two-story test-hut was carried out in chapter 4.

2.2.1.4. Components of CFD analysis framework

The salient features that are common in many commercial CFD codes consist of three main element; pre-processor, solver and post- processor, that are interconnected to attempt fluid flow problems. Figure 12 shows the interconnectivity of the three main elements. Their description and relevance in the CFD results are detailed in chapter 3.

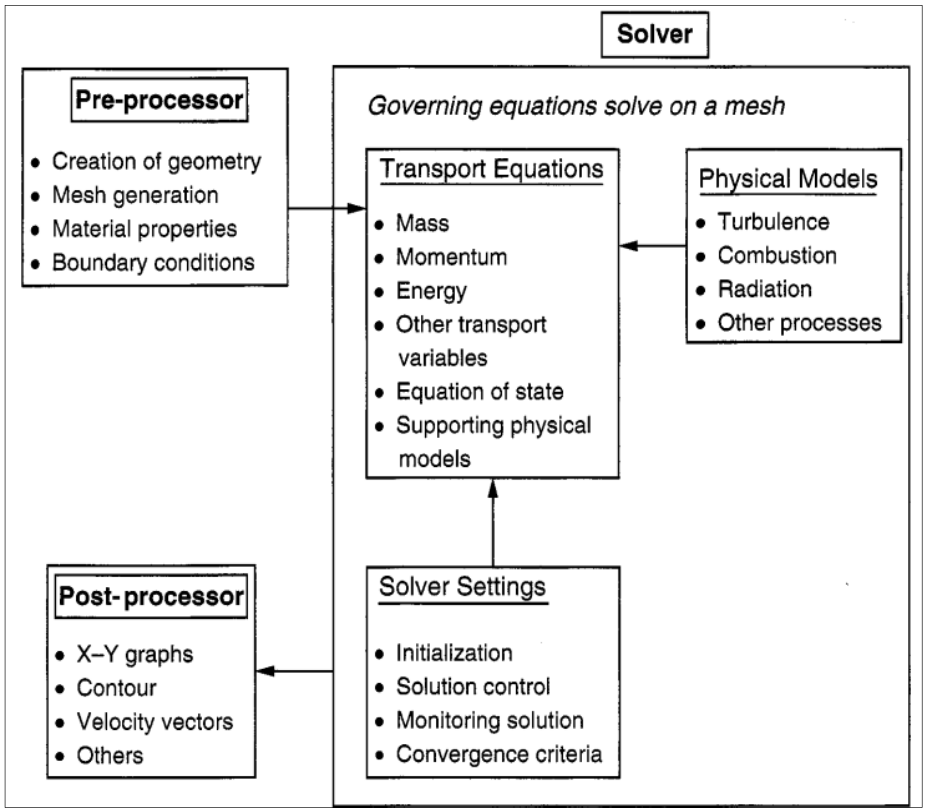

Figure 12: The interconnectivity functions of the three main elements within a CFD analysis framework (Tu et al., 2008).

2.2.2. Review of airflow through horizontal openings using CFD technique

CFD technique has had a rapid advance since its first application to simulate indoor airflows by Nielsen (1974). Similarly to Building Energy Simulation tools, nowadays,

CFD is extensively and intensively applied in the design stage of buildings to support evaluations of natural ventilation (Wu, 2012; Ramponi, 2012; Bangalee, 2012; Hussain, 2012; Carrilho Da Graça, 2012; Rundle et al., 2011) , HVAC system design (Tye-Gingras, 2012; Corgnati, 2013; Chiang, 2012), pollution dispersion and control (Siddiqui, 2012; Saha, 2012), fire and smoke control (Deckers, 2013; Cai, 2012; Chen J. C., 2005), and building envelope design (Pasut, 2012; Giancola, 2012; Suárez et al., 2012; Gagliano et al., 2012)

In terms of mass and energy transport inside multi-zone building, Riffat and Shao (1995) were one of the first to introduce a study of buoyancy-driven flow through horizontal opening using time-dependent CFD in a two-dimensional model. The computation revealed the highly transient flow patterns in the zones and across the horizontal opening showing that the air exchange rate between the two zones is continuously oscillating. They concluded that this dominant mode of air exchange correspond to intermittent pulses as shown in Figure 13 in which is observed that the flow rate through the horizontal opening present continuous fluctuations.

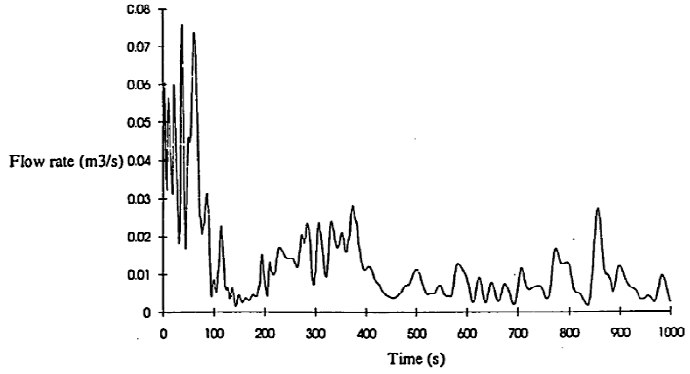

Figure 13: Time history of flow rate through the horizontal opening (Riffat and Shao, 1995)

Peppes et al. (2001) studied buoyancy driven airflow through a real stairwell based on CFD simulations. They found a relationship to predict the mass and heat transfer

through the horizontal opening where the coefficient of discharge C_d was rather independent of the opening size but it was affected by temperature difference as follow:

$$\dot{m} = \rho A C_d \sqrt{\Delta T g H / T} \quad (20)$$

$$\dot{q} = \rho c_p A C_d \sqrt{gH} (\Delta T)^{1.5} / T^{0.5} \quad (21)$$

In a subsequent study (Peppes et al., 2002) the authors extend the investigation to an experimental and numerical study for stairwells flow in a three storey building estimating the airflow rate through a stairwell using CFD method. Results show very good agreement with the corresponding values provided by the formulas proposed in the early study.

The limitation of the relationship found is that cannot be generalized since only two opening sizes were studied and one stair design was used.

Other study of buoyancy driven flow through horizontal opening was performed by Li (2007). He simulated the airflow through a square horizontal opening in a test room shown in Figure 14 using CFD technique. The simulations were performed using *k-ε standard* model and LES model. Previous experimental data show a bidirectional flow through the opening which is highly transient. The simulation of this transient pattern could not converge when *k-ε standard* model in a steady state was used while the LES model results agree well with measured data.

This study concluded that LES model is a suitable tool to predict airflow through a horizontal opening, however do not found relationship to describe it. Also, the simulation was performed for one opening size, thus more simulations considering different opening aspect ratios are required to obtain conclusions applicable to any case.

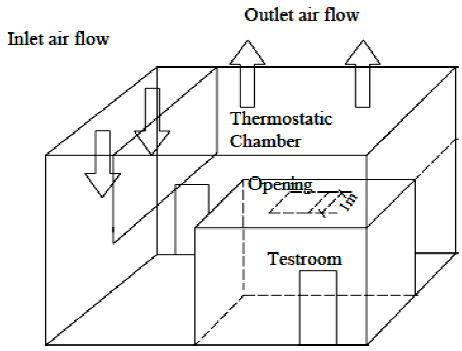

Figure 14: The experiment test cell layout (Li, 2007).

Vera et al. (2010) performed an experimental study of combined buoyancy airflows and mechanical ventilation in a two-story test-hut by means of CFD technique. They modeled cases with two different ventilation strategies; single ventilation with downward net flow through the opening and independent ventilation in each room. Similar conditions for the tested experimental cases were simulated extending for cases with additional ventilations rates and temperature difference between the two rooms. CFD simulations were performed in Airpak using indoor zero-equation turbulence model and the results verify that two- way airflow exists even in cases with warmer upper room. Temperature difference between the two rooms and ventilation rate strongly influence the interzonal mass airflow through the opening when the upper room is colder than the lower room. Empirical correlation between the upward mass airflow and the temperature difference between the two rooms were developed for cases with mechanical ventilation. Finally Vera et al., (2012) investigated the heat transfer through horizontal opening in a full scale two-story test-hut for the previously two ventilation strategies bases on cases simulated using CFD. Results demonstrated that upward heat fluxes through the opening are proportional to the temperature difference between the lower and the upper room. Heat fluxes were even found when the upper room is warmer than the lower room. Heat transfer through the opening is mainly caused by buoyancy driven flows with significant contribution from forced flows. Finally, mixed convective

heat transfer occurs through the opening and the combined effect can be predicted by the following correlation

$$Nu = 3.11Gr^{0.057}Re^{0.63} \quad (22)$$

The limitation of the previous correlation is that it was obtained for one opening size thus it should be evaluated for different opening sizes. Also, the previous study only considered cases with mixed convection but natural convection should be also studied since it is normally present in buildings.

2.3. Conclusion of literature review.

From literature review it is possible to conclude that airflow exchange through large horizontal openings has not been profoundly studied. More studied are required to obtain general relationship to describe heat and mass exchange through horizontal openings.

Table 1 shows a comparison of main results and conclusions obtained by previous experimental and CFD studies. It is possible to observe that most of the studies confirm that the airflow through the opening is complex and unstable and it is proportional to temperature difference between the rooms. However there is a lack of information in the following aspects:

- Most of the studies are carried out for natural convection, while only limited knowledge exists about mixed convection.
- Heat and mass exchange through the horizontal opening are affected by the relationship between opening size and thickness. However, most cases only studied fixed opening size with variable thickness. It is necessary to study airflow through horizontal opening for variable opening sizes.
- Most correlations for heat flow have been developed for natural convection in small scale models. This correlation could be not applicable for full scale cases.

- There are limits evaluations of the capabilities of different turbulence models to predict; i) indoor conditions in zones connected by horizontal opening, ii) mass airflow through the horizontal opening.

In consequence this thesis work has the objective to develop correlations capable to describe the heat flow through a horizontal opening separating two rooms via CFD technique. The correlations will be based on dimensionless numbers (Nu, Gr, Re) that describe the fluid. It is expected to develop correlations for different air conditions such as temperature difference between the lower and upper room of a full-scale two- story test- hut and ventilation strategies (natural and mixed convection), as well as the opening aspect ratios.

Table 1: Main conclusions of airflow through horizontal openings review

Author	Type of study	Phenomenon studied	Main conclusions	Correlations
Brown, 1962	Experimental	Natural convection	Heat and mass transfer rate increase with increasing partition thickness H.	• Heat transfer $\mathrm{Nu_H} = 0.0546\mathrm{Gr_H}^{0.55}\,\mathrm{Pr(L/H)}^{1/3}$
Epstein, 1988	Experimental	Natural convection	Recognizes four flow regimes as L/D is increased.	• Mass transfer $Q = 0.23(D^5 g\,\Delta\rho/\bar{\rho})^{1/2}(L/D)^{1/2}$
Heisleberg and Zhigang Li, 2007	Experimental	Natural convection	Regime (III) and (IV) from Epstein study could not be distinguished defining only one formula for both regimes.	• Mass transfer $\frac{Q}{(D^5 g\Delta\rho/\bar{\rho})^{1/2}} = 0.0077\left(\frac{L}{D}\right)^{-0.5}$ $0.55 < \frac{L}{D} < 4.455$
Zohrabian et al. 1989	Experimental	Natural convection	An increase in heat input resulted in an increase in velocity and in temperature of recirculation flow.	No correlation was found.
Cooper,1994	Experimental	Mixed convection	For relatively large pressure difference Δp, the flow is unidirectional; for relatively small to moderate Δp the flow is bidirectional.	No correlation was found.
Vera et al.2010	Experimental	Mixed convection	Interzonal air and moisture exchange are strongly linked to temperature difference between the two rooms. The mechanical ventilation significantly restricts the horizontal airflows.	No correlation was found.
Riffat and Shao,1995	CFD technique	Natural convection	The air exchange rate between the two zones is continuously oscillating.	No correlation was found.
Peppes et al.2002	CFD technique	Natural convection	The coefficient of discharge is affected by temperature difference. Volumetric airflow rate increased when the temperature difference increased.	• Mass and heat transfer $M = \rho A C_d\sqrt{\Delta T g H/T}$ $Q = \rho c_p A C_d\sqrt{gH}(\Delta T)^{1.5}/T^{0.5}$ Where $C_d = 11.85 Gr_H^{-0.2}$
Vera et al.2010	CFD technique	Mixed convection	Upward heat fluxes through the opening are proportional to the temperature difference between the lower and the upper room.	• Heat transfer $\mathrm{Nu/Re}^{1/2} = 36.86(\mathrm{Gr/Re}^2)^{0.08}$

3. Evaluation of two-eddy viscosity turbulence models to predict airflow in enclosed environments as training exercise for new CFD users

3.1. Abstract

Prediction of airflow pattern and velocities, temperature, moisture and pollutants concentration is required to design healthy and comfortable indoor environments. Computational Fluid Dynamics (CFD) is the most advanced technique to model and predict the airflow in enclosed environments. However, the main errors in CFD models and their results are linked to the human factor. Beginners on CFD modeling do not account with skills, experience and engineering judgment to generate robust and reliable CFD models. This process is not intuitive and new CFD users need guidance. This paper aims to provide more complete information on CFD modeling of basic natural, forced and mixed convection cases that would allow CFD beginners to acquire skills and confidence. CFD modeling includes mesh generation, setting convergence criteria and under-relaxation factors, and evaluating different turbulence models for each convection case. Results show that users´ expertise is needed in each step of CFD modeling, even for these basic convection cases.

Keywords: CFD; enclosed environments; new CFD users; turbulence models; CFD validation

3.2. Introduction

Indoor air distribution in buildings has significant impacts on thermal comfort, indoor air quality and energy efficiency. Important indoor air parameters are temperature and relative humidity; indoor pollutants concentration such as carbon dioxide (CO_2) and volatile organic compounds (VOC); indoor surface temperatures; and distribution of air velocity and air turbulence intensity (Zhai et al.,2007). Indoor airflow in building can be natural, forced or mixed and driven by different forces such as wind-induced infiltration, thermal buoyancy, and mechanical ventilation.

Computational Fluid Dynamics (CFD) technique has had a rapid advance since its first application to simulate indoor airflows by Nielsen (1974). Similarly to building energy simulation tools, nowadays, CFD is extensively and intensively applied in the design stage of buildings to support evaluations of natural ventilation (Wu et al. 2012; Ramponi and Blocken 2012; Bangalee et al., 2012; Hussain and Oosthuizen 2012; Carrilho da Graça et al., 2012; Rundle et al. 2011); HVAC system design (Tye-Gingras and Gosselin 2012; Corgnati and Perino 2013; Chiang et al., 2012); pollution dispersion and control (Siddiqui et al., 2012; Saha et al., 2012); fire and smoke control (Deckers et al. 2013; Cai and Chow 2012; Chen et al., 2005); and building envelope design (Pasut and De Carli 2012; Giancola et al. 2012; Suárez et al. 2012; Gagliano et al. 2012).

CFD is a well suited tool to model indoor air conditions for research and design because CFD modeling might save time and effort (Hajdukiewicz et al., 2013). For this reason CFD tools have had significant advances, thus CFD software are more accessible with user interfaces that facilitates students, researchers and engineers to perform CFD simulations of enclosed environments. However, this involves an important risk of obtaining erroneous results due to lack of user skills on CFD modeling and expertise to deal with indoor air specific engineering problems. Therefore, CFD codes and user skills need to be verified and validated to obtain reliable and successful CFD simulation results of indoor environmental conditions in buildings.

Although the American Institute of Aeronautics and Astronautics (AIAA, 1998) and American Society of Heating, Refrigerating and Air-conditioning Engineers (Chen and Srebric, 2001) provide different definitions of verification and validation, they pointed out that verification is focused on the CFD code, while validation is focused on the coupled user skills and the representation of the engineering problem by a CFD model. Verification consists on checking the capabilities of the CFD code to take into account the physical phenomena and identifying errors of the computational model and its solution. On the other hand, validation focuses on evaluating the coupled ability of the user and CFD model, first, to properly represent a specific indoor environments, and

secondly, to perform accurate indoor environmental simulation. Recently, Hajdukiewicz et al. (2013) proposed a process to achieve a valid CFD model for indoor environments. Besides verification and validation, they recommend a calibration methodology of the CFD model. This methodology consists of performing a parametric study to determine the influence of the boundary conditions on the results.

CFD modeling requires expertise to:

- Decide how to model a specific engineering problem. For instance, the physics of the problem could be represented as 2D or 3D and steady-state or transient.
- Define the geometry that represents the indoor environment engineering problem.
- Generate a proper mesh which includes deciding about size and meshing topology as well as testing grid independence.
- Set the fluid properties.
- Set the boundary condition such as wall boundary conditions (surface temperature, heat flux), air supply and outlets, heat and moisture sources and sinks, etc.
- Define solution algorithms, pressure or density based solution methods.
- Choose a proper turbulence model that provides reliable results for the characteristic airflow of the problem.
- Establish the numerical parameters such as differencing schemes, under-relaxation factors, time-step in case on transient problems, number of iteration, convergence criteria; etc.

Since several CFD codes have been already widely verified, errors to simulate indoor environments via CFD technique are mostly linked to the human factor. These errors are associated to user's attitude and their experience and training (Casey and Wintergeste, 2000). Errors in any step may cause unreliable results. Furthermore, inexperienced users may not realize that results are wrong. Nowadays, the high accessibility to commercial

CFD software with friendly user interfaces and colorful results increases the risk of errors and false confidence on results. Therefore, users must acquire confidence and expertise on CFD modeling before they obtain successful and robust simulations.

The “Best Practice Guidelines for Quality and Trust in Industrial CFD” published by the European Research Community on Flow, Turbulence and Combustion (Casey and Wintergeste, 2000) shows the need for CFD users training and provide guidelines to do this. Besides training and knowledge in CFD fundamentals, solution of realistic indoor environment cases is needed for new users. The guidelines for CFD modeling of AIAA (1998), ERCOFTAC (Casey and Wintergeste, 2000), ASHRAE (Chen and Srebric 2001), and Oberkampf and Trucano (2002) show procedures to validate CFD models based on comparing experimental results with CFD simulation results for an specific or various turbulence models. This procedure, for several cases, would help new CFD users to acquire confidence and expertise on CFD modeling of indoor environments. Section 2 shows extensive literature about validating CFD models.

The main focus of studies shown in Section 2 is to evaluate different turbulence models for natural, forced and mixed convection flows in enclosed environments. However, these works do not provide detailed information about parameters used on these CFD models and the engineering judgments applied to define the modeling parameters and how to generate a representative model of reality. This information is useful for new CFD user to acquire skill and confidence on CFD modeling.

In consequence, this paper aims to provide more complete information on CFD modeling of basic natural, forced and mixed convection cases that would allow CFD beginners to acquire skills and confidence. CFD validation of five k-ε and k-ω turbulence models is followed to show the criteria and engineering judgments used to model the cases of Ampofo and Karayiannis (2003) for natural convection (NC), Restivo (1979) for forced convection (FC) and Blay et al. (1992) for mixed convection (MC). The CFD validation process and datasets shown in this paper could be used as training exercises for new CFD users to acquire skills and expertise on CFD modeling.

3.3. Review on evaluating turbulence models and experimental studies

This paper proposes that CFD validation process according to CFD guidelines (i.e. AIAA, ASHRAE, etc.) is a proper methodology for training of inexperienced CFD users such as students, researchers and HVAC/building engineers. CFD validation has focused in a major part of the last two decades to evaluate different turbulence models. This requires experimental datasets to compare CFD results of predicted quantities with experimental measurements (i.e. air velocity, temperature, turbulent kinetic energy, etc.). The following sections summarize most recently studies in evaluating turbulence models, as well as basics experimental setups for NC, FC and MC that will be modeled on CFD as training exercises for new CFD users.

3.3.1. Evaluation of turbulence models

There is a large amount of work on evaluating turbulence models for indoor environments. Many works have focused on evaluating the capabilities of different turbulence models to predict the airflow pattern and indoor environmental parameters for natural, forced and mixed convection flows in laboratory enclosed cavities and in real offices or atriums. Table 2 summarizes some studies carried out during the last decade that evaluated several turbulence models in enclosed environments. Most studies focused on the evaluation of two-eddy viscosity models (*k*- ε standard, *k*-ε RNG, *k*-ε realizable, *k*-ω standard, *k*-ω SST, etc.). However, studies shown in Table 2 cover a broad range of turbulence models, from simpler turbulence models such as zero-equation model of Chen and Xu (1998) to more advanced models such as detached-eddy simulation models of Shur et al., (1999).

Table 2 also provides a performance evaluation of different turbulence models to predict temperature and velocity from “A” to “D” according to the information provided in the revised studies. “A”, “B”, “C” and “D” mean that errors between measurements and

simulations are less than 20%, between 20 and 30%, between 30 and 40%, and over 40%, respectively.

Table 2 shows that *k*- ε standard, *k*-ε RNG and *k*-ω SST have been widely evaluated. It is observed that several authors have evaluated *k*-ω standard and *k*-ω SST for NC, showing very good performance of these turbulence models to predict temperature and velocity. A couple of studies (Choi et al., 2004; Zhang and Chen, 2007) have also shown very good performance of v2f and its variation v2f-dav for NC.

For FC, *k*- ε standard and *k*-ε RNG show very good results for temperature and slightly lower performance for velocity. Zhang et al. (2007) showed that the v2f-dav and LES models also provide very good predictions of indoor air conditions for FC. The *k*-ω SST model was evaluated by Cao et al. (2011) and Zhang et al. (2007) but their results have been extremely different. In fact, while Cao et al. (2011) found the *k*-ω SST model provides excellent results, Zhang et al. (2007) found that its performance was poor.

For MC, evaluation errors fall under "A" or "B" ranges for all turbulence models, as shown in Table 2. Rohdin and Moshfegh (2011) evaluated several variants of *k*- ε models (standard, RNG and realizable) in large industrial rooms. While all these turbulence models predict well the airflow conditions, the RNG showed the best results even for pollutant transport in large rooms. Zhang et al., (2007) found that the zero-equation, *k*-ε RNG and v2f-dav predict well airflow conditions in enclosed cavities with low Raleigh number. Stamous and Katsiris (2006) evaluated several turbulence models in offices. They concluded that all evaluated models predict well temperature and velocity, however, the *k*-ω SST model performs better when a proper mesh is used.

3.3.2. Experimental studies

Complete datasets for experimental studies on indoor air conditions in enclosed cavities are needed to be able to validate CFD models. Since this paper recommends evaluating different two-equation eddy-viscosity models as training exercises for CFD´s new users,

Table 2: Literature review on performance of turbulence models

	Paper		Laminar	0-eq	LR *k*- ε	*k*- ε standard	*k*- ε realizable	*k*- ε RNG	*k*-ω standard	*k*-ω SST	*k*-ω BSL	v2f	V2f-dav	RSM	LES	DES	SMC-DH	EBM
Natural Convection	(Choi and Kim 2012)	Temperature																
		Air speed				C				B		A					A	A
	(Rundle et al. 2011)	Temperature																
		Air speed				C												
	(Zhang et al. 2007)	Temperature		B		C		A		A			A	A	A	C		
		Air speed		D		B		B		A			A	B	B	D		
	(Rundle and Lightstone 2007)	Temperature							A	A								
		Air speed							A	B								
	(Omri and Galanis 2007)	Temperature								A								
		Air speed								A								
	(Zitzmann, et al.,2005)	Temperature							A	A								
		Air speed							B	A								
	(Choi et al. 2004)	Temperature				B				B		A					A	
		Air speed				C				A		A					A	
Forced Convection	(Cao et al. 2011)	Temperature								A								
		Air speed								A								
	(Susin et al. 2009)	Temperature				A		B	B									
		Air speed																
	(Zhang et al. 2007)	Temperature		C		A		A		C			A	B	A	C		
		Air speed				B		B		C			B	B	B	C		
	(Posner, et al.m 2003)	Temperature																
		Air speed	B			B		A										
	(Voigt 2000)	Temperature																
		Air speed			A	A			A	C	A							

Table 2: Literature review on performance of turbulence models (continuation).

Mixed Convection	(Rohdin and Moshfegh 2011)	Temperature				B	B	B										
		Air speed				B	B	B										
	(Vera, Fazio, and Rao 2010)	Temperature		A														
		Air speed		A														
	(Zhang et al. 2007)	Temperature		A		A		A		A			A	B	A	B		
		Air speed		A		A		B		B			A	A	B	B		
	(Zhang and Chen 2007)	Temperature						A										
		Air speed						A										
	(Stamou and Katsiris 2006)	Temperature	B			B		B		A								
		Air speed	B			B		B		A								
	(Moureh and Flick 2003)	Temperature																
		Air speed				B	B							A				

* Letters indicate the errors between measurements and simulations: **A** for less than 20%, **B** for between 20 and 30%, **C** for between 30 and 40%, and **D** for over 40%, respectively

experimental data for basic convection flow problems is required. This paper shows the validation procedure for fundamental cases of natural, forced and mixed convection according to ASHRAE guidelines (Chen and Srebric 2001). Figure 15 shows the enclosed cavities for each convection flow, which are briefly described as follows:

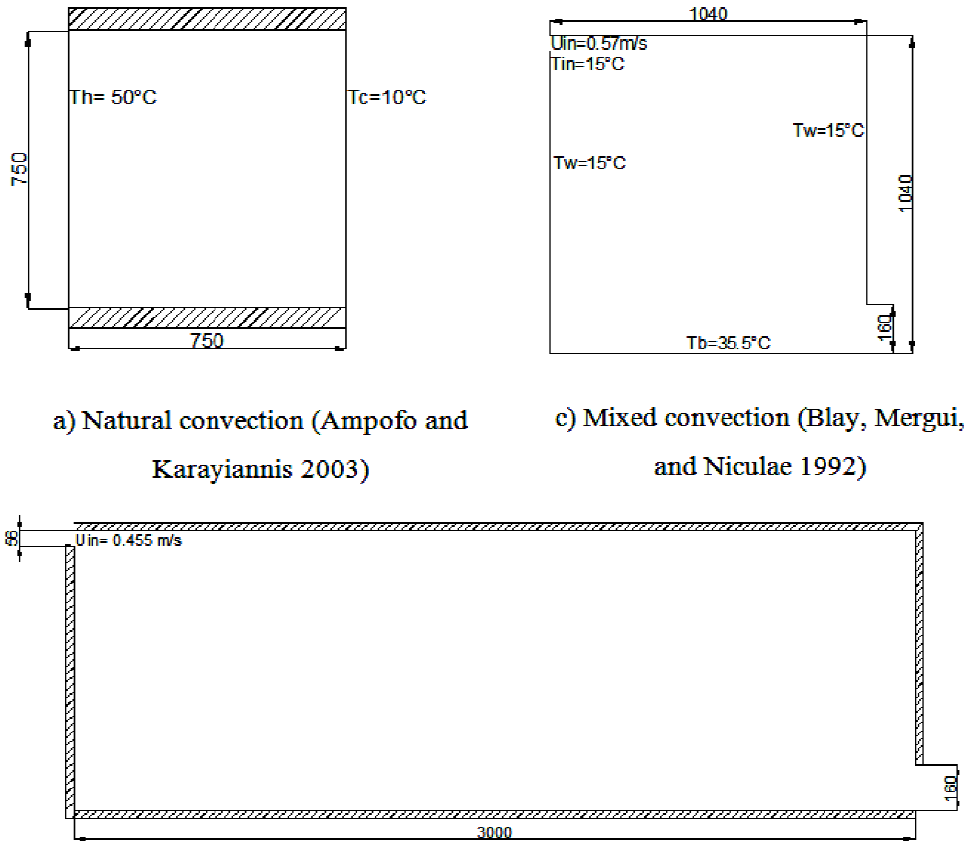

a) Natural convection (Ampofo and Karayiannis 2003)

c) Mixed convection (Blay, Mergui, and Niculae 1992)

b) Forced convection(Restivo 1979)

Figure 15: Experimental cavities for NC, FC and MC cases (dimensions are in mm)

- Natural convection: Ampofo and Karayiannis (2003) carried out a natural convection experiment in a square cavity where 2D flow occurs. This experiment consists in a cavity of 0.75 x 0.75 m and 1.5 m deep (Figure 15a) with hot and cold side walls at 50°C and 10°C, respectively; thus *Ra* number is 1.58×10^9. The top and bottom walls are highly insulated. The fluid properties are c_p = 1006.43

J/kg·°K, k = 0.0242 W/m·°K, μ = 1.7894x10^{-5} kg/m·s, and a molecular mass of 28.966 g/mol.

- Forced convection: The isothermal Annex 20 room of Restivo (1979) and described in Nielsen (1990) consists in a room with 2D forced convection flow (Figure 15b). The air supply is provided by an inlet slot at air velocity of 0.455 m/s and air temperature of 20°C. The room is 9.0 x 3.0 m, the inlet height is 0.168 m and the outlet height is 0.48 m. The kinematic viscosity of inlet air is 15.3x10^{6} m^{2}/s, thus Re is 5.000 based on the inlet height and its air conditions. According to Nielsen (1990), the turbulent intensity based on inlet conditions is 4%.
- Mixed convection: Blay et al. (1992) developed an experimental apparatus of 1.04 x 1.04 x 0.7 m giving a 2D flow (Figure 15c). Air is supplied from the inlet slot at temperature and air velocity of 15°C and 0.57 m/s, respectively. The outlets are placed at the floor level on the opposite wall. The wall temperature is 15°C while the floor temperature is 35.5°C. Thus, *Re* based on the inlet condition is 684. The measured turbulence intensity at the inlet is 6%.

3.4. CFD modeling of basic convection cases

The evaluation of five two-equation eddy-viscosity models is presented in this section according to guidelines for validation of CFD models. The objective of this evaluation is to provide information, criteria and engineering judgments used for CFD modeling of each convection case shown in Figure 15. Each case is an opportunity for CFD beginners to acquire skills and confidence on modeling indoor environments. Five two-eddy viscosity models are evaluated using FLUENT 13.0:

- *k*-ε standard (Launder and Spalding, 1974)
- *k*-ε RNG (Yakhot and Orszag, 1986)
- *k*-ε realizable (Shih et al., 1995)
- *k*-ω standard (Wilcox, 1988)

- *k*-ω SST (Menter, 1994)

For each convection case, the validation procedure follows the processes shown in Figure 16, which is an adaptation of the validation process proposed by Hajdukiewicz et al. (2013). The first step consists of generating an initial CFD model and test grid independency. This test consists of verifying that simulated results do not vary significantly for different mesh sizes. Thus, a mesh size is choosing among mesh sizes that passed the test balancing accuracy of results and computing time.

This initial model requires several inputs such as geometry that represents the problems, boundary conditions, parameters related to the physics of the problems (i.e. 2D or 3D, steady state or transient), initial mesh and turbulence model. To start verifying grid independency, a coarse mesh is set initially. Then, the number of mesh elements is increased consecutively and grid refinement is performed in certain zones (i.e. regions close to walls, inlet). Mesh size independency is achieved when close results are obtained. Once grid independency is obtained, a mesh size is chosen balancing accuracy of simulated results and computing time.

Then, the validation procedure is carried out. This implies that some parameters of the initial CFD model might need to be modified (i.e. under-relaxation factors, mesh refinements, etc.) to accommodate requirements of each model. Since the mesh is tested for independency of the results, the under-relaxation factors are modified in this study for each convection case and turbulence model to allow convergence and accurate simulation results.

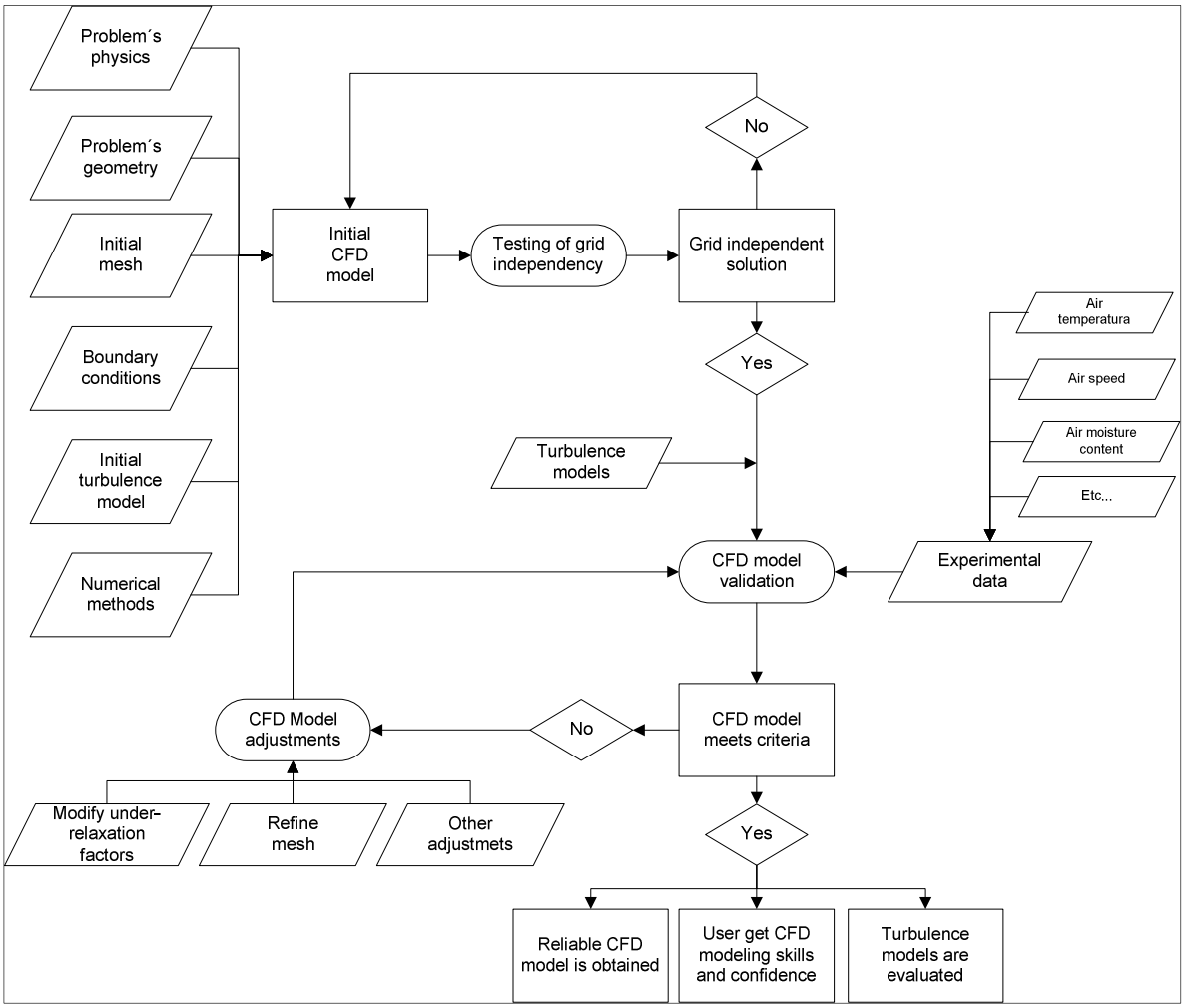

Figure 16: Process flow for CFD validation as exercise for new users to acquire CFD modeling skills.

3.4.1. Natural convection (NC)

3.4.1.1. Initial CFD model

The experiment shown in Figure 15a was modeled as 2D as reported by Ampofo and Karayiannis (2003). It was not possible to reach convergence when the problem was defined as steady-state. This result agrees with similar studies that have modeled the

same experiment (Rundle and Lightstone, 2007). Thus, the problem was modeled as transient with a time step size of 0.19 s. It is worthy to notice that time step setting is not straight forward. Smaller time-steps could allow more accurate results but it is more difficult to reach convergence. The initial turbulence model was set as *k*-ω standard because it shows good performance according to the literature review shown in Table 2. Table 3 shows the main CFD setup parameters for the initial CFD model.

Table 3: CFD setup parameters of NC case

General		**Under-Relaxation Factor**	
Time	Transient	Pressure	0.3
Gravity	y = -9.81 m/s^2	Density	1.0
Models		Body Forces	1.0
Energy	On	Momentum	0.7
Viscous	*k*-ω standard	Turbulent Kinetic Energy	0.9
Radiation	Off	Specific Dissipation Rate	0.8
Materials		Turbulent Viscosity	0.4
Fluid	Air	Energy	0.9
Density	Ideal gas	**Convergence Absolute Criteria**	
Solution Methods		Energy	0.0001
Scheme	SIMPLE	Continuity	0.001
Spatial discretization		x-velocity	0.001
Pressure	Standard	y-velocity	0.001
Density	Second Order Upwind	z-velocity	0.001
Momentum	Second Order Upwind	Turbulent Kinetic Energy	0.001
Turbulent Kinetic Energy	First Order Upwind	Specific Dissipation Rate	0.001
Specific Dissipation Rate	First Order Upwind	**Run Calculation**	
Energy	Second Order Upwind	Time step Size (s)	0.19

The hot and cold temperatures (Th and Tc in Figure 15a) were set as boundary conditions of the hot and cold side walls, respectively. The top and bottom walls were set as adiabatic because they were highly insulated, thus heat flows through theme are supposed to be negligible.

Convergence was difficult to reach. Convergence criteria were 10^{-3} for all parameters except for energy. Ansys, Fluent (2012) recommends a convergence criterion for energy of 10^{-6}. However, it was not possible to obtain convergence with this criterion. Thus, it was increased to 10^{-4} to reach convergence. Moreover, default under-relaxation factors

needed to be modified to obtain convergence. The sum of residual errors met convergence criteria at 2,023 iterations as shown in Figure 17. At this iterations number results were not satisfactory and simulations were performed until 4,000 iterations. Although the fluid flow is developed at 2,000 iterations as shown in Figure 18, the temperature distribution is right after 4,000 iterations only. Hot air rises along the hot wall while cold air drops down along the cold wall, and temperature stratification occurs.

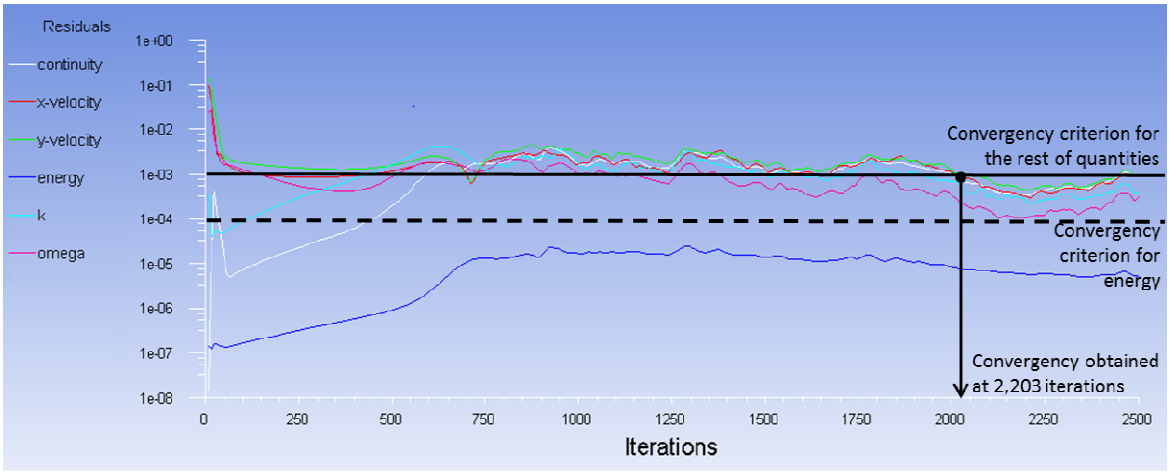

Figure 17: Residuals for NC case with *k*-ω standard.

3.4.1.2. Verification of grid independency

Since the simplified geometry of the experiment of Ampofo and Karayiannis (2003), the mesh is composed for quads elements in a uniform distribution (structured mesh) as shown in Figure 19a. The mesh was refined close to the walls to be able to transfer properly the boundary conditions to the air domain. In fact, large gradients of temperature and velocity occurs in the zone close to the walls, thus a finer mesh allow predicting these gradients more accurately. A coarser mesh is observed in the center of cavity where the air parameters show very low variation.

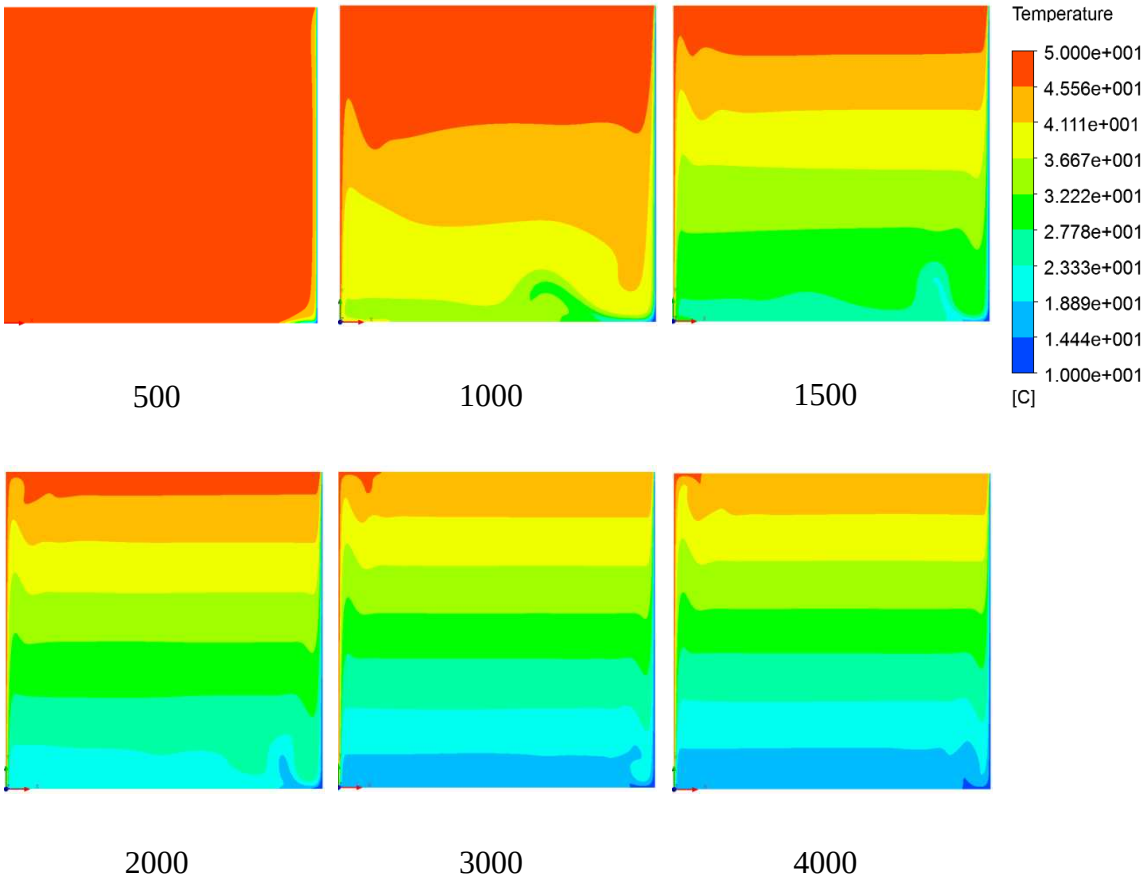

Figure 18: Temperature distribution for NC case at different iterations with *k*-ω standard

Grid independency verification was carried out for mesh sizes of 79x79, 94x94, 125x125 and 188x188. Figure 20a and Figure 21a shows the temperature and velocity at midheight of the square cavity (Y/H = 0.5). It is observed that all mesh sizes predict well the velocity and temperature in the center of the cavity at Y/H = 0.5. The maximum difference between the simulated and experimental data is 0.23% for mesh 94x94, which is negligible.

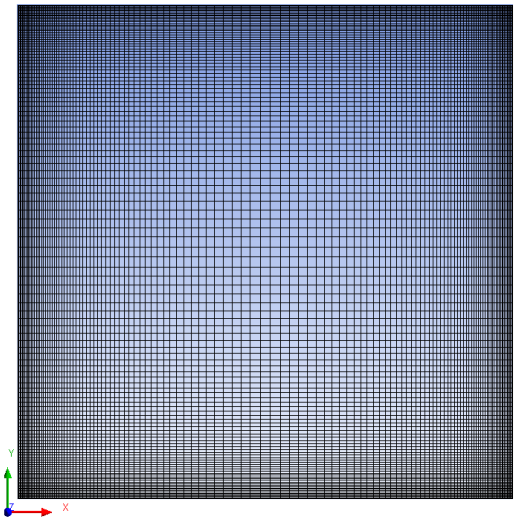

a) Mesh grid of 125x125 for NC case

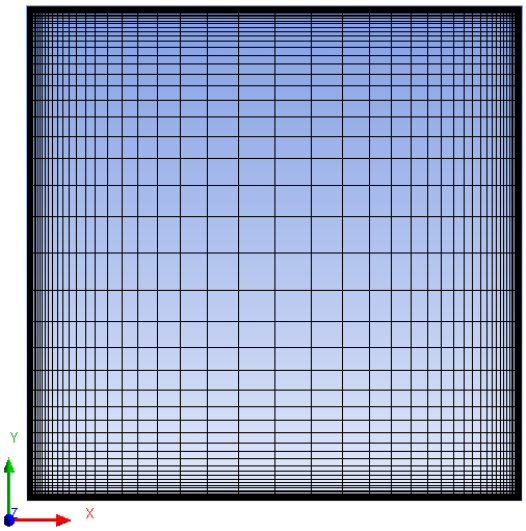

c) Mesh grid of 60x60 for MC case

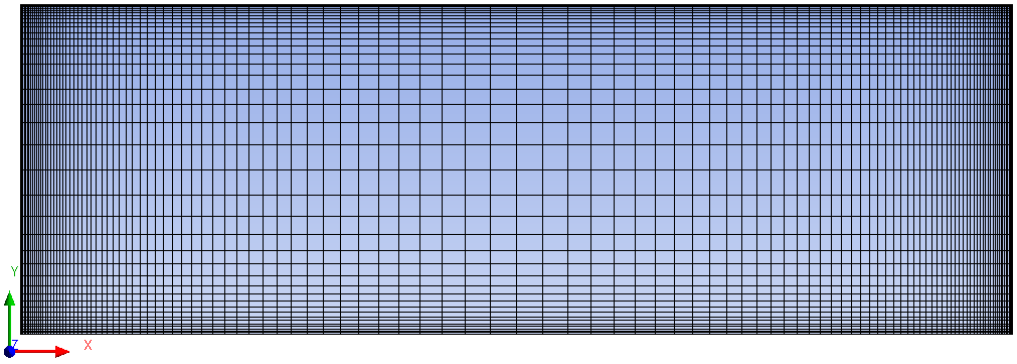

b) Mesh grid of 40x120 for FC case

Figure 19: Mesh grid of initial CFD model for NC, FC and MC cases.

Nevertheless, Figure 20b shows that the CFD model with mesh 125x125 predicts better the temperature drop close to the hot wall. Also, Figure 21b shows that the coarsest mesh predicts very well the velocity close to the hot and cold walls, while the other meshes underpredict it significantly between X/L 0.01 and 0.05. Based on the overall

performance, the mesh size of 125x125 is chosen to proceed with the CFD validation process.

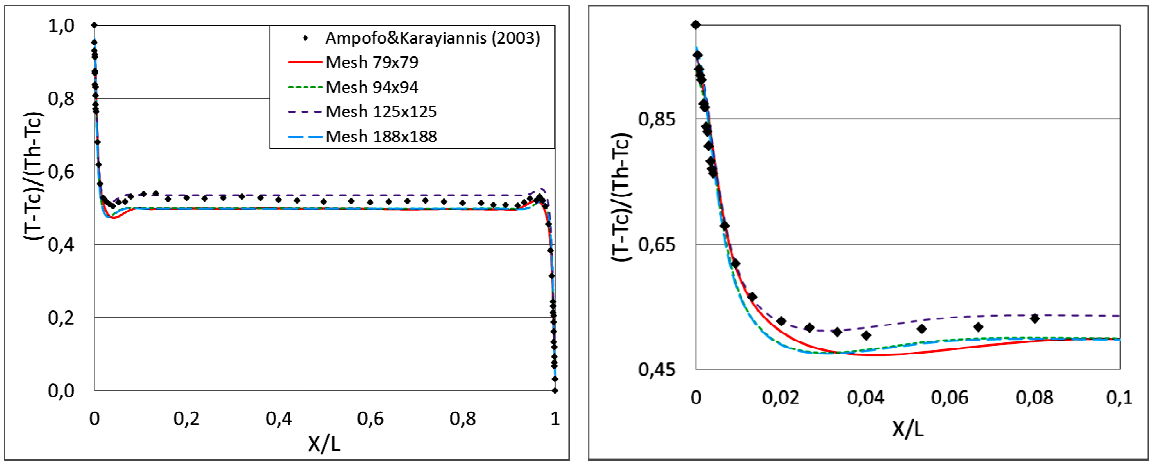

(a) (b)

Figure 20: Grid independency test: a) Dimensionless temperature along Y/H =0.5. b) Dimensionless temperature close to the hot wall.

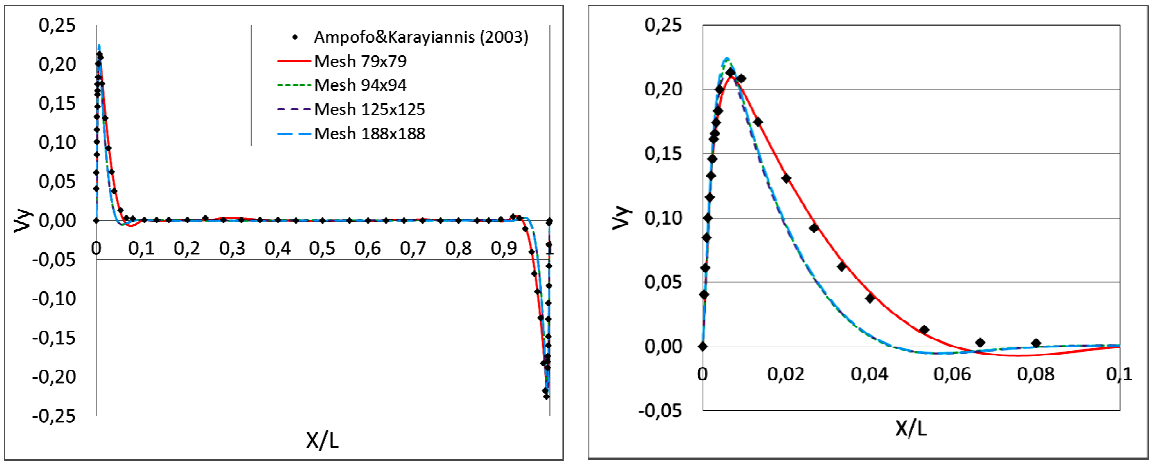

(a) (b)

Figure 21: Grid independency test: a) Velocity along Y/H =0.5. b) Velocity close to the hot wall in m/s.

3.4.1.3. CFD model validation

CFD validation is carried out comparing the simulation results for five turbulence models and experimental data reported in Ampofo and Karayiannis (2003) for temperature and velocity at Y/H = 0.5. Overall, Figure 22a and Figure 23a show that all evaluated turbulence models predict very well the temperature and velocity distribution at midheight of the square cavity. The five two-eddy viscosity models are able to predict the large variation of temperature and velocity close to the hot and cold walls as well as the constant temperature and velocity at the middle section of the cavity.

Despite this good overall performance of all evaluated *k*-ε and *k*-ω models, their performance vary significantly in the region close to walls. Figure 22b shows that *k*-ω standard predicts better the temperature variation close to the hot wall, while the model *k*-ω SST presents the largest variation from the experimental results. Furthermore, Figure 23b shows that both variation of *k*-ω model (standard and SST) do not predict the variation of velocity close to the hot walls as well as the *k*-ε models. The *k*-ω SST overpredicts the peak velocity and underpredicts the velocity drop in the outer border of the boundary layer. The simulated results with *k*-ω SST show differences up to 13.4% with experimental data, which is the largest difference among evaluated two-eddy viscosity models. Similar limitations of *k*-ω SST to predict velocity in the boundary layer were found also by Rundle and Lighstone (2007) and Zitzmann et al. (2005). On the other hand, the *k*-ε RNG and realizable show excellent performance predicting the air velocity close to the hot and cold walls.

These results show that convergence was difficult to reach even for this basic NC case. The problem needed to be modeled as transient and under-relaxation factors and convergence criterion for energy were modified to get convergence and reliable results. Modification of these factors is not intuitive and requires specialized knowledge.

Also, it was found that simulated results in the region close to walls vary significantly among turbulence models. Accurate predictions of what happen in this region are crucial

because the heat and mass transfer between walls and air occurs in this zone. This could have great influence on the predicted room air conditions (temperature, velocity, moisture content, pollutant concentration). This fact emphasizes the need of CFD beginners to be aware that choosing the right turbulence model to indoor environmental conditions. New CFD users need to get experience on CFD modeling. Otherwise, the CFD model and results may not be reliable.

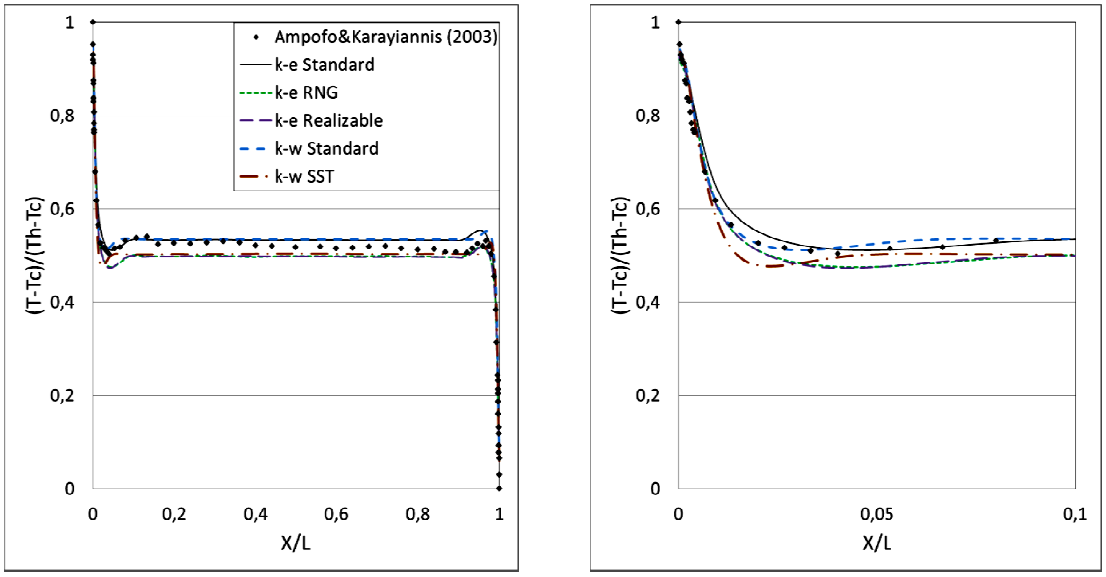

(a) (b)

Figure 22: Performance of two-eddy viscosity models for NC: a) Dimensionless temperature along Y/H =0,5. b) Dimensionless temperature close to the hot wall.

3.4.2. Forced convection (FC)

Since a similar process to NC case was carried to create the initial CFD model and verification of grid independency for FC case, this section focuses on the validation procedure via the evaluation of the turbulence models. Table 4 shows the main CFD setup parameters for the *k*-ε RNG model. The experimental setup of Restivo (1979) was modeled as 2D and steady-state. Since this setup is isothermal, the air inlet supply is the

main factor that influences the airflow pattern. Figure 19b shows a structured grid of 40x120 quad elements. The mesh was refined close to the walls and inlet supply to properly transfer the heat and mass flow from the boundaries to the air domain.

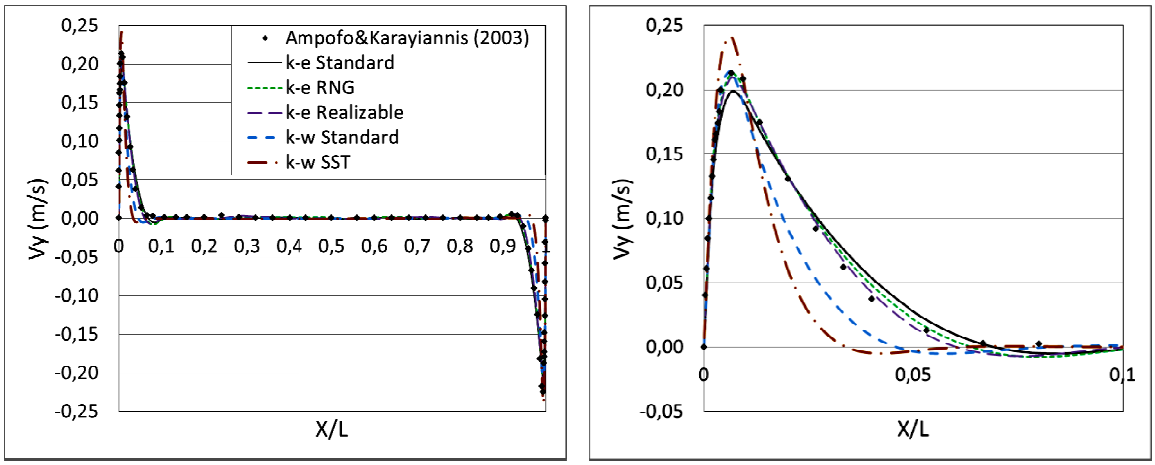

(a) (b)

Figure 23: Performance of two-eddy viscosity models for NC: a) Dimensionless temperature along Y/H =0,5. b) Dimensionless temperature close to the hot wall

Table 4: CFD setup parameters of FC case

General		**Under-Relaxation Factor**	
Time	Steady-state	Pressure	0.3
Gravity	y = -9.81 m/s^2	Density	1.0
Models		Body Forces	1.0
Energy	On	Momentum	0.7
Viscous	*k*-ε RNG	Turbulent Kinetic Energy	0.9
Radiation	Off	Specific Dissipation Rate	0.8
Materials		Turbulent Viscosity	0.4
Fluid	Air	Energy	0.9
Density	Ideal gas	**Convergence Absolute Criteria**	
Solution Methods		Energy	0.000001
Scheme	SIMPLE	Continuity	0.001
Spatial discretization		x-velocity	0.001
Pressure	Standard	y-velocity	0.001
Density		z-velocity	0.001
Momentum	Second Order Upwind	Turbulent Kinetic Energy	0.001
Turbulent Kinetic Energy	First Order Upwind	Specific Dissipation Rate	0.001
Specific Dissipation Rate	First Order Upwind		
Energy	First Order Upwind		

The same under-relaxation factors used for NC case were used in this CFD model. Although convergence criterion for energy was more stringent for FC case, convergence was obtained in short time (650 iterations). Figure 24 shows the airflow pattern for the initial CFD model. It is observed a clockwise airflow with a strong jet flow under the ceiling due to the air inlet. This result is in good agreement with other CFD simulation studies (Olmedo and Nielsen 2010).

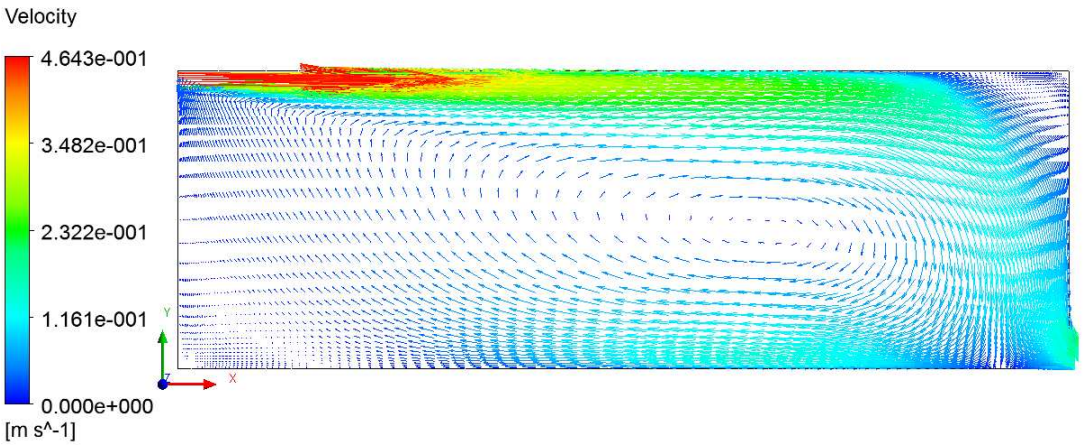

Figure 24: Airflow pattern for initial CFD model.

The evaluation of the five turbulence models is carried out for velocity at the vertical plane at X = 2 m. Results of each turbulence model and experimental data reported in Nielsen (1990) are shown in Figure 25. It can be observed that all turbulence models predict the general airflow pattern, a jet flow close to the top wall of the experimental cavity, and a reverse flow close to the bottom wall. Overall, velocities predicted by all evaluated *k*-ε and *k*-ω models are in good agreements with measured velocities along the cavity height at x = 2 m. However, significant differences on predicted velocities among turbulence models are observed close to the top and bottom walls. In this zone, the *k*-ε standard and RNG predict very well the reverse flow close to the floor and the jet flow close to the ceiling, showing the best performance with differences lower than 7% (or 0.009 m/s) with the experimental data. Otherwise, the *k*-ε realizable model shows the largest differences, 21.3% or 0.05 m/s.

Similarly to NC case, significant variation of simulated air velocity close to the floor is found among turbulence models, and the *k*-ε RNG predict well the whole air domain. In contrast with NC case, *k*-ε realizable shows poor performance predicting air velocity. This result evidences that the performance of turbulence models could strongly depend on the quantity predicted and airflow type.

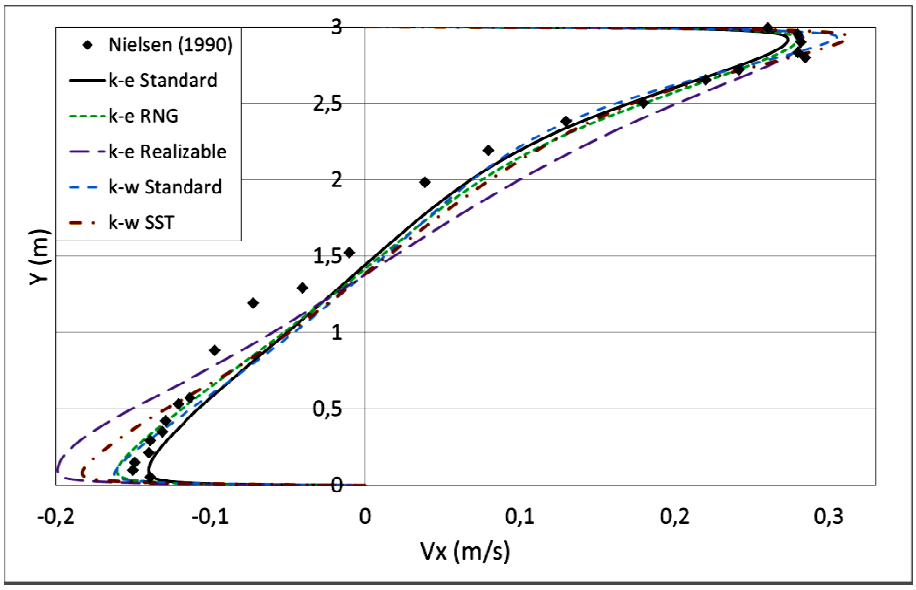

Figure 25: Performance of two-eddy viscosity models to predict temperature along x = 2m for FC case.

3.4.3. Mixed convection (MC)

The mixed convection experiment of Blay et al. (1992) is modeled via CFD technique. This experiment has been widely used to validate new CFD models. The airflow is influenced by inertia forces due to the air supply and buoyancy forces due to the temperature differences on the walls.

Figure 19c shows the mesh of 60x60 elements used to model this experiment. Table 5 summarizes the main setup parameters of CFD modeling with the *k*-ε realizable.

Convergence was obtained at 350 iterations. However, different under-relaxation factors were used to allow obtaining accurate results.

Figure 26 shows the flow pattern obtained with different turbulence models and those observed experimentally by Blay et al. (1992). It is observed that all evaluated turbulence models predicts well the clockwise airflow pattern. However, *k*-ε realizable and both *k*-ω models predict a large eddy in the upper-right corner of the cavity that is not predicted by the *k*-ε standard and RNG models. Due to the lack of more detailed experimental data showing this eddy, it is not possible to get conclusions about the accuracy of the turbulence models to predict this particular feature of the airflow.

Table 5: CFD setup parameters of MC case

General		**Under-Relaxation Factor**	
Time	Steady-state	Pressure	0.3
Gravity	y = -9.81 m/s^2	Density	1.0
Models		Body Forces	1.0
Energy	On	Momentum	0.6
Viscous	*k*-ε realizable	Turbulent Kinetic Energy	0.8
Radiation	Off	Specific Dissipation Rate	0.8
Materials		Turbulent Viscosity	0.4
Fluid	Air	Energy	1.0
Density	Ideal gas	**Convergence Absolute Criteria**	
Solution Methods		Energy	0.000001
Scheme	SIMPLE	Continuity	0.001
Spatial discretization		x-velocity	0.001
Pressure	Standard	y-velocity	0.001
Density		z-velocity	0.001
Momentum	Second Order Upwind	Turbulent Kinetic Energy	0.001
Turbulent Kinetic Energy	First Order Upwind	Specific Dissipation Rate	0.001
Specific Dissipation Rate	First Order Upwind		
Energy	First Order Upwind		

This section focuses on validation procedure and evaluation of the turbulence models. The validation is based on the velocity and temperature measurements carried out at the middle height (Y = 0.52 m) and middle width (X = 0.52) of the cavity as shown in Figure 15c. Figure 27 and Figure 28 shows the temperature and velocity at X = 0.52 and Y = 0.52, respectively. In Figure 27a and Figure 28a, it is observed that *k*-ω models

significantly underpredict the temperature by 1°C along the midwidth and midheight of the cavity. On the other hand, the simulation results of temperature for *k*-ε models are in good agreement with experimental data. Among the *k*-ε models, the realizable variant shows a better performance because it accurately predicts the temperature distribution close to the boundary layer and along the core of the cavity. The maximum differences between the experimental and simulation data for *k*-ε realizable are 0.97% and 1.3% at Y = 0.52 m and X = 0.52 m, respectively.

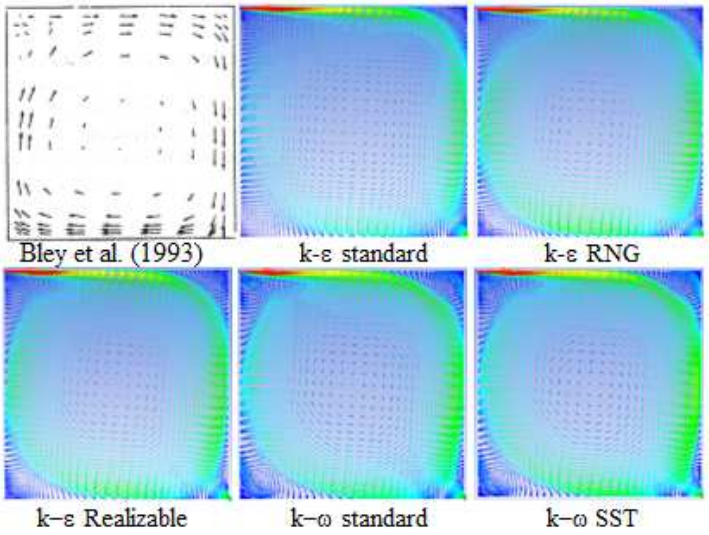

Figure 26: Comparison of airflow pattern for different turbulence models and experiment.

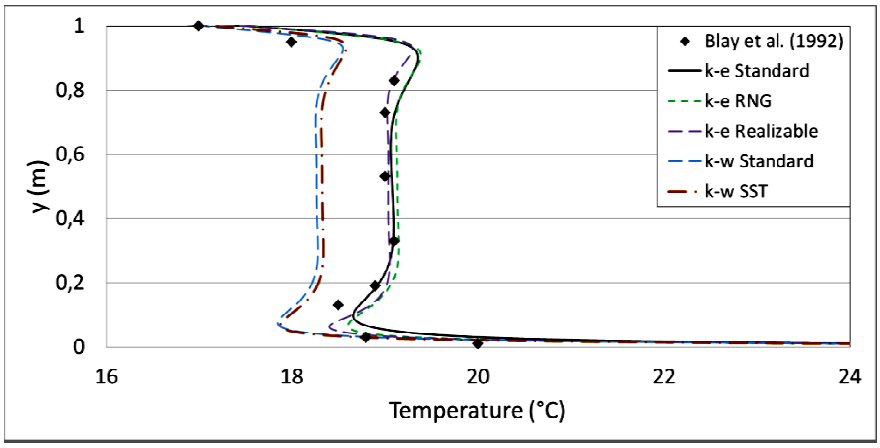

(a)

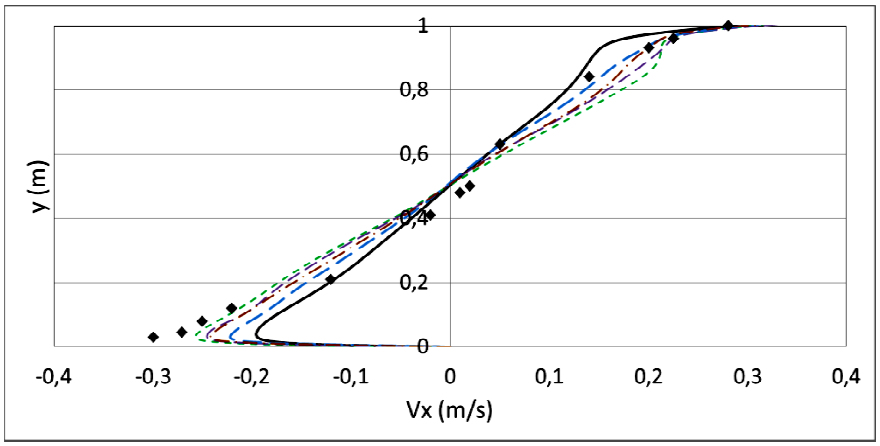

(b)

Figure 27: Performance of CFD model to predict temperature and air velocity at X = 0.52 m for MC case.

Velocity profiles at X = 0.52 m and Y = 0.52 m are shown in Figure 27b and Figure 28b. It is observed that all turbulence models predict the general pattern of the airflow but large discrepancies occur close to the walls. The standard versions of the *k*-ε and *k*-ω models predict better the air velocities in the regions far from the walls. Also, both turbulence models predicts well the air velocities close to the top wall at X = 0.52 and

close to the right wall at Y = 0.52 m. However, these models significantly underpredict the reverse flow close to the bottom wall at X = 0.52 m and the vertical velocity close to the left wall at Y = 0.52 where maximum differences are close to 0.1 m/s. In these zones where large velocity gradients occur, the *k*-ε RNG model performs better.

In this case, it can be observed similar results than that for NC and FC cases. However, performance of turbulence models to predict temperature across de air domain varies more significantly. It is notorious that *k*-ω models underpredict temperature not only close to walls but also across the cavity core.

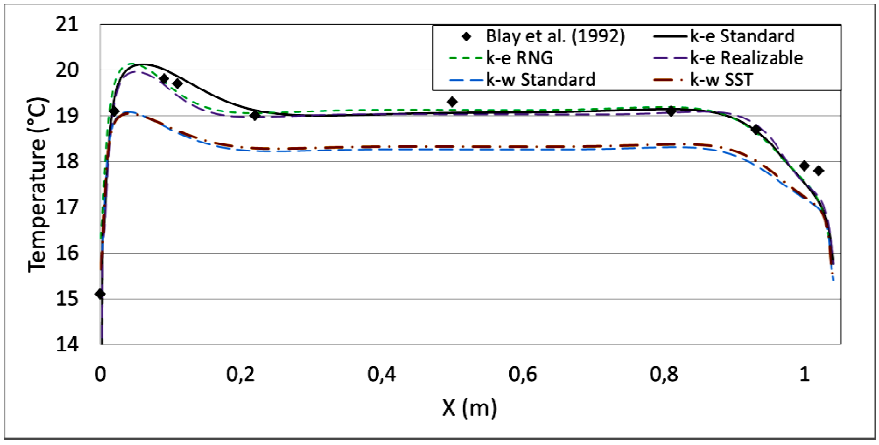

(a)

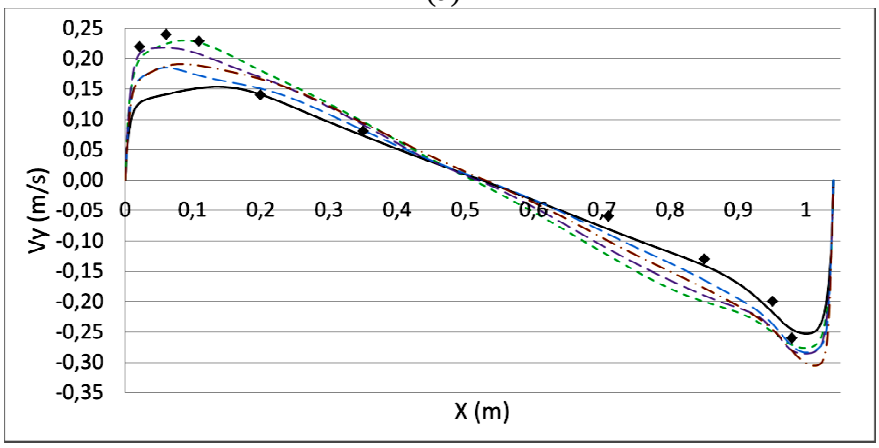

(b)

Figure 28: Performance of CFD model to predict temperature and air velocity at Y = 0.52 m for MC case.

3.5. Discussion and final remarks

CFD modeling is not an intuitive process and requires taking decisions about several parameters such as representative geometry, mesh size and topology, convergence criteria, under-relaxation factors, turbulence model, among others. The main source of errors in CFD modeling is the lack of users' expertise.

The main objective of this study was to provide more complete CFD modeling information of basic natural, forced and mixed convection flows that allows CFD beginners to acquire skills and confidence on CFD modeling. This paper provides a procedure, criteria and engineering judgment to evaluate five k-ε and k -ω turbulence models. Modeling these three basics flow of natural, forced and mixed convection in enclosed environments with different two-eddy viscosity models is proposed as exercise for new CFD users to obtain expertise on CFD modeling.

The results evidences that reliable and robust CFD results require users' skills on CFD modeling, even for the basics indoor airflows studied in this paper. The main general conclusions that can be drawn from this study are:

- Overall, the five evaluated *k-ε* and *k-ω* model performs well predicting air velocity and temperature. However, their accuracy depends on the convection type, quantity predicted and regions of the air domain. Therefore, the use of the right turbulence models is crucial to obtain reliable results. Literature review provides evidence about which turbulence models perform better for different cases. However, studies from different authors is not always in good agreement due to particularities of the case studied and other CFD modeling parameters that also influences the results (i.e. mesh size and topology).
- Predicted indoor conditions for temperature and air velocity in the boundary layer region might vary significantly among *k-ε* and *k-ω* models. Accurate predictions of what happen in this region are crucial because the heat and mass transfer between walls and air occurs in this zone. This could have great

influence on the predicted room air conditions (temperature, velocity, moisture content, pollutant concentration). This fact strongly support that new CFD users need to acquire skills on CFD modeling even for the basic convection flows reviewed in this paper.

- Convergence cannot be given for granted, especially for natural convection cases. The setting up of time step and under-relaxation factors is needed, which involves advanced knowledge and expertise of the CFD modeler even for basic indoor environmental problems.
- The basic convection cases studied in this paper are good exercises to get skills on CFD modeling of indoor environments. This paper provides information and engineering judgment that allow new CFD users to properly model these cases and obtain robust and reliable CFD models and results.

4. Evaluation of two eddy-viscosity turbulence models to predict indoor air conditions and interzonal air transport through a horizontal opening in a full-scale two-story test-hut for natural and mixed convection using CFD technique.

4.1. Abstract

Building design has the objective to achieve healthy, comfortable and productive indoor environments for the occupants in balance with energy efficiency. Interior building openings such as stairwells are important paths for exchange of heat, air, moisture, and pollutants. Interzonal airflow through horizontal openings has not been profoundly studied due its highly transient and unstable nature. Therefore, there is very limited available experimental data. Computational Fluid Dynamics (CFD) is an excellent tool to study this phenomenon. However, there are very few studies that have applied CFD to study the airflow in indoor environments with interzonal heat and mass exchanges through horizontal openings and evaluate the mass exchange through these openings. This paper evaluates the performance of five two eddy-viscosity turbulence models, *k*-*ε* standard, *k*-*ε* RNG, *k*-*ε* realizable, *k*-*ω* standard and *k*-*ω* SST, to predict indoor air conditions and upward mass airflows through a horizontal opening in a full-scale two-story test-hut. This study involves 6 cases with different temperatures gradients between the two floors and three ventilation strategies that represent natural and mixed convection. The main results show that temperatures are well predicted by all turbulence models while simulated air speeds present larger variations among turbulence model used. Overall, the k-ε standard model is the most accurate model to predict indoor temperatures and air speeds, and upward mass airflows through the opening for natural convection, whereas the k-ε realizable model is the most accurate model for mixed convection.

4.2. Introduction

Staircases of multi-storey houses and buildings are the main paths for interzonal air, moisture, heat and pollutants exchange between different floors. Heat and mass transport through stairwell openings could have significant effects on building energy consumption, indoor air quality, ventilation effectiveness, and fire and smoke spread in building fires. Despite the importance of heat and mass exchange through horizontal opening in buildings, there is very limited information for natural (Brown and Solvason, 1962; Epstein, 1988; Riffat and Kohal, 1994; Peppes et al., 2001; Blomqvist and Sandberg, 2004; Heiselberg and Li, 2009) and mixed convection (Vera et al., 2010a, 2010b; Tan and Jaluria, 2001; Klobut and Sirén, 1994; Cooper 1995). Most of these studies have been carried out in small-scale experiments and used saline water instead air. Full-scale experiments using air as fluid are expensive, time consuming and complex to be carried out. For this reason, there have been some attempts to study this phenomenon by means of Computational Fluid Dynamics (CFD).

Few authors have used CFD technique to study the airflow exchange through horizontal opening, and most of them have focused on buoyancy-driven flows. Riffat and Shao (1995) performed one of the first studies on natural convection flow through horizontal opening using a transient and two-dimensional CFD simulation. The CFD results revealed the highly transient flow patterns at the horizontal opening. The air exchange rate between the two zones was continuously oscillating and with intermittent pulses. The predicted air exchange rate between the two zones obtained via CFD showed a good agreement with experimental data of Riffat et al. (1994), thus a relative difference of 10.5% was found. This study does not indicate the turbulence model used to solve the Navier-Stokes equations.

Peppes et al. (2001) presented the measurements and the CFD modeling of buoyancy-driven flow through a stairwell connecting two individual floors in order to study the mass and heat transfer between the floors. Airflow rate was measured using the tracer gas technique. They noted that the airflow rate between the two floors was determined

by the size and geometry of the opening separating the floors and by the air temperature differences between the upper and lower rooms. With the experimental data, the authors proposed relations to obtain the mass and heat flow rate through the stairwell opening. The experimental cases were simulated using CFD technique. The k-ε RNG model was chosen because of it ability in predicting both high and low Reynolds number flows. The relative differences between the CFD and experimental results for airflow rates through the opening remained below 11.6% for all the experiments. In a subsequent study, Peppes et al., 2002, the authors extended the investigation to an experimental and numerical study of a three-story building. The same previous turbulence model was used and the CFD and experimental data showed a very good agreement too.

Li (2007) also studied natural convection flows through square horizontal openings via CFD. He modeled a three-dimensional test-room with an upper opening. Simulation were time dependent and two turbulence models were evaluated, the k-ε standard and Large Eddy Simulation (LES). The LES model was able to capture the bidirectional flow observed experimentally and agrees well with measurements. Otherwise, the k-ε standard turbulence model showed poor performance because the airflow rate through the opening was significantly underpredicted.

More recently, Vera et al., (2010a) carried out a unique experiment on interzonal air and moisture transport through horizontal opening in a full-scale two-story test-hut dominated by mixed convection. Indoor air conditions across the test-hut and mass flow rates through the opening under different scenarios were measured experimentally. Vera et al. (2010b) extended the experimental study by means of CFD simulations. CFD simulations were performed using indoor zero-equation turbulence model (Chen and Xu, 1998). The CFD results verified that two- way airflow exists even in cases with warmer upper room. The CFD model was extensively validated and CFD results agreed well with the experimental data for air speed, temperature, humidity ratio and interzonal mass airflows.

In the view of the foregoing, it is self-evident that there is a scarcity of studies on evaluating turbulence models to predict, first, indoor air conditions in rooms connected by an horizontal opening, and secondly, the heat and mass exchange through these openings. In contrast, there is extensive literature showing the evaluation of turbulence models to predict indoor air conditions in single cavities or rooms for different convection regimes. These studies cover a broad variety of turbulence models, from the simplest models such as zero-equation (Zhang et al, 2007) to more complex models such as Detached Eddy Simulation models (Zhang and Chen, 2007, Zhang et al, 2007). The two-eddy viscosity turbulence models such as k- ε and k-ω are the most widely models evaluated for single enclosed cavities i.e Posner et al, 2002; Choi et al, 2004; Zhang et al, 2007; Rundle and Lighstone, 2007, Susin et al, 2009; Cao et al, 2010; Rohdin and Moshfegh , 2011; Choi and Kim, 2012. Overall, k-ε and k-ω models evidence good performance to predict indoor airflow conditions, and the accuracy of these two-eddy viscosity models is significantly associated to the convection regime (natural, forced or mixed). In consequence, the objective of this paper is to evaluate five two-eddy viscosity turbulence models (k-ε standard, k-ε RNG, k-ε realizable, k-ω standard and k-ω SST) in terms of predicting: i) the indoor air conditions in a full-scale two-story test-hut with heat and mass exchange through an horizontal opening connecting two floors, and ii) the mass exchange rate across the horizontal opening.

The evaluation of the turbulence models is based on experimental results obtained by Vera et al. (2010a) in a full-scale two-story test-hut. The experimental results correspond to indoor air conditions such as temperature and air speed across the test-hut and upward mass flow rates through the horizontal opening. Simulated CFD results for each turbulence model are compared with experimental results at different locations for each case of natural and mixed convection.

4.3. Full-scale two-story test-hut description

A two-story full-scale test-hut representing a typical wood-framed house was built in a previous study (Vera et al., 2010a). It consists of two rooms with internal dimensions of 3.62 m x 2.44 m x 2.43 m each and a horizontal opening of 1.19 m x 0.91 m and 0.22 m thick. The opening connects the two rooms and allows heat and mass airflow exchange. Figure 29a shows an schematic isometric view of the test-hut. A baseboard heater was located at the bottom part of the north wall in each room to provide the desired indoor temperature varying the mean heating power. A moisture source, named as heat source in Figure 29a, is placed in the lower room producing moisture at a constant rate. The average temperature differences between the lower and upper room, ΔT, ranged from 0.2°C to 2.8°C, thus the upper room was colder than the lower room for all cases.

Three ventilation strategies were studied as shown in Figure 30. These ventilation strategies correspond to natural convection (NC, scenario I) and mixed convection (MC, scenarios II and IV). Air speed across the full-scale two-story test-hut were measured by 19 omnidirectional anemometers (hot-sphere type, model HT- 412 probes and HT-428 transducers from Sensor Electronic and Measurement Equipment, Poland), while the indoor temperature was monitored by 64 sensors (Vaisala Humitter 50Y and HMP50). All sensors are distributed along the test- hut at different heights forming lines from the floor of the lower room to the ceiling of the upper room. Figure 29b shows the location of these sensors in the lower room. More details about test setup and measuring process can be found in Vera (2009).

Table 6 summarizes the experimental conditions of cases of Vera, 2009 that are numerically studied in this paper.

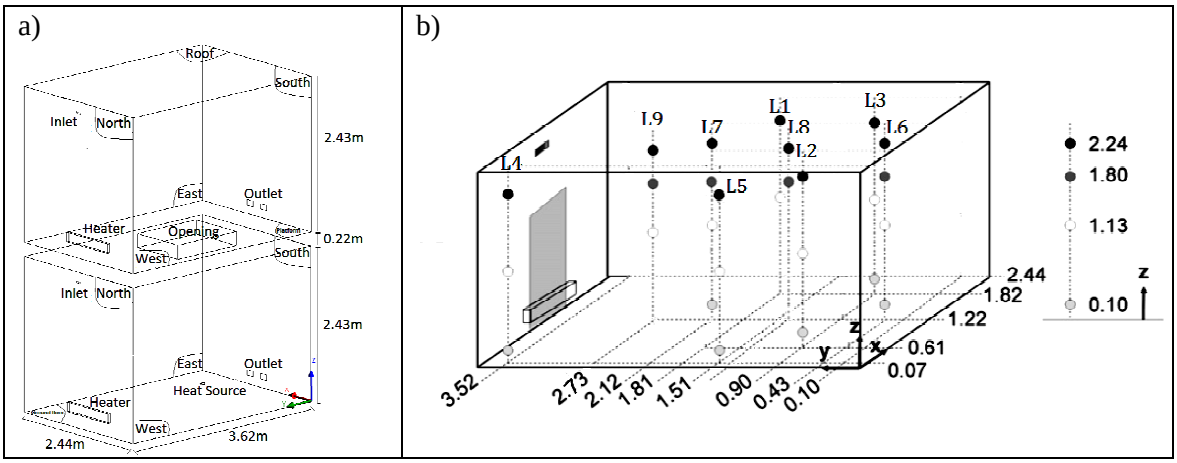

Figure 29: a) Two-story test-hut CFD geometry model, (b) Plan view of lines distribution of experimental data

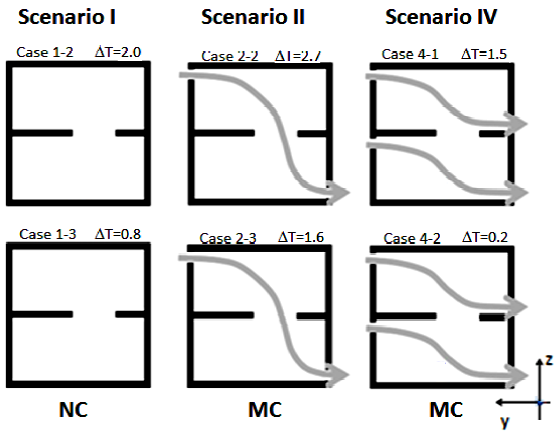

Figure 30: Scenarios tested: no ventilation (scenario I), single ventilation with downward net flow through the opening (scenario II), and independent ventilation in each room (scenario IV).

4.4. CFD model

A CFD model of the full-scale two-story test-hut was developed to simulate the indoor environment using commercial CFD software, Ansys Fluent v.14.0 (Ansys 14, 2012). The airflow pattern and temperature distribution are governed by the conservation laws of mass, momentum and energy. Five two eddy-viscosity turbulence models were

evaluated in this study. These models were *k-ε* standard (Launder and Spalding., 1974), *k-ε* RNG (Yakhot and Orszag, 1986), *k-ε* realizable (Shih et al., 1995), *k-ω* standard (Wilcox, 1988) and *k-ω* SST (Menter, 1994). The *k-ε* models are the most popular models for indoor airflow simulations due their robust performance, whereas the *k-ω* models present a newer formulation for the near wall treatment which might make them more accurate and robust for indoor environment conditions. These models were chosen due their accuracy in the assessment of indoor environment conditions and because they have been widely validated for indoor airflow in single-zone enclosed cavities (Zhang and Chen, 2007; Rundle and Lighstone, 2007; Zitzmann and Cook, 2005 ; Choi et al., 2004; Susin et al., 2009 ; Zhang Z. et al., 2007; Posner, et al., (2002); Voigt, 2000; Rohdin and Moshfegh, 2011; Stamou and Katsiris, 2006; Moureh, 2003).

Table 6: Cases and experimental conditions (Vera, 2009)

Parameters	Case 1-2	Case 1-3	Case 2-2	Case 2-3	Case 4-1	Case 4-2
ΔT	3.9	3.0	3.7	2.9	2.9	0.3
Supply air condition:						
Inlet airflow rate 1 (m/s)	-	-	3.65	3.59	1.96	1.96
Inlet Temperature 1 (°C)	-	-	17.97	18.04	17.81	18.20
Inlet airflow rate 2 (m/s)	-	-	-	-	1.76	1.72
Inlet Temperature 2 (°C)	-	-	-	-	18.01	17.90
Baseboard heater 1 (w/m2)	554.08	698.63	660.80	607.08	421.58	344.50
Baseboard heater 2 (w/m2)	-	409.54	-	244.43	216.81	660.80
Heat source (w/m2)	6508.42	6508.42	6508.42	6508.42	6508.42	6508.42
Wall surface temperatures lower room (°C)						
North wall	19.9	22.6	20.5	20.3	20.1	19.2
East wall	18.9	21.2	18.8	18.8	18.8	18.4
South wall	18.3	20.7	18.4	18.6	18.3	17.6
West wall	18.6	21	18.7	18.7	18.6	18.4
Ground floor	18	19.1	18.1	18.2	17.91	18.6
Ceiling	20.9	23.6	21.2	21	20.78	19.6
Wall surface temperatures upper room (°C)						
North wall	17.6	20.1	16.6	16.5	17.8	20
East wall	16.9	19.4	16.2	17.2	17.2	18.8
South wall	16.6	18.7	15.6	16.5	16.4	18.3
West wall	16.9	19.4	16.2	17.2	17.2	18.7
Floor	18.69	19.8	16.9	17.8	17.63	17.9
Ceiling	17.6	20.4	16.8	18	17.94	20.8

4.4.1. Geometry

The full-scale two-story test-hut was modeled in CFD. Walls were considered as zero-thickness and adiabatic. The experimental surface temperatures at different locations for each case were set as boundary conditions. The heat source was considered as a small cylinder of sensible heat of 85 W. The ventilation inlets and outlets were rectangular sections of 96.5mm wide by 21.8 mm high and 135 mm wide by 85 mm high, respectively. The baseboard heaters were modeled as rectangular objects of 0.045 m x 0.15 m x 0.920 m.

4.4.2. Numerical solution method

In order to predict the main conditions of the indoor airflow across the test-hut, temperatures and air speeds, and the interzonal mass airflow rate through the horizontal openings, steady-state and 3-dimensional simulations were performed in Ansys Fluent v.14.(Ansys 14, 2012) . A second order upwind differencing scheme was chosen to achieve higher accuracy of the solutions. Boussinesq approximation was considered, thus density is taken into account as a constant value in all solved equations, except for the buoyancy term. The convergence criteria were 10^{-6} for energy and 10^{-3} for the other variables. In order to obtain convergence, the under-relaxation factors were set between 0.15 and 0.5 for momentum; between 0.5 and 0.85 for pressure; 1.0 for density, body forces, turbulent viscosity and energy; and 0.8 for turbulent kinetic energy and turbulent dissipation rate. The SIMPLE (semi implicit-method for pressure linked equation) was chosen as a default pressure- velocity coupling algorithm.

4.4.3. Grid verification

An hexahedral unstructured mesh (Figure 31a) was built with finer cells near to the walls, inlet, outlets, baseboard heater and heater source to ensure a proper transfer of boundary conditions to the air domain. Grid verification is needed to evaluate that CFD results are mesh independent. It is usual to carry out the mesh verification comparing the

CFD results among the tested meshes with the experimental results. In this study three different meshes were tested, Δ1 , Δ2 and Δ3 as shown in Table 7. Δ1 is the finest mesh while Δ3 is the coarsest mesh. Figure 31b shows, as example, the simulated and the experimental results of air temperature for these three meshes at lines 1, 8 and 9 of case 2-3. It can be seen that the results of the coarsest (Δ3) and medium (Δ2) meshes are very close and in excellent agreement with experimental data, while the results of the finest mesh (Δ1) are not as good as the results for the other meshes.

Table 7: Grid elements and refinement ratio for three different mesh sizes

Δ1	Δ2	Δ3	r32	r21
1,065,895	493,575	153,769	1.48	1.29

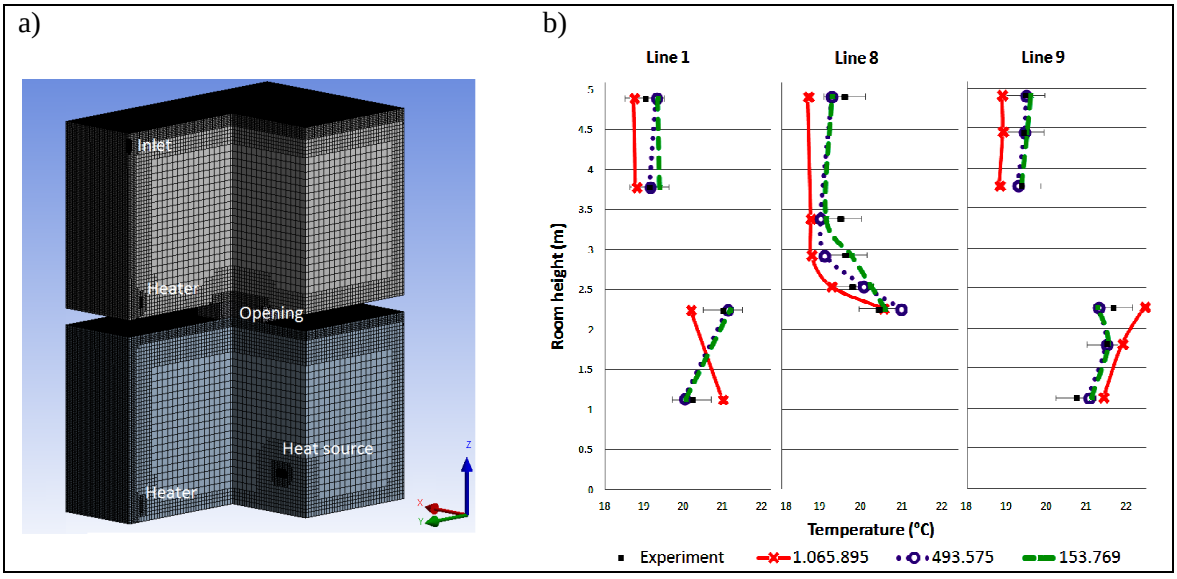

Figure 31: a) Computational mesh grid used. b) Predicted vertical temperatures at various points along vertical lines at different locations of the test-hut for three mesh densities for case 2-3.

Previous qualitative analysis does not allow concluding which mesh is a good balance between accuracy and computing time. Therefore, a quantitative analysis to verify grid independency is performed based on the quantification of the uncertainty of the grid

convergence by means of the estimation of the grid convergence index, CGI (Roache, 1994; Hajdukiewic et al., 2013). This index can be seen as the error estimator associated with the grid resolution and indicates how much the solution would change with a further refinement of the grid. The GCI is defined as

$$\mathrm{GCI}^{\mathrm{fine}} = \mathrm{Fs}\frac{\varepsilon}{\mathrm{r}^{\mathrm{p}}-1} \tag{23}$$

$$\mathrm{p} = \frac{\ln\left|\frac{\mathrm{f_{coarse}}-\mathrm{f_{medium}}}{\mathrm{f_{medium}}-\mathrm{f_{fine}}}\right|}{\ln \mathrm{r}} \tag{24}$$

$$\varepsilon = \frac{\mathrm{f_{coarse}}-\mathrm{f_{fine}}}{\mathrm{f_{fine}}} \tag{25}$$

$$\mathrm{r} = \left(\frac{\Delta\mathrm{fine}}{\Delta\mathrm{coarse}}\right)^{1/3} \tag{26}$$

where Fs is the safety factor equal to 1.25 when comparing three grids (Roache, 1994); p is the order of convergence that has been calculated as the average p value over the sensor at the nine lines presented in Figure 29b thus it is equal to 5.1; ε is the relative error between the coarse ($\mathrm{f_{coarse}}$) and fine ($\mathrm{f_{fine}}$) grid solutions; r is the refinement ratio between the number of grid elements of the fine mesh and the coarse mesh for a 3D mesh. GCI_{21} in this study, corresponds to the grid convergence error due to the refinement from mesh $\Delta 2$ (medium size) to mesh $\Delta 1$ (the finest mesh). Similarly, it is defined $\mathrm{GCI}_{32}^{\mathrm{coarse}}$ as the grid convergence error due to passing from the coarsest mesh $\Delta 3$ to the medium mesh $\Delta 2$.

The GCI indexes for case 2-3 are shown in Table 8 for air temperature data at several locations of lines 1, 8 and 9 as examples of the all GCI index. The GCIs obtained when refining from mesh $\Delta 2$ to $\Delta 1$ are close to the accuracy of temperature measurements (2%) while GCIs for refining mesh $\Delta 3$ to $\Delta 2$ are much smaller for all measurement points. This means that all meshes are accurate enough and can be used for further analysis nevertheless mesh $\Delta 1$ with 1,065,895 elements would have a higher computational cost than meshes $\Delta 3$ and $\Delta 2$ without achieving more accurate results. The

convergence error is much smaller when the mesh is refined from the coarsest to the medium mesh. This suggests that mesh Δ2 with 493,575 elements represents a good balance between accuracy and computing time.

Table 8: Grid convergence index for indoor temperatures for three mesh sizes.

z (m)	Experiment (°C)	Δ1	Δ2	Δ3	e32	e21	GCI 32 (%)	GCI 21 (%)
Line 1								
1.13	20.20	20.98	20.00	20.06	0.003	-0.047	0.056	-2.159
2.245	20.99	20.17	21.10	21.19	0.004	0.046	0.088	2.137
3.78	19.11	18.77	19.12	19.39	0.014	0.019	0.276	0.879
4.895	19.00	18.72	19.28	19.34	0.003	0.030	0.057	1.388
Line 8								
2.26	20.44	20.54	20.98	20.58	-0.019	0.022	-0.377	1.001
2.54	19.80	19.27	20.08	20.24	0.008	0.042	0.162	1.930
2.929	19.63	18.79	19.12	19.76	0.034	0.017	0.675	0.800
3.387	19.50	18.78	19.01	19.15	0.007	0.012	0.149	0.569
4.91	19.59	18.71	19.29	19.29	0.000	0.031	0.007	1.428
Line 9								
1.13	20.73	20.88	21.04	21.13	0.004	0.008	0.082	0.351
1.8	21.50	21.90	21.50	21.55	0.002	-0.018	0.048	-0.853
2.26	21.66	21.46	22.29	22.28	-0.001	0.039	-0.011	1.788
3.78	19.35	18.81	19.25	19.35	0.005	0.024	0.105	1.094
4.45	19.42	18.90	19.42	19.50	0.004	0.028	0.077	1.295
4.91	19.45	18.88	19.47	19.59	0.006	0.031	0.122	1.452

4.4.4. General CFD results

The CFD model of the full-scale two-story test-hut predicts two main parameters of the airflow, temperature and air speed distributions. Figure 32 shows the location of two vertical planes used to show CFD model results.

Figure 33, Figure 34 and Figure 35 show, as example, these CFD results for cases 1-2 dominated by natural convection and case 2-3 and 4-1 dominated by mixed convection. These figures reveals that bidirectional airflow exchange occurs through the horizontal opening and significant differences of the airflow conditions and pattern are observed between the cases.

Figure 33 shows the velocity and temperature contours for case 1-2. This case represents a natural convection scenario due the “no ventilation” strategy used. The length of the vectors indicates the high air velocity in both upper and lower room and through the opening. The air velocity in case 1-2 is much higher than case 2-3 (Figure 34) and cases 4-1(Figure 35) which represent mixed convection scenarios. The flow pattern is dominated by vortices in all studied cases. In case 1-2 the major vortex is identified in the upper room in the left side of the upward flow while a smaller vortex is formed in the right side. At the lower room, another vortex can be identified at the left side of the downward airflow. The air exchange between the zones takes place at the horizontal opening, where the upward and downward flow seems to take place in the same part of the opening but in opposite directions. The warmer air from the lower room comes from the baseboard heater and flows along the ceiling, and then it flows upward through the right half of the opening into the upper room causing the temperature rise. The downwards cold air takes place at the same right half of the opening. Also, it is possible to see a stratified fluid inside the room, with the main flow of warm air coming from the baseboard heater and heat source flowing upward through the opening and the temperature increases from bottom to the top level of the test-hut.

Case 2-3 shown in Figure 34 represents a scenario of mixed convection produced by single ventilation with downward net flow through the opening. The airflow pattern presents a vortex in the upper room in the right side of the upward flow. The length of the velocity vector indicates that the air speed is higher in the upper room than in the lower room. There, the air velocity is close to zero except in the upward flows produced by the baseboard heater and heat source and the downward flow coming from the opening. In the upper room, the main air velocity is produced by the jet flow entering through the inlet at the top of the south wall. This jet flow moves along the ceiling and then moves downward over the right wall to finally flow downward through the center of the opening into the lower room. The warm airflow, coming from the baseboard heater and heat source at the lower room, moves upward until the ceiling and flows upward through the left half of the opening into the upper room causing the temperature

there to rise. Comparing to case 1-2, Figure 33 shows that the air velocity for mixed convection is in general much lower than natural convection. Also, for mixed convection is easier to see that the upward and downward flows occur in different parts of the opening.

Figure 35 shows the case 4-1 which represents a scenario of mixed convection produced by independent ventilation in each room. As in case 2-3, the airflow pattern presents a vortex in the upper room in the right side of the upward flow. The overall indoor air behavior in this case is similar to case 2-3 in which velocity vector indicates that the air speed is higher in the upper room than in the lower room. However, in case 4-1 the general air speed is higher than in case 2-3, that can be due the independent ventilation in each room that contributes with the air movement. Despite a downward flow through the opening is observed, the upward warm flow coming from lower room into the upper room seems to be greater and with a major velocity. The jet flow entering through the inlet in the lower room contributes to create a vortex which may hinder the upward airflow coming from the baseboard heater. The airflow from the heat source moves upward until the ceiling and then flows upward through opening into the upper room next to the downward flow.

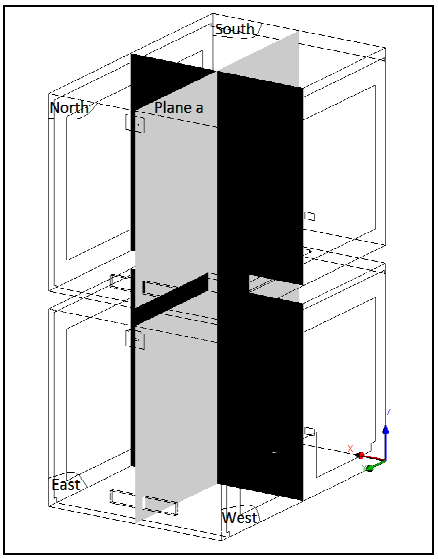

Figure 32: Location of vertical planes. Plane a) x=1.22m and plane b) y=1.81m

Case 1-2

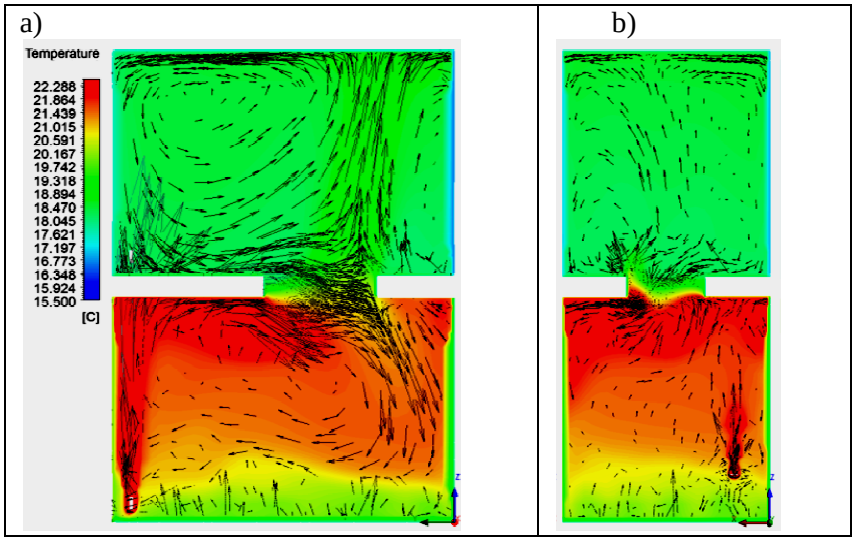

Figure 33: Visualization of warm convective currents when the lower room is warmer for no ventilation strategy: a) longitudinal cross section at x= 1.22m, b) longitudinal cross section at y=1.81 m

Case 2-3

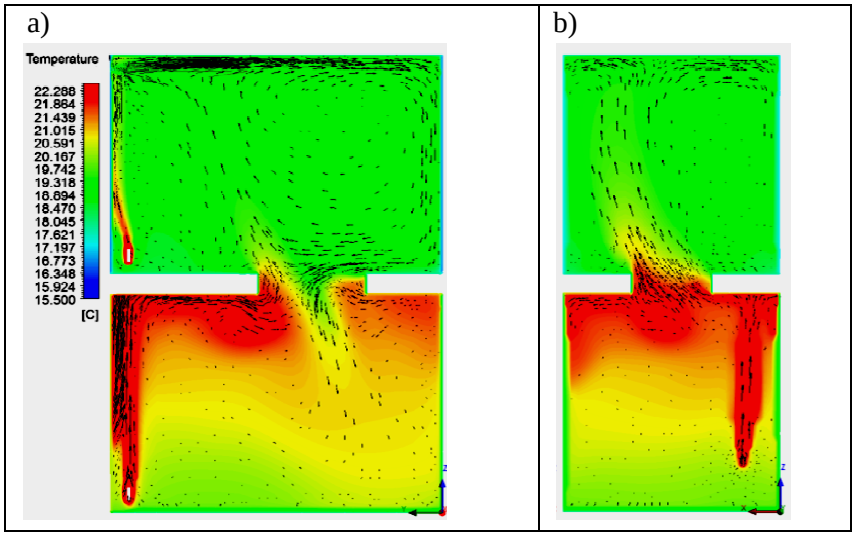

Figure 34: Visualization of warm convective currents when the lower room is warmer for single ventilation with downward net flow through the opening: a) longitudinal cross section at x= 1.22m, b) longitudinal cross section at y=1.81 m, c) temperature volume rendering of two-story test- hut .

Case 4-1

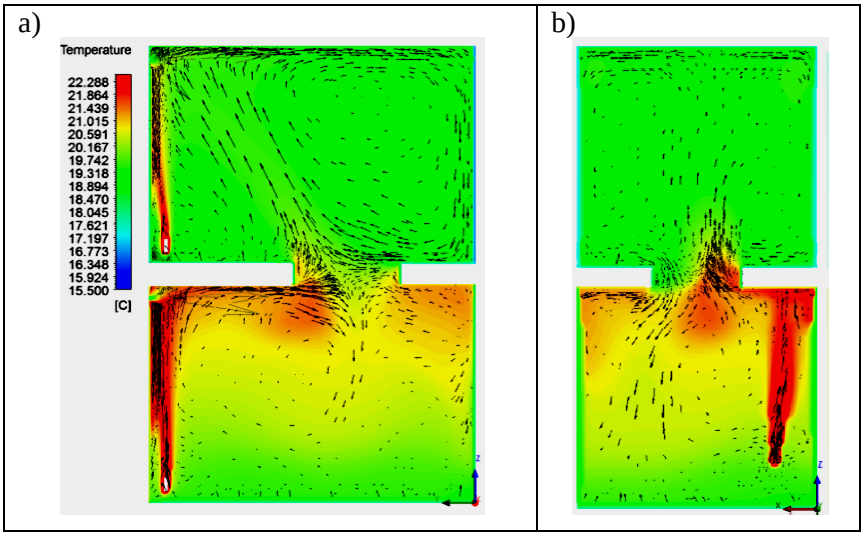

Figure 35: Visualization of warm convective currents for a warmer lower room and independent ventilation in each room: a) longitudinal cross section at x= 1.22m, b) longitudinal cross section at y=1.81 m.

Despite that CFD is a technique well validated to predict indoor air conditions in buildings, there is no extensive validation of turbulence models to predict these conditions and mass exchange in enclosed environments with horizontal opening between floors. The next section presents the evaluation of five k-ε and k-ω turbulence models to predict these quantities under this scenario.

4.5. Evaluation of turbulence models

4.5.1. Evaluation of turbulence models to predict indoor temperature and air speed distribution.

In this section five two-eddy viscosity turbulence models are evaluated in terms of their capability to predict indoor air conditions (temperature and air speed) under the scenario of heat and mass exchange through an horizontal opening that connects two flows. The

evaluated turbulence models are *k-ε* standard, *k-ε* RNG, *k-ε* realizable, *k-ω* standard and *k-ω* SST. These models have been evaluated extensively to predict indoor air quantities in single rooms and cavities (Zhang and Chen, 2007; Rundle and Lighstone, 2007; Zitzmann and Cook, 2005; Choi et al., 2004; Susin et al., 2009; Zhang Z. et al., 2007; Posner, et al., (2002) ; Voigt, 2000; Rohdin and Moshfegh, 2011 ; Stamou and Katsiris, 2006 ; Moureh J. F., 2003).

The evaluation of turbulence models consists on comparing the simulated results with experimental data across the full-scale two-story test-hut shown in Figure 31b.

This paper performs the evaluation of the turbulence models for six different cases with warmer lower room under three ventilation strategies, which corresponds to two cases of natural convection and four cases of combined buoyancy and forced driven flows. Table 6 summarizes the main boundary conditions measured and reported by (Vera, 2009). A CFD model for each case was built and indoor temperature and air speed was obtained for each evaluated turbulence models.

The evaluation of the five two-eddy viscosity models is carried out, first, qualitatively comparing the experimental and CFD simulation results of temperature and air speed at different poles. The qualitative analysis allows resolving if the enclosed environment can be predicted by the turbulence models. Secondly, a quantitative evaluation is performed based on the normalized root-mean-square error (RMSE). The following sections present these results and evaluations. Due to length limitations of the paper, results for only three cases are shown (1-2, 2-3 and 4-1).

4.5.1.1. Qualitative comparison between predicted and measured data.

Figure 37c, line 9 represent the supply jet flow into the room at the top of upper room for case 2-3 and at the top of upper and lower room for case 4-1. For case 2-3 CFD turbulence models predicts accurately air speed in this line, except for *k-ω* standard model which presents an overall different behavior in the upper room. At the top of the

upper room only *k*-ε realizable model predicts accurately air speed while other models have a difference of ~0.2 m/s. For case 4-1, all turbulence models predict accurately air speed in line 9 with difference lesser than 0.1 m/s, except for *k*-ε RNG model which present an overall different behavior. This shows that the inlet was properly modeled by most models.

For all cases, line 9 and line 4 represent the effect of baseboard heater in temperature distribution while line 5 represents the heat source effect in temperature distribution. All the turbulence models can predict temperature profiles close to measured data with a highest difference found of 1°C considering all studied cases. Pronounced temperature stratification of 2°C-3°C exist in the lower room with the lowest temperatures found close to the floor and highest temperatures at the top. Temperature is more uniform in the upper room. This indicates that baseboard heater and heat source effects were properly modeled.

Line 8 represents the air conditions through the opening. Figure 36 shows that temperature distribution was well predicted by all turbulence models with difference between predicted and experimental data lower than 1°C, excepting for Case 1-2 (Figure 36a) in which the predicted temperature profile is around 2°C underpredicted. Line 8 in Figure 37 shows the velocity distribution at the opening which presents more discrepancies between predicted and measured data than temperature profiles. Although predicted data from all turbulence models are not totally far of measured values, each data point is better predicted by a different turbulence model and it is not easy to determinate which model has the best overall behavior.

For all cases, the results graphed showed an accurate prediction of the indoor environment. A wide range of computational parameters, model inputs, experimental accuracy etc. might have influenced the discrepancy in CFD predictions. For this reason, a comparison of the overall prediction of temperature distribution and air velocity distribution per model based on the error difference was performed in order to

determinate which model is the best in predict indoor environment for natural convection and mixed convection.

4.5.1.2. Quantitative comparison between predicted and measured data.

Although predicted data from all turbulence models are in good agreement with experimental values, each data point is better predicted by a different turbulence model, which make difficult to establish which turbulence model has the best overall performance. In consequence, a quantitative analysis is required.

Table 9 and Table 10 show the percentage of error of the data predicted by each turbulence model based on the experimental data. The error is calculated for each available sensor distributed into the test-hut as shows Figure 31b. These tables show only data for case 2-3 as example. In this case, the maximum error in temperature prediction considering all predicted values is 9.2% (1.88°C) in line 8 for *k*-*ε* realizable model. For air velocity the maximum error was exceptionally 300% (0.14 m/s) in line 9 for *k*-*ε* RNG model at one point. This large error can be attributed to the small magnitude of velocity that ranges between 0.05 and 0.15 m/s. Thus, small variation of 0.1 m/s results in a large error.

The previous analysis is not enough to determinate the ability of the turbulence model in predict the indoor environment. Since one model may have better prediction at one location but worse in another, it is necessary to apply an extra technique to compare the overall prediction performance quantitatively. The normalized root-mean-square error (RMSE) index is applied based on the procedure describing by Wanga and Zhai, 2012. RMSE is used to evaluate how far the prediction deviates from the experimental data, considering first the uncertainty in the experiment, and then normalizing the deviation by the absolute value of measurement data. The RMSE is defined as

$$\mathrm{RMSE}(\mathrm{P},\mathrm{M}) = \sqrt{\frac{\sum_{i=1}^{n} \delta_{pm}(|P(i)-M(i)|-e(i))^2}{\sum_{i=1}^{n} M(i)^2}} \qquad (27)$$

$$\delta_{pm} = \begin{cases} 1 | \mathrm{P(i)} - \mathrm{M(i)} > e(i) \\ 0 | \mathrm{P(i)} - \mathrm{M(i)} < e(i) \end{cases} \quad (28)$$

Where P(i) and M(i) are the prediction and the measurement datasets at certain locations, respectively, and e(i) is the uncertainty of the test instrument in the experiment. The RMSE was calculated for all available data location. Thus the index was calculated with 56 data point for temperature distribution and 12 data point of air speed distribution shown in Figure 31b. Then the RMSE of the cases for each convection type was averaged to obtain a unique value of RMSE for each turbulence model and convection type. Table 11 and Table 12 show the RMSE indexes for temperature and air speed for natural convection (cases 1-2 and 1-3) and mixed convection (cases 2-2, 2-3, 4-1 and 4-2), respectively.

The results show that the *k*-ε standard model has the lowest deviations from experimental data to predict air temperature and speed in the cases of natural convection (cases 1-2 and 1-3), which represents the best overall performance among turbulence models. The average RMSE indexes are 0.019 for temperature and 0.134 for air speed. For mixed convection (cases 2-2; 2-3; 4-1 and 4-2), the *k*-ε realizable model reveals the lowest RMSE indexes of 0.014 and 0.429 for temperature and air speed, respectively. Despite that a specific turbulence model show better performance for each characteristic convection flow, all turbulence models present a similar RMSE for temperature in natural and mixed convection cases.

Therefore, the five evaluated two-eddy viscosity models perform well and can be used in further studies and analysis. Otherwise, larger values of RMSE and variations among turbulence models evidence that air speed is not predicted by all turbulence models with the same accuracy, so that it is necessary to know the most accurate model for further analysis.

a) Case 1-2

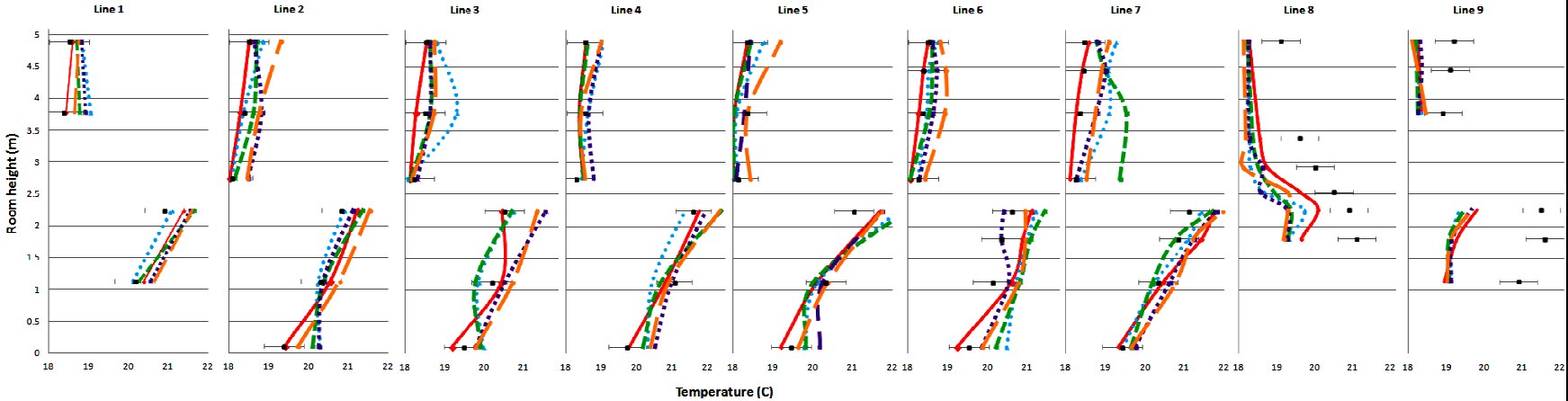

b) Case 2-3

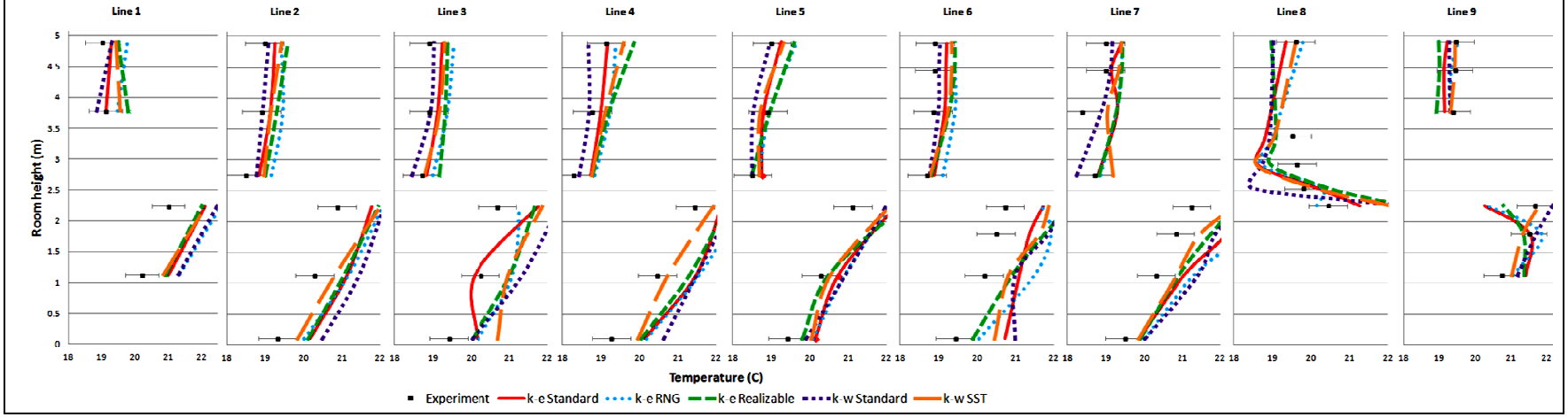

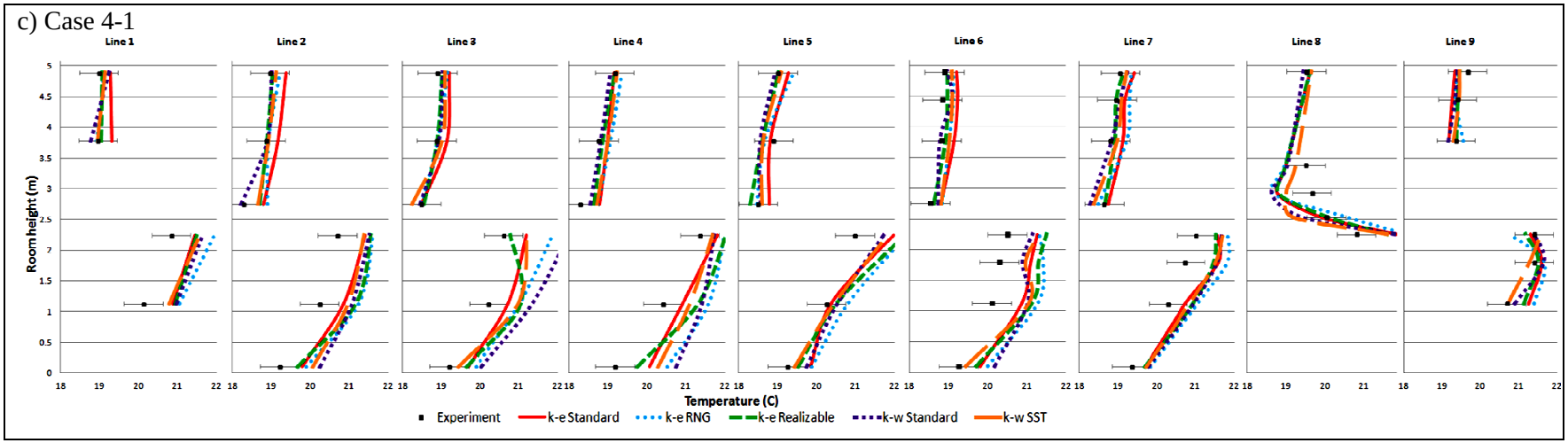

Figure 36: Comparison between the simulated and measured temperatures for a) case 1-2, b) case 2-3, c) case 4-1

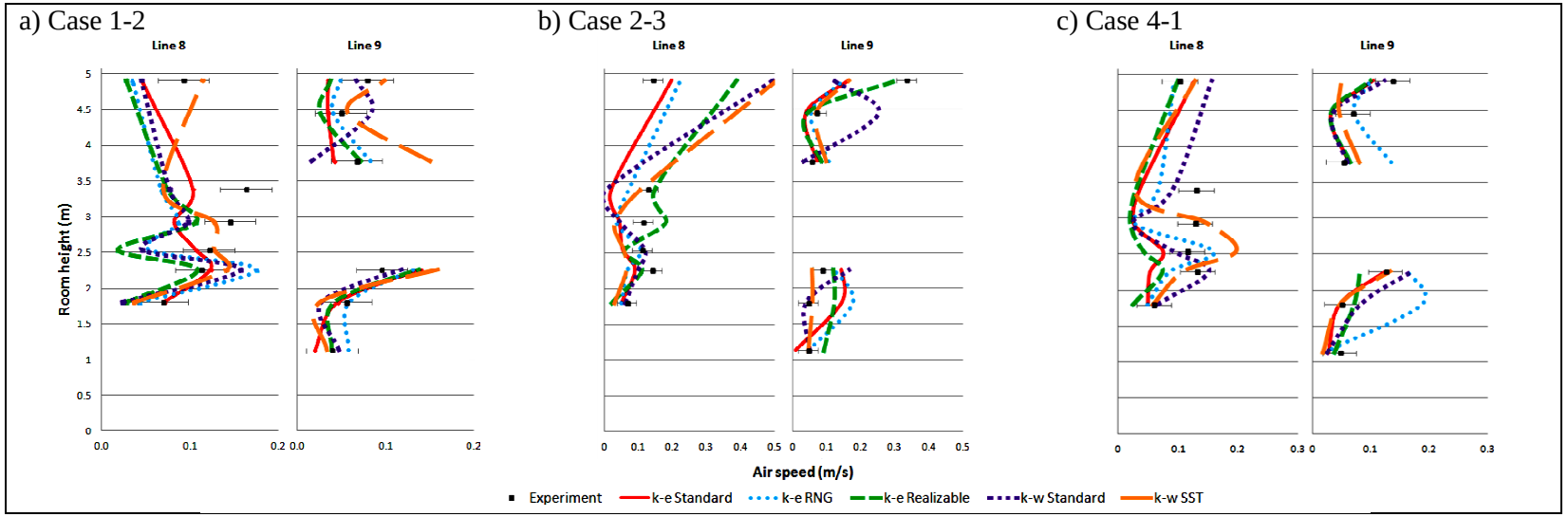

Figure 37: Comparison between the simulated and measured air speeds for a) case 1-2, b) case 2-3, c) case 4-1

Table 9: Percentage error measured and simulated indoor data for temperature distribution in case 2-3

	Temperature											
	Location z (m)	Measured	k-ε Standard	% error	k- ε RNG	% error	k- ε Realizable	% error	k-ω Standard	% error	k- ω SST	% error
Line 1	1.13	20.20	21.00	3.99	21.33	5.62	20.93	3.61	21.29	5.44	20.85	3.23
	2.25	20.99	22.10	5.31	22.58	7.60	22.01	4.88	22.46	7.02	22.13	0.05
	3.78	19.11	19.12	0.08	19.46	1.85	19.78	3.52	18.84	1.41	19.55	0.02
	4.90	19.00	19.28	1.48	19.76	3.99	19.48	2.53	19.29	1.54	19.42	0.02
Line 2	0.10	19.32	20.16	4.35	20.01	3.58	20.11	4.12	20.48	6.02	19.83	0.03
	1.13	20.28	21.12	4.13	21.17	4.36	21.05	3.77	21.43	5.68	20.81	0.03
	2.25	20.86	21.76	4.31	22.05	5.69	21.94	5.16	22.08	5.83	21.99	0.05
	2.75	18.49	18.83	1.84	19.16	3.63	18.99	2.75	18.76	1.50	18.96	0.03
	3.78	18.90	19.12	1.16	19.45	2.96	19.29	2.08	18.92	0.11	19.13	0.01
	4.90	18.97	19.24	1.40	19.41	2.32	19.58	3.22	19.07	0.54	19.42	0.02
Line 3	0.10	19.41	20.16	3.84	20.20	4.06	20.04	3.27	20.04	3.25	20.70	0.07
	1.13	20.24	20.09	0.74	21.10	4.21	21.02	3.85	21.35	5.46	20.97	0.04
	2.25	20.69	21.76	5.19	21.28	2.83	21.68	4.80	22.29	7.73	21.87	0.06
	2.75	18.71	18.83	0.63	18.99	1.54	19.17	2.49	18.45	1.35	18.77	0.00
	3.78	18.88	19.12	1.22	19.37	2.59	19.32	2.31	18.94	0.27	19.16	0.01
	4.90	18.89	19.24	1.81	19.55	3.45	19.39	2.62	19.03	0.70	19.29	0.02
Line 4	0.10	19.28	20.13	4.44	20.18	4.69	20.05	4.01	20.65	7.09	19.96	0.04
	1.13	20.47	21.47	4.89	21.55	5.23	21.30	4.04	21.50	5.01	20.74	0.01
	2.25	21.45	22.13	3.14	22.69	5.78	22.27	3.80	22.42	4.51	21.93	0.02
	2.75	18.30	18.73	2.35	18.83	2.92	18.79	2.67	18.44	0.76	18.76	0.03
	3.78	18.77	18.99	1.16	19.23	2.46	19.21	2.35	18.70	0.40	19.11	0.02
	4.90	19.13	19.16	0.18	19.38	1.31	19.86	3.84	18.68	2.37	19.59	0.02
Line 5	0.10	19.43	20.14	3.67	20.10	3.46	19.81	1.94	19.91	2.47	20.05	0.03
	1.13	20.30	20.74	2.19	20.92	3.06	20.49	0.94	20.93	3.12	20.54	0.01
	2.25	21.12	22.24	5.29	22.09	4.59	22.41	6.08	21.99	4.11	22.09	0.05
	2.75	18.51	18.74	1.25	18.69	0.95	18.49	0.13	18.49	0.10	18.69	0.01
	3.78	18.90	18.79	0.60	18.96	0.30	18.96	0.30	18.52	2.02	18.71	0.01
	4.90	19.01	19.24	1.20	19.66	3.39	19.59	3.04	18.96	0.28	19.32	0.02

Table 9: Percentage error of measured and simulated indoor data for temperature distribution in case 2-3 (continuity)

Line 6	0.10	19.43	20.73	6.71	20.06	3.25	19.89	2.40	20.99	8.07	20.46	0.05
	1.13	20.18	21.10	4.57	21.49	6.50	20.91	3.63	20.99	4.01	20.82	0.03
	1.80	20.49	21.37	4.26	21.93	7.00	21.76	6.16	21.86	6.66	21.62	0.06
	2.25	20.73	21.72	4.77	21.69	4.61	22.41	8.11	22.17	6.95	21.86	0.05
	2.75	18.69	18.89	1.08	19.12	2.30	18.82	0.70	18.77	0.42	18.79	0.01
	3.78	18.84	19.16	1.65	19.44	3.14	19.27	2.27	19.00	0.83	19.25	0.02
	4.45	18.90	19.19	1.55	19.44	2.86	19.41	2.73	19.02	0.63	19.35	0.02
	4.90	18.90	19.21	1.65	19.42	2.72	19.43	2.79	19.04	0.75	19.35	0.02
Line 7	0.10	19.49	19.86	1.89	20.01	2.67	19.89	2.07	20.02	2.74	19.85	0.02
	1.13	20.31	21.05	3.66	21.32	4.97	20.91	2.98	21.42	5.49	20.85	0.03
	1.80	20.82	22.17	6.47	22.61	8.58	21.76	4.50	21.87	5.06	21.48	0.03
	2.25	21.24	22.43	5.61	22.71	6.91	22.41	5.51	22.60	6.41	22.41	0.06
	2.75	18.71	18.79	0.45	18.87	0.86	18.82	0.61	18.25	2.46	19.19	0.03
	3.78	18.36	19.29	5.07	19.27	4.97	19.27	4.96	18.88	2.84	19.04	0.04
	4.45	18.99	19.14	0.79	19.40	2.17	19.41	2.23	19.12	0.71	19.34	0.02
	4.90	18.98	19.40	2.21	19.44	2.40	19.43	2.34	19.17	0.97	19.41	0.02
Line 8	2.26	20.44	21.27	4.06	20.16	1.37	22.32	9.22	22.29	9.06	22.03	0.08
	2.54	19.80	20.19	1.96	20.29	2.49	20.46	3.31	18.48	6.67	20.11	0.02
	2.93	19.63	18.60	5.23	18.70	4.75	18.95	3.48	18.74	4.54	18.57	0.05
	3.39	19.50	18.82	3.47	19.01	2.50	19.10	2.04	18.93	2.92	19.05	0.02
	4.91	19.59	19.35	1.25	19.79	1.03	18.98	3.14	19.02	2.91	19.60	0.00
Line 9	1.13	20.73	21.42	3.34	21.06	1.59	21.36	3.08	21.18	2.17	21.02	0.01
	1.80	21.50	21.53	0.18	21.86	1.70	21.34	0.74	21.70	0.97	21.33	0.01
	2.26	21.66	20.25	6.48	20.30	6.25	20.78	4.06	22.16	2.34	21.80	0.01
	3.78	19.35	19.13	1.13	19.29	0.30	18.91	2.25	19.29	0.30	19.29	0.00
	4.45	19.42	19.11	1.57	19.31	0.57	18.99	2.18	19.26	0.79	19.40	0.00
	4.91	19.45	19.20	1.30	19.50	0.24	18.97	2.47	19.26	0.97	19.42	0.00
Average				2.80		3.40		3.24		3.18		0.08

Table 10: Percentage error of measured and simulated indoor data for air speed in case 2-3.

	Velocity											
	Location z (m)	Measured	k- ε Standard	% error	k- ε RNG	% error	k- ε Realizable	% error	k- ω Standard	% error	k- ω SST	% error
Line 8	1.8	0.06	0.05	21.95	0.05	24.73	0.02	67.99	0.06	5.16	0.03	55.65
	2.26	0.14	0.09	36.21	0.07	52.73	0.11	21.49	0.10	29.40	0.06	54.07
	2.54	0.11	0.05	51.58	0.11	3.89	0.06	47.27	0.12	8.50	0.06	48.88
	2.929	0.11	0.04	61.07	0.03	69.95	0.18	60.52	0.05	58.78	0.03	74.11
	3.387	0.13	0.02	83.91	0.07	45.05	0.15	15.39	0.01	95.60	0.11	17.03
	4.91	0.14	0.20	39.27	0.22	57.38	0.39	175.23	0.50	250.69	0.51	258.52
Line 9	1.13	0.05	0.01	81.13	0.05	4.22	0.09	101.78	0.05	9.58	0.05	3.78
	1.8	0.04	0.14	227.27	0.18	300.91	0.12	177.05	0.04	13.16	0.06	33.18
	2.26	0.09	0.14	64.14	0.12	40.46	0.12	36.09	0.16	88.26	0.06	34.25
	3.78	0.06	0.07	28.75	0.11	90.00	0.08	49.27	0.03	42.35	0.10	76.61
	4.45	0.07	0.04	45.29	0.05	22.71	0.04	41.86	0.25	258.19	0.07	2.14
	4.91	0.33	0.17	50.57	0.15	55.51	0.31	8.38	0.12	64.08	0.17	50.60
Average				65.93		63.96		66.86		76.98		59.07

Table 11: RMSE index for natural convection cases.

Case	Temperature RMSE					Case	Velocity RMSE				
	k-ε standard	k- ε RNG	k- ε realizable	k-ω standard	k- ω SST		k- ε standard	k- ε RNG	k- ε realizable	k- ω standard	k- ω SST
1-2	0.031	0.034	0.035	0.032	0.033	1-2	0.221	0.319	0.407	0.292	0.234
1-3	0.006	0.005	0.008	0.010	0.006	1-3	0.047	0.320	0.193	0.241	0.277
Average	**0.019**	0.0200	0.022	0.021	0.020	Average	**0.134**	0.319	0.30	0.267	0.256

Table 12: RMSE index for mixed convection cases

Case	Temperature RMSE					Case	Velocity RMSE				
	k-ε standard	k- ε RNG	k- ε realizable	k-ω standard	k- ω SST		k- ε standard	k- ε RNG	k- ε realizable	k- ω standard	k- ω SST
2-2	0.021	0.018	0.010	0.019	0.020	2-2	0.514	0.282	0.501	0.423	0.631
2-3	0.016	0.021	0.018	0.024	0.015	2-3	0.520	0.525	0.383	0.676	0.651
4-1	0.008	0.016	0.011	0.015	0.009	4-1	0.520	0.525	0.383	0.676	0.651
4-2	0.022	0.024	0.018	0.017	0.018	4-2	0.432	0.388	0.448	0.337	0.251
Average	0.017	0.020	**0.014**	0.019	0.016	Average	0.497	0.430	**0.429**	0.528	0.540

4.5.2. Evaluation of turbulence models to predict the mass airflow through the horizontal opening.

This study is not only focused on evaluate the performance of turbulence models to predict indoor conditions in a scenario with interzonal heat and mass exchange across an horizontal opening connecting two floors, but it also aims to evaluate the capability of the turbulence models to predict the mass exchange across the horizontal opening. Therefore, this section evaluates the ability of the *k-ε* standard model for cases 1-2 and 1-3 and the *k-ε* realizable for cases 2-2 to 4-2 to predict the upward mass airflows through the horizontal opening. The experimental data of Vera, 2009 are used to perform this evaluation.

The total upward mass airflow, ma_{up}, through the opening can be calculated from simulated results as the sum of the mass airflow in each cell, ma_i, in the middle plane of the opening (z = 2.54m) as follows:

$$ma_i(kg/s) = A_i * \rho_i * V_{z_i} \quad (29)$$

$$ma_{up}(kg/s) = \sum_1^N ma_i \text{ ; If } ma_i > 0 \quad (30)$$

$$ma_{down}(kg/s) = \sum_1^N ma_i \text{ ; If } ma_i < 0 \quad (31)$$

where $A_i = A/N$. A is the horizontal opening area (m^2) and N is the number of cells in the middle plane. Since the mesh grid into the opening (plane XY) is uniform, the area of cells is equal to Ai. V_{z_i} is the vertical component of the air velocity in each cell and ρ is the air density defined as Eq. 32. Ti is the temperature in each cell of the opening in Kelvin.

$$\rho_i(kg/m^3) = \frac{101.325}{287.055 * T_i} \quad (32)$$

Table 13 and Figure 38 show the measured and simulated upward mass airflow rates for all the cases studied. It is observed that the *k-ε* realizable model predicts the mass airflow through the opening in a good agreement with measured data for all mixed convection cases. The predicted upward mass airflows are very close to the measurements. The highest difference is found in case 4-2 where the percentage error is 8.5%, while the lowest difference is for case 2-2 with an error of 1.31%.

Results of *k-ε* standard model for natural convection cases are not as good as the results found for mixed convection cases. In particular, the predicted mass airflow rate for case 1-2 (37.08 x 10-3 kg/s) is much lower than the measured value (61.00 x 10^{-3} ± 16.5 x 10^{-3} kg/s). This result might evidences the difficulty to predict mass airflow through horizontal openings when buoyancy forces dominates the mass exchange. Although the airflow through a horizontal opening has not been extensively studied, the available literature shows that the airflow pattern is highly unstable for natural convection. Therefore, it is expected this phenomenon would be difficult to be predicted.

Table 13: Comparison of measured and simulated upward mass airflow through the opening.

Cases	Measured upward mass airflows (kg/s) (x 10^{-3})	Uncertainty (relative) in upward airflow (%)	Predicted upward mass airflows (kg/s) (x 10^{-3})	Upward mass airflow difference (kg/s) (x 10^{-3})	% error between predicted and measured values (%)
NC					
Case 1-2	61	16.5	37.08	23.9	39.21
Case 1-3	24.1	5.1	29.40	5.3	21.99
MC					
Case 2-2	53.5	3.6	54.20	0.7	1.31
Case 2-3	48.2	3.3	44.70	3.5	7.26
Case 4-1	41.7	5.2	38.24	3.4	8.3
Case 4-2	20.5	3.1	18.76	1.7	8.49

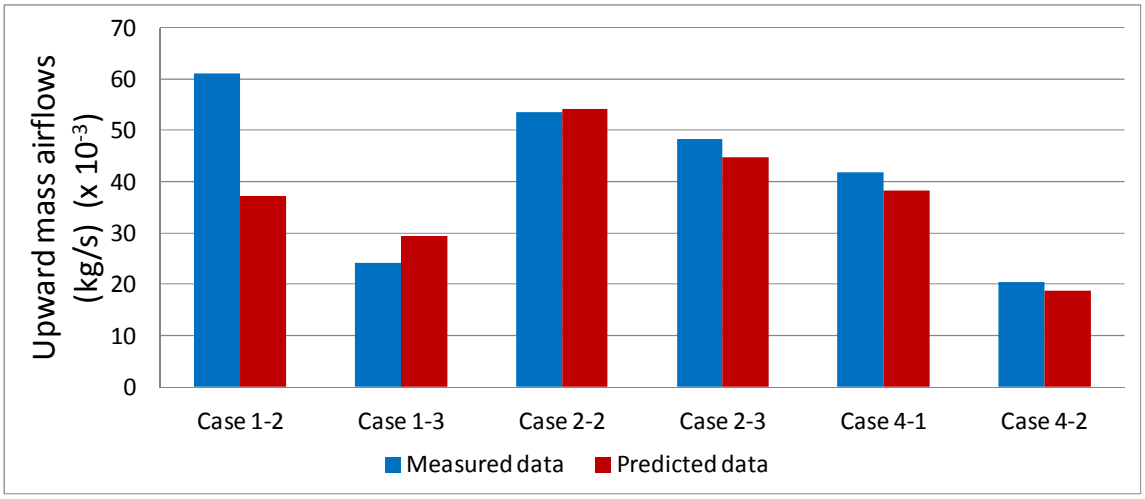

Figure 38: Measured and simulated upward mass airflow rates for all the cases studied

4.6. Conclusions

Interior building openings such as stairwells are important paths for exchange of heat, air, moisture, and pollutants. Interzonal airflow through horizontal openings has not been profoundly studied due its highly transient and unstable nature.

Few authors have used CFD technique to study the airflow exchange through horizontal opening. However, there is a scarcity of studies on evaluating turbulence models to predict, first, indoor air conditions in rooms connected by an horizontal opening, and secondly, the heat and mass exchange through these openings.

This paper focused on the evaluation of five two-eddy viscosity turbulence models, *k*-ε standard, *k*-ε RNG, *k*-ε realizable, *k*-ω standard and *k*-ω SST, in terms of predicting: i) the indoor air conditions in a full-scale two-story test-hut with heat and mass exchange through an horizontal opening connecting two floors, and ii) the mass exchange rate across the horizontal opening for cases of natural and mixed convection. Simulated CFD results for each turbulence model were compared with experimental results (Vera et al., 2010a) at different locations. From the study it can be concluded:

- Visualization of warm convective currents into the two-story test-hut for temperature and velocity distributions indicate that the flow pattern is dominated by vortices and a complex two way airflows exist through the horizontal opening for all cases with a warmer lower room.
- The low value of RMSE index indicates that all the turbulence models predicted temperature distribution in a good agreement with experimental data. Considering all turbulence models, the RMSE index lies between 0.019 and 0.022 for natural convection while for mixed convection cases the RMSE lies between 0.014 and 0.02.
- For air velocity, all turbulence models can predict a similar profile of air speed distribution; however the models present deviations with experimental data at the horizontal opening. For natural convection RMSE index for air speed considering predictions from all turbulence models lies between 0.13 and 0.3 while for mixed convection it lies between 0.42 and 0.54.
- Based on RMSE index, the k-ε standard model is the most accurate model in predict temperature and air speed distribution in a full-scale two-story test-hut and the interzonal mass airflows through horizontal opening for natural convection
- Based on RMSE index, k-ε realizable model is the most accurate model in predict temperature and air speed distribution in a full-scale two-story test-hut and the interzonal mass airflows through horizontal opening for mixed convection cases

CFD technique is able to predict the indoor environment and mass airflows through a horizontal opening for a full-scale two-story test-hut. The turbulences models found contribute to the knowledge about interzonal mass and heat airflow through horizontal openings and improves the building design focused in achieve a comfortable and healthy indoor environment for occupants and energy efficiency.

5. Heat transfer correlations to predict upward heat flux through a horizontal opening for natural and mixed convection.

5.1. Abstract

Interior building horizontal opening such as stairwells are important paths for exchange of heat, air, moisture and pollutants through different zone of a building. This exchange will affect the healthy and comfortable indoor environment for the occupants and the energy efficiency of buildings. Unlike vertical openings, only few authors have found empirical correlations to describe the heat transfer through horizontal opening in natural convection regime and mixed convection regime. This lack of studies is mainly caused by the highly transient and unstable nature of the airflow at horizontal openings, therefore there are limited available information about the interzonal heat exchange through horizontal opening in buildings. This paper studies the upward heat transfer through a horizontal opening in a full-scale two-story test-hut using CFD technique. The main results are two empirical correlation to describe the heat exchange through a horizontal opening for natural and mixed convection regimes. Theses correlations are based on dimensionless fluid numbers (Nu, Gr, Re, Pr) and are applicable for different air conditions such as; temperature difference between the lower and upper room, ventilation strategies (natural and mixed convection) and opening aspect ratios.

5.2. Introduction

Consideration of interzonal airflow is an important aspect in building design because it allows the mass and energy transport inside building. Interzonal airflow exchange could have important effect on building energy consumption, indoor air quality, comfort of occupants, and ventilations effectiveness among other.

An important way in which airflow transport can take place in a multizone building is through large vertical and horizontal openings. There are different investigations

describing the airflow exchange through vertical opening for natural and mixed convection flows, however airflow through horizontal opening have not been profoundly studied and the lack of experimental data and the transient and unstable flow pattern found at the opening for natural convection cases are the main reasons.

Only few authors have found empirical correlations for the heat transfer in natural convection regime and mixed convection regime. These correlations are based on dimensionless numbers as Grashof and Nusselt for natural convection, and Nusselt and Reynolds for mixed convection.

The first study in considered airflow transport through horizontal opening was introduced by Brown (1962). He presented an experimental investigation about natural convection flow across square horizontal partitions for heavier fluid above the partition using air as the fluid medium. In this situation an unstable condition in the opening and an exchange of lighter and heavier fluid is observed. Also, Brown determined that the heat and mass transfer rate increased with increasing partition thickness and defined a mean curve from the experimental data as follow

$$Nu_H = 0.0546 Gr_H^{0.55} Pr(L/H)^{1/3} \quad (33)$$

Where L is the length of the square partition, Nu_H is the Nusselt number based on partition thickness, Gr_H is Grashof number based on partition thickness and Pr is Prandtl number.

In an extended study, Vera et al., (2010) carried out an experimental study about interzonal air and moisture transport through horizontal opening in a full scale two-story test-hut. The study extended the cases with buoyancy driven flows to cases with combined buoyancy airflows and mechanical ventilation and cases with warmer upper room than the lower room. The results show that interzonal air and moisture exchange through the horizontal opening are strongly linked to the temperature difference between the two rooms. In a subsequent study, Vera et al. (2012) investigated the heat transfer

through a horizontal opening connecting two rooms based on simulated cases using CFD. Results demonstrated that upward heat fluxes through the opening are proportional to the temperature difference between the lower and the upper room. Heat transfer through the opening is mainly caused by buoyancy driven flows with significant contribution from forced flows. Thus, mixed convective heat transfer occurs through the opening and the combined effect can be predicted by the following correlation

$$\mathrm{Nu}/\mathrm{Re}^{1/2} = 36.86\left(\mathrm{Gr}/\mathrm{Re}^{2}\right)^{0.08} \quad (34)$$

There is a lack of studies and validated empirical correlations of mixed convective and natural convective heat transfer through horizontal opening. Only one study has been carried out for natural convection and mixed convection and they only studied fixed opening surfaces. It is necessary to study airflow through horizontal opening for variable opening sizes. In addition, there are not evaluations of the capabilities of different turbulence models to predict; i) indoor conditions in zones connected by horizontal opening, ii) mass airflow through the horizontal opening.

Thus, in this chapter the CFD technique will be used to extend the available experimental data (Vera et al., 2010) of air distribution in a full- scale two-story test-hut with a horizontal opening connecting two rooms. The two-story test-hut will be simulated with the same dimensions of the original configuration but with new sizes of the opening. A range of temperature differences between the upper and lower room will be considered and two ventilation strategies will be tested to study air distribution for natural convection and mixed convection regimes.

The objective is to obtain enough simulated data to develop an empirical correlation for the heat flux through a horizontal opening applicable for different opening dimensions and convective regimes.

5.3. Methodology

5.3.1. CFD simulations

In the previous chapter 4 it was concluded that CFD technique is able to predict the indoor environment for a two-story test-hut and the air and heat exchange through the horizontal opening. The indoor air in the studied cases was under natural convection or mixed convection regimes depending on the ventilation strategy used.

The study determined that the most accurate turbulence model to predict both indoor air distribution and mass airflow exchange through the opening was the *k-ε* standard for a natural convection state and *k-ε* realizable for a mixed convection state. In this study, the turbulence models found will be used to extend the available experimental data (Vera et al., 2010) of the indoor air distribution in a two- story test-hut and the airflow exchange through the horizontal opening.

Thirty two cases will be modeled with combinations of four opening aspect ratios “AR". The opening aspect ratio is $\mathrm{AR} = \mathrm{side\ (S)/length\ (L)}$, with S=1m for all cases and L is 0.8 m, 1 m, 1.35 m and 2 m depending on the case.

Figure 39 shows the opening geometry variation of the cases tested and a plan view of the opening aspect ratios "AR" used. A smaller opening AR means a larger superficies area of the opening. The rooms temperature difference ranged between 1°C and 4.8°. This is considered as the difference of average temperature in the lower room less the average temperature in the upper room.

Two ventilation strategies were analyzed: Ventilation I ("no ventilation") that respect a case with pure natural convection; and ventilation II ("single ventilation with downward net flow through the opening ") where mixed convection dominates de airflow. Table 14 summarizes the main conditions of the cases tested.

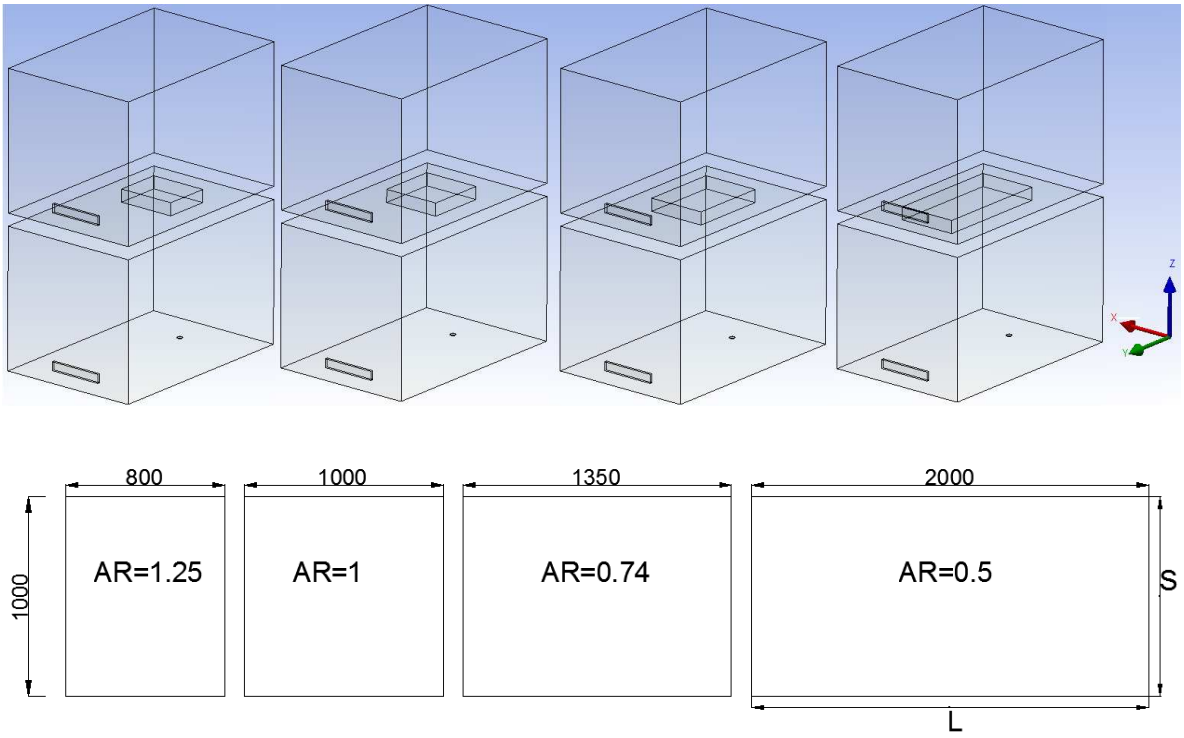

Figure 39: Full-scale two-story test-hut with different opening ratios (dimensions are in mm).

Table 14: Description of cases tested.

Case	Ventilation	Area (m^2)	AR	ΔT	Case	Ventilation	Area (m^2)	AR	ΔT
1	I	0.80	1.25	4.8	17	II	0.80	1.25	4.6
2	I	1.00	1	4.3	18	II	1.00	1	3.7
3	I	1.35	0.74	4.1	19	II	1.35	0.74	4.0
4	I	2.00	0.5	3.6	20	II	2.00	0.5	2.7
5	I	0.80	1.25	3.6	21	II	0.80	1.25	3.8
6	I	1.00	1	3.2	22	II	1.00	1	3.6
7	I	1.35	0.74	3.3	23	II	1.35	0.74	3.2
8	I	2.00	0.5	2.9	24	II	2.00	0.5	2.5
9	I	0.80	1.25	2.8	25	II	0.80	1.25	3.6
10	I	1.00	1	2.4	26	II	1.00	1	3.0
11	I	1.35	0.74	2.5	27	II	1.35	0.74	2.8
12	I	2.00	0.5	2.4	28	II	2.00	0.5	2.3
13	I	0.80	1.25	1.3	29	II	0.80	1.25	2.1
14	I	1.00	1	1.4	30	II	1.00	1	2.0
15	I	1.35	0.74	1.0	31	II	1.35	0.74	1.6
16	I	2.00	0.5	1.5	32	II	2.00	0.5	1.5

5.3.2. Derivation of heat flux exchange through the opening.

The upward heat flow through the opening q_{up} is a useful quantity to be analyses and represent the heat exchange between the lower and upper room. The upward heat flux is calculated based on mean temperatures of the two rooms. In this way, q_{up} is obtained from upward mass airflows through the opening (F_{12}) calculated from CFD simulations for each case.

$$F_{12\_i}(kg/s) = A_i * \rho_i * V_{z_i} \quad (35)$$

$$F_{12}(kg/s) = \sum_1^N F_{12\_i} \text{ ; If } F_{12\_i} > 0 \quad (36)$$

Where $A_i = A/N$. A is the horizontal opening area (m^2) and N is the number of cells in the middle plane. Since the mesh grid into the opening (plane XY) is uniform, the area of the cells are equal to Ai. V_{z_i} is the vertical component of the air velocity in each cell and ρ is the density of the air defined as $\rho_i(kg/m^3) = \frac{101.325}{287.055 * T_i}$ with T_i the temperature of each cell.

Then, the upward heat flux q_{up} is obtained as follow

$$q_{up} = c_p * F_{12} * \Delta T \quad (37)$$

Where c_p is the air specific heat (J/kg·K) and ΔT is the temperature difference between lower and upper room considering the mean temperature.

Depending on the phenomenon studied, there are different dimensionless numbers which describe a fluid. If the flow is driven by buoyancy forces the fluid is under a natural convection regime and the heat transfer can be represented by

$$Nu = c_1 Gr^l \quad (38)$$

where Nu is Nusselt number and Gr is Grashof number.

$$Nu = \frac{q_{up} L_c}{A \Delta T k} \tag{39}$$

$$Gr = \frac{g \beta \Delta T {L_c}^3}{\nu^2} \tag{40}$$

where q is the heat flux (J/s), g is the acceleration due to gravity (m/s^2), k is the air thermal conductivity (W/m·K) ,ν is the kinematic viscosity (m^2/s), A is the opening area where heat flux occurs (m^2), ΔT is the temperature difference between the lower and upper room (K) and L_c is the characteristic length which depends on the geometry by which fluid is transported. Since the convective heat flux of interest corresponds to the vertical flow through the opening, the characteristic length is the thickness (H) of the opening (Brown, 1962 and Vera et al., 2012).

Brown (1962) found that the exponent l in eq. 38 was equal to 0.55 for a square opening with different thickness.

If the flow is driven by pressure differences the fluid is under forced convection regime. If natural and forced convection are comparable in magnitude the flow is under mixed convection regime. The parameter that typically has been used to characterize mixed convection is Gr/Re^2 and the heat transfer can be represented by

$$\frac{Nu}{Re^{1/2}} = c_2 \left(\frac{Gr}{Re^2}\right)^{C_3} \tag{41}$$

where *Re* is the Reynolds number.

$$Re = \frac{U L_c}{\nu} \tag{42}$$

U is the characteristic velocity of the fluid (m/s). In this case, the characteristic length *Lc* used for Reynolds number is the hydraulic diameter (D_h) of the horizontal opening which for a closed channel correspond to $Dh = 2LS/(L+S)$ where L and S are the length dimensions of each side of the opening. The same characteristic length was used

for Zohrabian et al. (1989) who studied a similar configuration in a study of buoyancy driven flow in a half-scale stairwell model.

Vera et. al (2012) found that the constant C_3 in eq. 41 was equal to 0.083 for a specific opening.

5.4. Results

5.4.1. Heat flux through the opening

Figure 40 shows the linear correlation between the upward heat transfer, q_{up}, and the temperature difference ΔT for ventilation I and ventilation II. A greater upward flow is produced when the temperature difference between the lower and upper room is increased. In addition, it is observable that q_{up} is significantly influenced by the aspect ratio of the opening and at the same ΔT the upward heat flux is greater if opening area increased. This is expected since there is a larger path for heat flow exchange if the opening has more surface area.

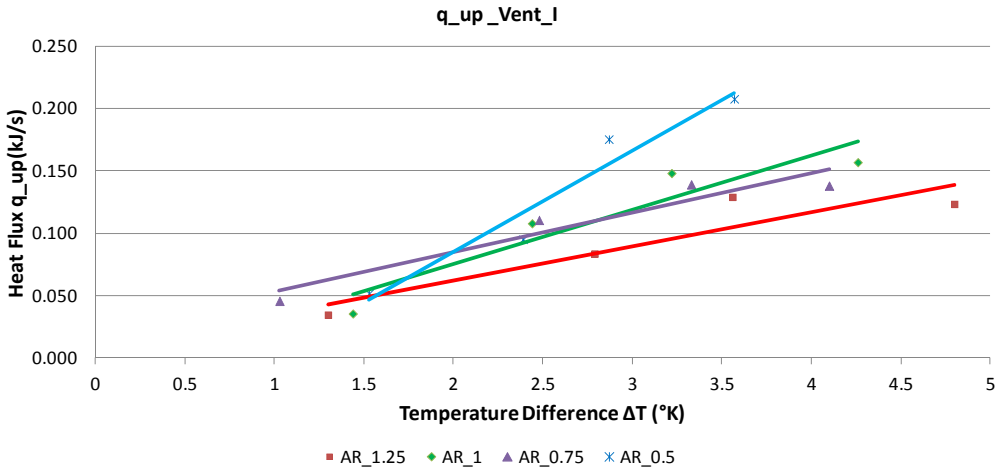

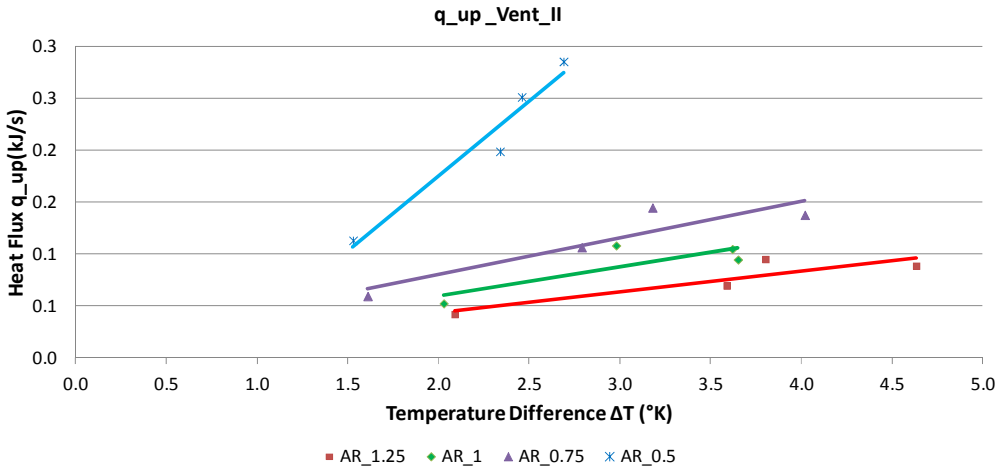

Figure 40: Variation of the upward heat transfer (q_{up}) through the opening versus ΔT

Figure 41 compares the upward heat flux through the opening for ventilation I and II at different opening AR. A greater opening AR means a smaller opening superficies area (Table 14). It is observable that for greater AR the upward heat transfer through the opening is greater for "no ventilation" strategy (Vent_I) than for "single ventilation with downward net flow through the opening" strategy (Vent_II). In contrast, for smaller opening AR the upward heat transfer through the opening for Vent_II is larger than for Vent_I.

This means that the pressure difference forces due to the jet flow introduced into the room may affect the upward airflow in a more significant than the buoyancy forces when a larger opening area is used. While if a smaller opening area is used, the effect of pressure difference forces is not significant enough in the upward air movement in comparison with the buoyant effect.

In addition, a larger upward heat flux is observable when a smaller opening AR is used.

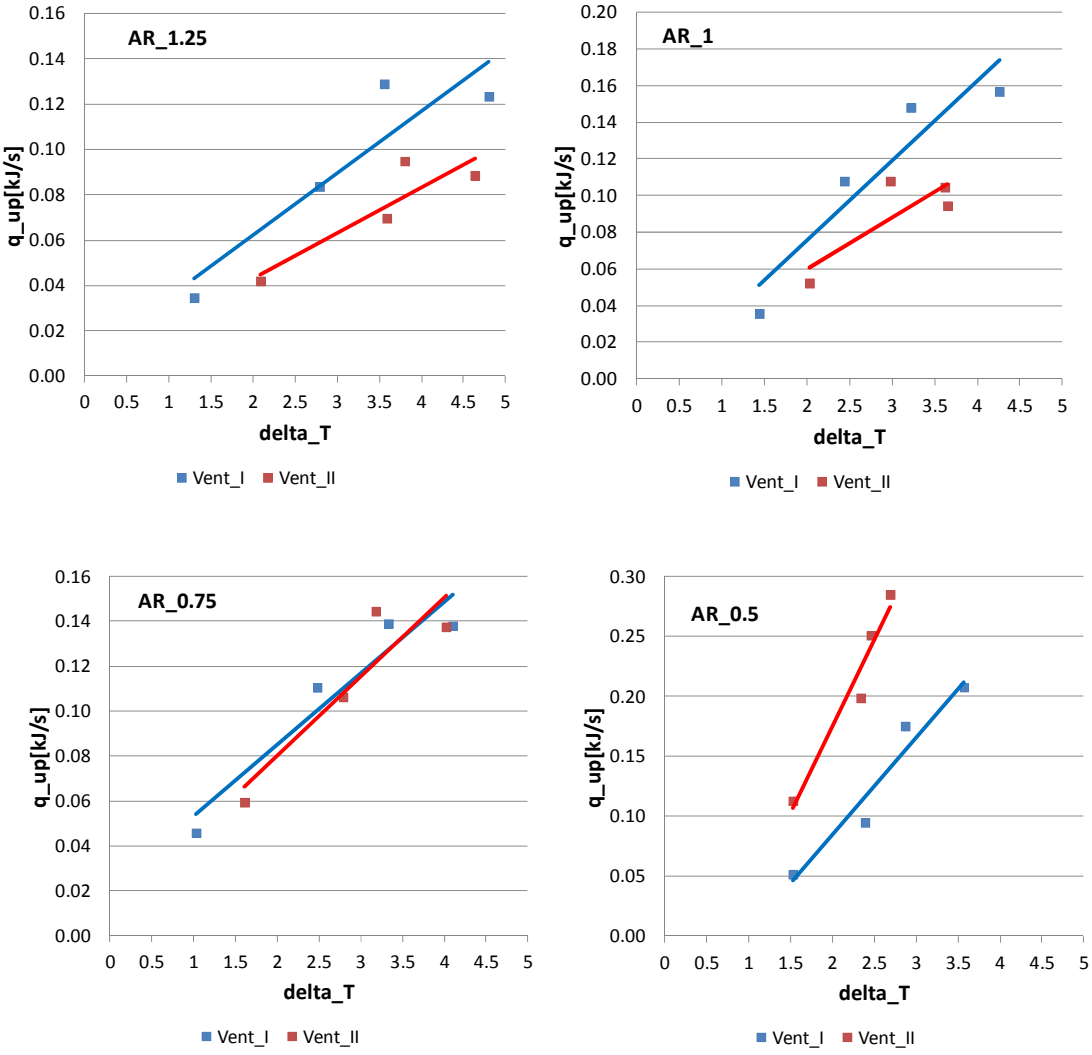

Figure 41: Variation of the upward heat transfer through the opening versus ΔT depending of the opening area.

5.4.2. Analysis for natural convection cases: Ventilation I

In this section the cases 1 to 16 (Table 14) will be studied with the objective to obtain correlation between dimensionless numbers of the fluid and the dimensions of the opening. These cases correspond to “no ventilation” strategy, therefore a natural convection regime is present into the test-hut and the analysis is based on the Nusselt and Grashof number. For these cases, the Nu number ranged from 379 to 1010 while Gr

number ranged from $2.81x10^6$ to $6.93x10^6$, both numbers based on the opening thickness.

Figure 42 shows the relationship between the Grashof and the Nusselt number. It show that when the Grashof number increases then Nusselt number increases, which means that an increases on temperature difference produce an increase on heat flux, similar to previous studies have noted (Vera et al., 2010, Zohrabian et al., 1989 and Peppes et al.,2001). Moreover, it is observed that the aspect ratio of the opening influences the heat flow. In consequence, it is necessary to formulate a correlation which includes the opening dimensions such as the opening thickness (H) and the hydraulic diameter (D_h). This adaption allows the formulation of a unique relationship applicable to any opening dimensions.

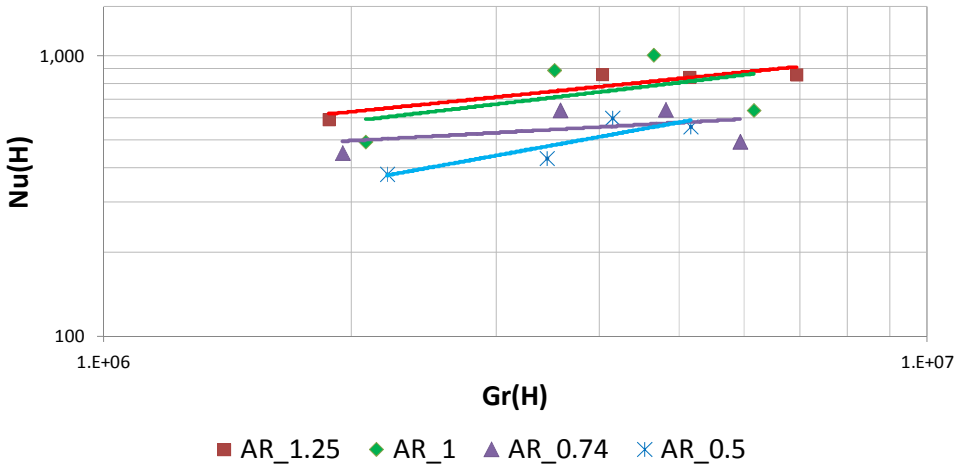

Figure 42: Variation of the Grashof number versus Nusselt number for ventilation I

Figure 43 shows the relationship between Nusselt number and Grashof number when the dimensions of the opening are included by means of the opening thickness (H) and the hydraulic diameter (Dh). From this relationship is possible to define a correlation to predict heat transfer through the horizontal openings with a $R^2 = 0.4$

$$Nu = 36.9 * Pr * Gr^{0.31} \left(\frac{H}{D_h}\right) \quad (43)$$

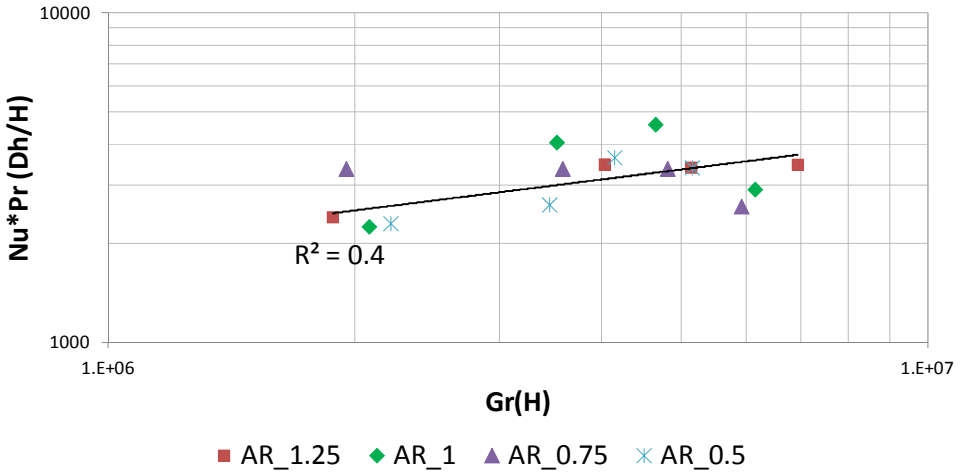

Figure 43: Heat transfer correlation for a horizontal opening under non ventilation strategy.

Figure 44 shows the heat transfer predicted by correlations found by Brown (1962) for natural convection and the correlation developed in this study, using experimental data of (Vera, 2009). The correlation found in this study is close to the experimental data, whereas the correlation found by Brown underpredicts the heat transfer through the horizontal opening.

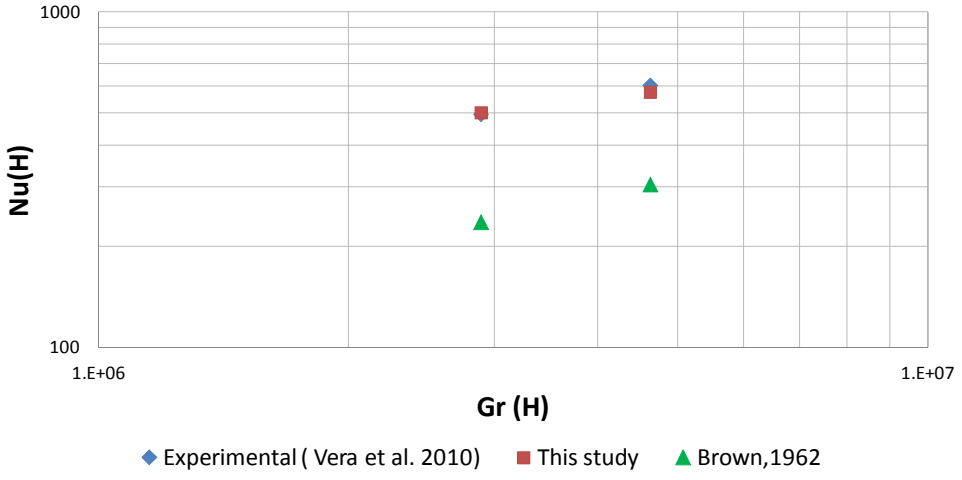

Figure 44: Heat transfer correlations for natural convection for experimental data.

5.4.3. Analysis for mixed convection cases: Ventilation II

In this section the cases 17 to 32 (Table 14) will be studied with the objective to obtain a correlation that represents the heat flow through the opening for mixed convection. These cases correspond to "single ventilation with downward net flow through the opening". This strategy make that airflow exchange through the opening is affected by natural and forced convection at the same time.

If the flow is driven by both pressure difference and buoyancy forces at the same time, the fluid is under a mixed convection regime. The parameter that typical has been used to characterize mixed convection is Gr/Re^2, also called Richardson number. In the two extreme cases heat transfer can occurs driven by pure forced convection and $Ri \to 0$ or driven by pure natural convection and $Ri \to \infty$. The mixed convection is believed to occur between these two limit when $Gr/Re^2 \cong 1$ but is not completely clear. Kitamura and Mitsuishi (2010) reported that the range for mixed convection is between 1.5 and 11. Siebers (1983) reported a Ri between 0.7 and 10 for mixed heat transfer from a vertical plane with horizontal flow. Saha et al. (2006) reported a forced convection for Ri between 0 and 0.1, a mixed convection for Ri near to 1 and natural convection for Ri larger than 10.

To determinate the fluid regime, the Ri number was calculated using Reynolds number based on the hydraulic diameter of the upward fluid section. This is because the area of the upward fluid is less than the opening area. Thus, the Ri number for cases with ventilation II are between 0.1 and 1.72 which can be considering as a mixed regime based on the studies presented above.

To obtain correlations that describe the upward heat flux, the Reynolds number was calculated based on the hydraulic diameter of the opening. This characteristic length is chosen because is a known variable for any studied configuration, unlike the characteristic length of the upward flow area.

The Grashof number based on the opening thickness ranged from $2.21x10^6$ to $6.69x10^6$, while the Reynolds number based on the hydraulic diameter of the opening ranged from 2827 to 8448.

For a mixed regime, the negative slope between Nu and Gr/Re^2 in Figure 45 indicates that the heat transfer decrease when the pressure difference forces decrease. This negative relationship was detected in a previous study of turbulent mixed convection in a horizontal tube (Grassi and Testi, 2006).

At the same time, it is observed that aspect ratio of the opening strongly influences the heat transfer through the opening. When the opening is smaller the heat transfer tends to be less governed by pressure difference effect; while for higher openings, the heat transfer is mainly governed by forced convection. In this way, it is necessary to formulate a correlation which includes the opening dimensions such as the opening thickness (H) and the hydraulic diameter (D_h). This adaption allows the formulation of a unique relationship applicable to any opening aspect ratio.

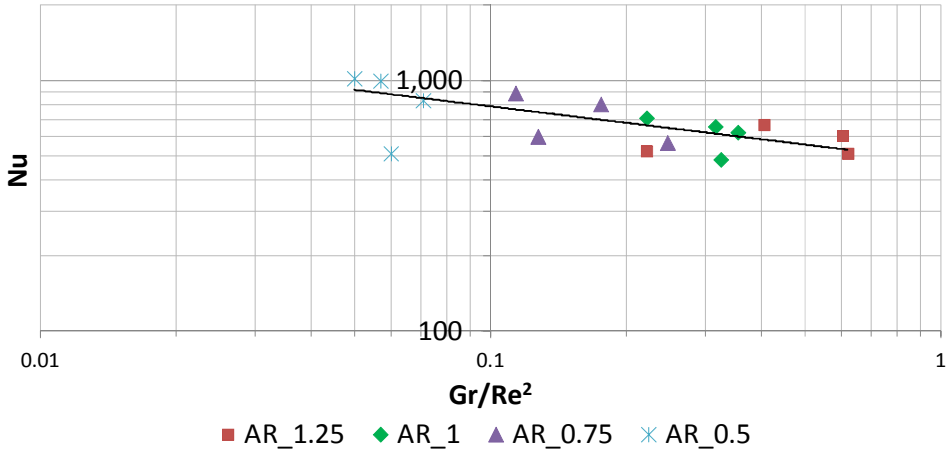

Figure 45: Range of Richardson number for cases with ventilation II and different AR.

Figure 46 shows the upward heat transfer flux through the opening. The opening is represented by the opening thickness (H) and the hydraulic diameter (D_h) thus the

dimensions of the opening can vary. It is possible to define a correlation with a R^2=0.86 as follow

$$\mathrm{Nu} = 35.81 * \mathrm{Re}^{1/2} * \left(\frac{\mathrm{Gr}}{\mathrm{Re}^2}\right)^{-0.2} \left(\frac{\mathrm{H}}{\mathrm{D_h}}\right)^{2} \quad (44)$$

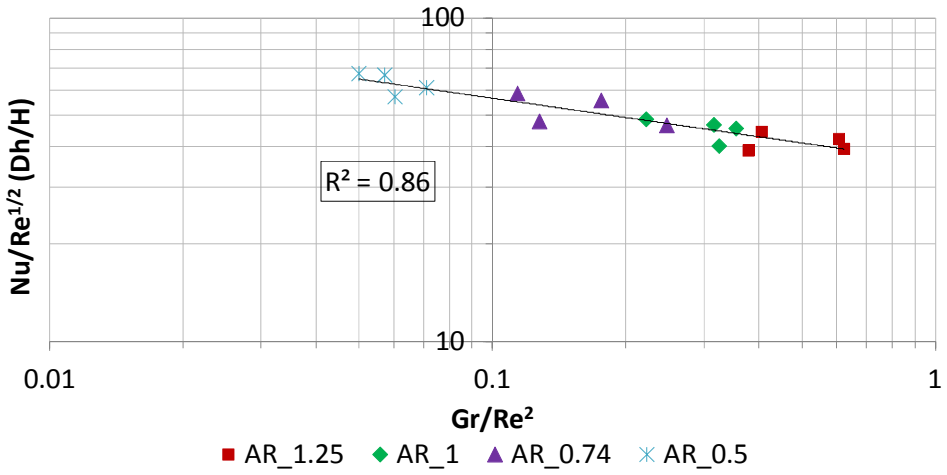

Figure 46: Heat transfer correlation for a horizontal opening under single ventilation with downward net flow through the opening strategy.

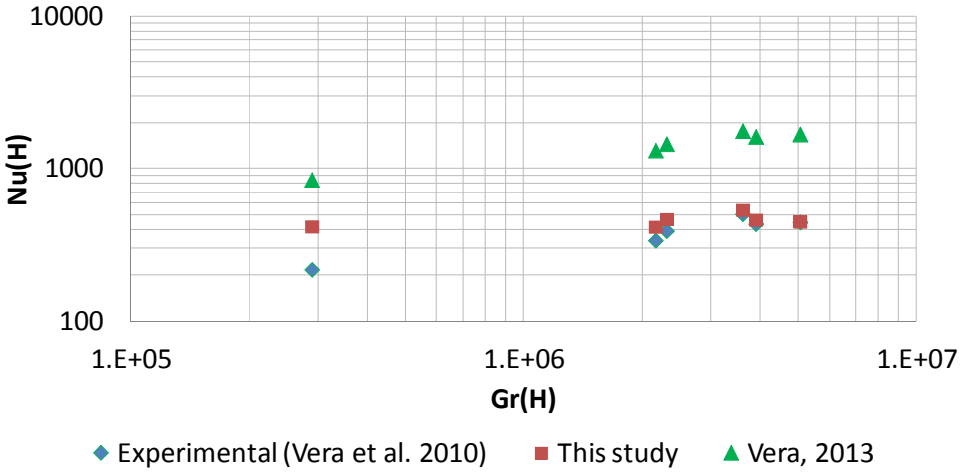

Figure 47: Heat transfer correlations for mixed convection applied to experimental data.

Figure 47 represents the heat transfer predicted by the previously correlation found together with the empirical correlation found by Vera et al., (2013) for mixed convection cases applied to experimental data (Vera, 2009). The correlation found by Vera overpredicts the heat transfer through the horizontal opening while the correlation found in this study is very close to experimental data.

5.5. Conclusions of analysis

In this chapter the CFD technique was used to predict the indoor air conditions of a two-story test-hut with a horizontal opening connecting two rooms. A range of temperature differences between the upper and lower room, different opening aspect ratio (AR) and two ventilation strategies were tested to study the air distribution for natural convection and mixed convection regimes. The objective was to obtain enough simulated data to develop an empirical correlation for the heat flux through a horizontal opening for different opening dimensions and convective regimes.

From the results of this study the following conclusions can be drawn:

- Upward heat transfer through the horizontal opening is strongly linked to the temperature difference between the lower and the upper room. A larger upward heat flux is observed when the upper room was much colder. This agrees with the studied developed by Peppes (2002) and Vera (2010).
- Upward heat transfer through the horizontal opening is significantly influenced by the opening aspect ratio. Larger upward heat flux is observed if a larger opening is used. This shows that the upward heat flow through a horizontal opening is affected by both; the aspect ratio as shown in this study and the opening thickness as was indicated before (Brown, 1962) (Epstein M. , 1998).
- Inertia forces significantly contribute to upward heat transfer through the opening in a mixed convection regime.
- For larger opening sizes (>~1.5m^2) the upward heat flux through the opening is greater for a mixed regime than for natural convection. On the other hand, for

smaller opening sizes (<~1.5m^2) the upward heat flux through the opening generated for natural convection regime is greater than for mixed convection regime.

- A correlation to describe the upward heat flux for natural convective heat transfer was found as follows:

  $$\mathrm{Nu} = 36.9 * Pr * \mathrm{Gr}^{0.31} \left(\frac{\mathrm{H}}{\mathrm{D_h}}\right)$$

- A correlation to describe the upward heat flux for mixed convective heat transfer was found as follows:

  $$\mathrm{Nu} = 35.81 * \mathrm{Re}^{1/2} * \left(\frac{\mathrm{Gr}}{\mathrm{Re}^2}\right)^{-0.2} \left(\frac{\mathrm{H}}{\mathrm{D_h}}\right)^2$$

- Correlations for natural convection and mixed convection predict the indoor air distribution for a two-story hut with a horizontal opening in a good agreement with the experimental data (Vera et al., 2010).

6. Conclusions

Building design has the objective to achieve a comfortable and healthy building environment for the occupants with high energy efficiency. Both, indoor environment conditions and energy consumption could be significantly influenced by heat and mass exchange through building zones.

Multizone heat and mass flows mainly occurs through large vertical and horizontal openings.

For the past 50 years, a wide variety of building energy simulation tools have been developed, which provide users with key building performance indicators such as heating and cooling energy demand, temperature, humidity and costs, with the objective to achieve building's designs more comfortable for occupants considering energy efficiency; the problem is that they consider in a basic manner the airflow exchange through horizontal openings in general. This is consequence of limited studies related with airflow through large horizontal openings and lack of validated correlations to describe heat flow.

One way to enhance the study of airflow through horizontal openings has been the incorporation of CFD technique in building design. CFD can be used to model temperature distribution and air movement within spaces that allows designers to know building performance under different options before they are built and select the most effective solutions.

Consequently, the main objective of this thesis was to develop correlations that represent the heat transfer through a horizontal opening such as staircases opening. This correlation associates fluid dimensionless numbers and the dimensions of a horizontal opening through the use of CFD technique.

The main conclusions that can be obtained from the CFD simulations and numerical analysis developed are presented below according to the topic covered.

6.1. Evaluation of two-eddy viscosity turbulence for basic convective uses as training CFD exercise.

Modeling of three basics natural, forced and mixed convection flows in enclosed environments evidences that CFD modeling is not an intuitive process and requires taking decisions about several parameters such as representative geometry, mesh size and topology, convergence criteria, under-relaxation factors, turbulence model, among others. The main conclusions are:

- Reliable and robust CFD results require users' skills on CFD modeling, even for basics indoor airflows.
- The five evaluated two-eddy viscosity turbulence models (*k*-ε standard, *k*-ε RNG *k*-ε, *k*-ε realizable, *k*-ω standard and *k*-ω SST) perform well predicting air velocity and temperature. However, their accuracy depends on the convection type, quantity predicted and regions of the air domain. Predicted indoor conditions for temperature and air velocity might vary significantly especially in the boundary layer region where the heat and mass transfer between walls and air occurs.
- For natural convection case, the five evaluated turbulence models predict well the temperature and velocity in the core's cavity. While *k*-ω standard predicts better the temperature variation close to the hot wall, the *k*-ε RNG and realizable show excellent performance predicting the air velocity close to the hot and cold walls.
- For mixed convection, the five evaluated *k*-ε and *k*-ω model predict well the clockwise airflow pattern across the cavity. While the *k*-ε realizable shows a better performance predicting the temperature distribution close to the boundary layer and along the core of the cavity, the standard versions of the *k*-ε and *k*-ω models predict better the air velocities in the regions far from the walls.

- Convergence cannot be given for granted, especially for natural convection cases. Several authors agree that convergence is difficult to reach for NC when they are modeled as steady-state, thus it is needed to model them as transient. This means the setting up of time step and under-relaxation factors is needed, which involves advanced knowledge and expertise of the CFD modeler even for basic indoor environmental problems.

6.2. Evaluation of two eddy-viscosity turbulence models to predict indoor air conditions and interzonal air transport through a horizontal opening in a full-scale two-story test-hut under natural and mixed convection using CFD technique.

This section was focused on the evaluation of five two-eddy viscosity turbulence models (*k*-ε standard, *k*-ε RNG *k*-ε, *k*-ε realizable, *k*-ω standard and *k*-ω SST) to predict indoor environment (airflow pattern and temperature distribution) and the mass airflow through the opening for a two-story test-hut with a horizontal opening. The predicted data was validated with extensive experimental data from Vera et al. (2010). The objective was to determinate the most accurate model to predict indoor environment and the airflow through a horizontal opening for natural and mixed convection.

- Visualization of warm convective currents for temperature and velocity distributions indicates that the flow pattern is dominated by vortices. A complex two way airflows exist through the horizontal opening for all cases with a warmer lower room.
- The temperature distribution is well predicted by all turbulence models for all cases so the model used for a further analysis can be selected under the criteria needed for the specific studied case. However is not the same for velocity distribution, where the simulated result presented more discrepancies depending

on the turbulence model used and it is necessary a previous analysis before select one.

- The RMSE index is a good tool to evaluate how far the prediction deviates from the experimental data when a large number of data is used. The low RMSE index value and the low variation between models indicate that all turbulence models can predict indoor conditions in a good agreement with experimental data although some model may be more accurate than other.
- Based on RMSE index, the *k-ε* standard model is the most accurate model in predicting indoor temperature and air speed distribution in cases with natural convection, while *k-ε* realizable model is the most accurate model for cases with mixed convection in a two-story test-hut with a horizontal opening.
- The previously selected turbulence models predict the mass airflow through the horizontal opening presenting a good agreement with experimental data.

6.3. Heat transfer correlations to predict upward heat flux through a horizontal opening for natural and mixed convection.

The *k-ε* standard model and *k-ε* realizable model were used to determinate correlations to describe the airflow and heat flow through horizontal opening. These correlations can be applied for any initial air condition and opening aspect ratio.

Thirty two new cases of a two-story test-hut were modeled with combinations of four opening aspect ratios *"AR"* and temperature difference between the upper and lower room. The main conclusions are:

- Heat transfer through the opening is affected by temperature difference between the lower and the upper room, thus for a larger ΔT a larger upward heat flux is observed.

- Heat transfer through the opening is affected by opening aspect ratio, where if a larger opening is used, a greater upward heat flux is observed.
- Inertia forces significantly contribute to the mixed convective heat transfer through the opening.
- For larger opening sizes (>~1.5m^2) the upward heat flux through the opening is greater for a mixed convection regime, while for smaller opening sizes (<~1.5m^2) the upward heat flux through the opening is greater for a natural convection regime.
- A correlation for natural convective heat transfer was constructed as follow:

  $Nu = 36.9Pr * Gr^{0.31} \left(\frac{H}{Dh}\right)$
- A correlation for mixed convective heat transfer was constructed as follow:

  $Nu = 35.81 * Re^{1/2} * \left(\frac{Gr}{Re^2}\right)^{-0.2} \left(\frac{H}{Dh}\right)^2$

7. Contributions and future work

7.1. Contributions

The work developed in this thesis allows contributing to the understanding of the heat exchange through horizontal opening found in buildings as staircases opening, attic hatch, chimneys and fireplace penetrations among other.

This thesis has developed correlations that describe the heat transfer through a horizontal opening for cases with buoyancy driven flows and cases with combined buoyancy and forced drive flows. These correlations associate the fluid dimensionless numbers and the dimensions of a horizontal opening.

The correlations developed were obtained from CFD simulations of a two-story test-hut which allow studying cases with variations in the opening sizes and ventilation strategies. That allows extends the existing numerical studies of heat flow exchanging

through the horizontal openings developed only for buoyancy driven flows and specifics opening geometries without variations tested.

Moreover the use of CFD technique in this thesis work allows extending the information about the difficulties of using this technique and the required modeler skill to achieve good results. Basic cases found in literature were modeled as a training exercise for new CFD users. Also, the introduction of CFD technique in buildings design contributes to obtain detailed information of the building behavior before it is built.

7.2. Future work

Based on the performed research, new questions are proposed in order to increase knowledge of airflow through horizontal openings.

- The two-story test-hut used for this study has a horizontal opening like a staircase opening. It is proposed to incorporate a stair into the two-story test-hut and evaluate the correlation found for heat transfer through the horizontal opening considering the new geometry.
- Studies of scenarios considering warmer upper room are needed to evaluate the impact of the heat sources and their locations in the vertical heat and mass exchange.
- The mixed convection regime was studied for a specific ventilation rate. It is propose to extend the cases considering variations in the ventilation rates and evaluate its influence in the upward heat transfer through the opening.
- It is recommended to extend the experimental and CFD data to a three –story building model. Thus it is possible to evaluate the correlations found in predicting airflow through different zones for a larger range of cases.
- It is recommended to evaluate the impact of an accurate prediction of the interzonal mass and heat flow on the performance of the building energy simulation tools.

REFERENCES

AIAA. (1998). Guide for the Verification and Validation of Computational Fluid Dynamics Simulations. American Insitute of Aeronautics and Astronautics.

Allard, F., & Utsumi, Y. (1992). Airflow through large openings. *Energy and Buildings, 18*(2), 133-145.

Allocca, C., Chen, Q., & Glicksman, L. R. (2003). Design analysis of single-sided natural ventilation. *Energy and Buildings, 35*(8), 785-795.

Ampofo, F., & Karayiannis, T. (2003). Experimental benchmark data for turbulent natural convection in an air filled square cavity. *International Journal of Heat and Mass Transfer*, 3551-3572.

Anderson, J. D. (1995). Computational Fluid Dynamics. En *The basics with applications.* (págs. 23-31). New York: McGraw-Hill, Inc. .

Angirasa, D. (2000). Mixed convection in a vented enclosure with an isothermal vertical surface. *Fluid Dynamics Research 26*, 219-233.

Ansys 14. (2012). Ansys Inc.

Ansys Inc. (2012). Ansys 14.0 Theory guide.

ASHRAE. (1977). *Standads for natural and mechanical ventilation. ANSI/ASHRAE standard 62-73.* American Society of Heating, Refrigerating, and Air-Conditioning .

ASHRAE. (2004). Thermal Environmental Conditions for Human Occupancy. *ANSI/ ASHRAE standard 55* .

Bangalee, M. Z. (2012). Wind driven natural ventilation through multiple windows of a building: A computational approach. *Energy and Buildings, 45*, 317-325.

Belleghem, M. V., Steeman, M., Willockx, A., Janssens, A., & Paepe, M. D. (2011). Benchmark experiments for moisture transfer modelling in air and porous materials. *Building and Environment*, 884-898.

Blay, D., Mergui, S., & Niculae, C. (1992). Confined turbulent mixed convection in the presence of a horizontal buoyant wall jet. *In Fundamentals of Mixed Convection, ASME HTD 213.*

Blomqvist, C., & Sandberg, M. (2004). Air Movements through Horizontal Openings in Buildings – A Model Study. *The International Journal of Ventilation, 3*(1), 1-10.

Bornoff, R. (31 de Enero de 2011). *Mentor Graphics Blog*. Recuperado el 29 de Abril de 2013, de http://blogs.mentor.com/robinbornoff/blog/2011/01/31/floefd-hvac-module-taking-built-environment-cfd-simulation-to-the-next-level/

Brown, W. (1962). Natural convection through rectangular openings in partitions—2: Horizontal partitions. *International Journal of Heat and Mass Transfer, 5*(9), 869-881.

Brown, W., & Solvason, K. (1962). Natural convection through rectangular openings in partitions—1: Vertical partitions. *International Journal of Heat and Mass Transfer, 5*(9), 859–862.

Cai, N. C. (2012). Air Flow through the Door Opening Induced by a Room Fire under Different Ventilation Factors. *Procedia Engineering, 43*, 125-131.

Cao, G., Ruponen, M., Paavilainen, R., & Kurnitski, J. (2011). Modelling and simulation of the near-wall velocity of a turbulent ceiling attached plane jet after its impingement with the corner. *Building and Environment, 46*(2), 489-500.

Carrilho Da Graça, G. M. (2012). Thermal and airflow simulation of a naturally ventilated shopping mall. *Energy and Buildings, 50*, 177-188.

Casey, M., & Wintergeste, T. (2000). ERCOFTAC Special Interest Group on Quality and Trust in Industrial CFD - Best Practice Guidelines.

Celik IB. (2004). Procedure for estimation and reporting of discretization error in CFD applications. In: Statement on the control of numerical accuracy of the journal of luids engineering (editorial policy): ASME Fluids Engineering Division.

Chen, J. C. (2005). Numerical Investigation of Fire Smoke Transport in the Tsinghua University Sports Center. *Tsinghua Science & Technology, 10*, 618-622.

Chen, Q., & Srebric, J. (2001). *How to Verify, Validate and Report Indoor Environment Modeling CFD Analyses.* Atlanta: ASHRAE.

Chen, Q., & Xu, W. (1998). A zero-equation turbulence model for indoor airflow simulation. *Energy and Buildings, 28*(2), 137-144.

Cheung, J. O., & Liu, C.-H. (2011). CFD simulations of natural ventilation behaviour in high-rise buildings in regular and staggered arrangements at various spacings. *Energy and Buildings, 43*(5), 1149-1158.

Chiang, W.-H., Wang, C.-Y., & Huang, J.-S. (2012). Evaluation of cooling ceiling and mechanical ventilation systems on thermal comfort using CFD study in an office for subtropical region. *Building and Environment, 48*, 113-127.

Choi, S. K., & Kim, S. O. (2012). Turbulence modeling of natural convection in enclosures: A review. *Journal of Mechanical Science and Technology*, 283-297.

Choi, S.-K., Kim, E.-K., Wi, M.-H., & Kim, S.-O. (2004). Computation of a turbulent natural convection in a rectangular cavity with the low-reynolds-number differential stress and flux model. *KSME International Journal, 18*, 1782-1798.

CNE. (2 de Agosto de 2008). *COMISIÓN NACIONAL DE ENERGÍA.* Recuperado el 26 de Abril de 2013, de http://www.cne.cl/: http://www.cne.cl/noticias/otros/238-gobierno-lanza-nueva-campana-de-energia-gracias-por-tu-energia-sigamos-haciendolo-bien

Cooper, L. Y. (1995). Combined buoyancy- and pressure- driven flow through a shallow, horizontal, circular vent. *Journal of Heat Transfer, 117*, 659-667.

Corgnati, S. P. (2013). CFD application to optimise the ventilation strategy of Senate Room at Palazzo Madama in Turin (Italy). *Journal of Cultural Heritage, 14*, 62-69.

Crawley, D., Hand, J., Kummert, M., & Griffith, B. (2005). Contrasting the capabilities of building energy performance simulation programs.

D.Blay, Mergui, S., & Niculae, C. (1992). Confined turbulent mixed convection in the presence of a horizontal buoyant wall jet. *Fundamentals of Mixed Convection, ASME HTD 213*, 65-72.

Deckers, X. H. (2013). Smoke control in case of fire in a large car park: CFD simulations of full-scale configurations. *Fire Safety Journal, 57*, 22-34.

EnergyPlus, E. S. (15 de Abril de 2013). *Energy efficiency and renewable energy (EERE).* Recuperado el 29 de abril de 2013, de http://apps1.eere.energy.gov/buildings/energyplus/energyplus_features.cfm

Epstein, M. (1998). Buoyancy-driven exchange flow through small openings in horizontal partitions. *Journal of Heat Transfer, 110*(4), 885-893.

Favarolo, P., & Manz, H. (2005). Temperature-driven single-sided ventilation through a large rectangular opening. *Building and Environment, 40*(5), 689-699.

Gagliano, A., Patania, F., Nocera, F., Ferlito, A., & Galesi, A. (2012). Thermal performance of ventilated roofs during summer period. *Energy and Buildings, 49*, 611-618.

Giancola, E. S. (2012). Experimental assessment and modelling of the performance of an open joint ventilated façade during actual operating conditions in Mediterranean climate. *Energy and Buildings, 54*, 363-375.

Grassi, W., & Testi, D. (2006). Heat Transfer Correlations for Turbulent Mixed Convection in the Entrance Region of a Uniformly Heated Horizontal Tube. *J. Heat Transfer , 128*(10), 1103-1107.

Hajdukiewicz, M., Geron, M., & Keane, M. M. (2013). Formal calibration methodology for CFD models of naturally ventilated indoor environments. *Building and Environment, 56*, 290-302.

Harriman, L., Brundrett, G., & Kittler, R. (2001). *Humidity control design guide for commercial and institutional buildings.* Artlanta, USA: American Society of Heating, Refrigerating and Air Conditioning Engineers.

Heiselberg, P., & Li, Z. (2007). Experimental study of buoyancy driven natural ventilation through horizontal openings. *The International Conference on Air Distribution in Rooms, Roomvent.* Helsinki: VBN Publication Aalborg University.

Heiselberg, P., & Li, Z. (2009). Buoyancy Driven Natural Ventilation through Horizontal Openings. *International Journal of Ventilation, 8*(3), 219-231.

Hotta, T. K., & Venkateshan, S. P. (2012). Natural and Mixed Convection Heat Transfer Cooling of Discrete Heat Sources Placed Near the Bottom on a PCB. *WORLD ACADEMY OF SCIENCE, ENGINEERING AND TECHNOLOGY*(68), 526-533.

Hussain, S. O. (2012). Numerical investigations of buoyancy-driven natural ventilation in a simple atrium building and its effect on the thermal comfort conditions. *Applied Thermal Engineering, 40*, 358-372.

Incropera, F. P., DeWitt, D. P., Bergman, T. L., & Lavine, A. S. (2006). Fundamentals of Heat and Mass Transfer,6th edition. Hoboken, NJ: John Wiley & Sons.

ISO 7730. (2005). *Ergonomics of the thermal environment - Analytical determination and interpretation of thermal comfort using calculation of the PMV and PPD indices and local thermal comfort criteria.* International Organization for Standardization.

Kitamura, K., & Mitsuishi, A. (2010). Fluid flow and heat transfer of mixed convection over heated horizontal plate placed in vertical downward flow. *International Journal of Heat and Mass Transfer*(53), 2327-2336.

Klobut, K., & Sirén, K. (1994). Air flows measured in large openings in a horizontal partition. *Building and Environment, 29*(3), 325-335.

Launder, B., & Spalding., D. (1974). The numerical computation of turbulent flows. *Computer Methods in Applied Mechanics and Energy, 3*, 269–289.

Li, Z. (2007). *Characteristics of buoyancy driven natural ventilation through horizontal openings.* Aalborg: PhD Thesis definded public at Aalborg University.

Menter, F. (1994). Two-equation eddy-viscosity turbulence models for engineering applications. *AIAA Journal, 32*, 1598–1605.

Metais, B., & Eckert, E. R. (1964). Forced, Mixed, and Free Convection Regimes. *J. Heat Transfer, 86*(2), 295-296.

Moureh, J., & Flick, D. (2003). Wall air–jet characteristics and airflow patterns within a slot ventilated enclosure. *International Journal of Thermal Sciences*, 703–711.

Musser, A., & McGrattan, K. (2002). Evaluation of a Fast Large-Eddy-Simulation Model for Indoor Airflows. *Journal of Architectural Engineering / Volume 8 / Issue 1 / TECHNICAL PAPERS*, 10-18.

Neal, A. (2006). A study in computational fluid dynamics for the determination of convective heat and vapour transfer coefficients. *A thesis in the Department of Building, Civil and Environmental Engineering*. Montreal, Quebec, Canadá: Concordia University.

Nielsen, P. V. (1974). *Flow in air conditioned room.Ph.D.* Technical University of Denmark.

Nielsen, P. V. (1990). Specification of a two-dimensional test-case. *Dept. of Building Technology and Structural Engineering, Aalborg Universitetscenter*. Denmark.

Nitatwichita, C., Khunatornb, Y., & Tippayawongb, N. (2008). Investigation and characterization of cross ventilating flows through openings in a school classroom. *Journal of the Chinese Institute of Engineers, 31*(4), 587-603.

Oberkampf, W. L., & Trucano., T. G. (2002). Verification and validation in computational fluid dynamics. *Progress in Aerospace Sciences, 38*(3), 209-272.

Omri, M., & Galanis, N. (2007). Numerical analysis of turbulent buoyant flows in enclosures: Influence of grid and boundary conditions. *International Journal of Thermal Sciences*, 727–738.

Özcan, S. E., Vranken, E., & Berckmans, D. (2009). Measuring ventilation rate through naturally ventilated air openings by introducing heat flux. *Building and Environment, 44*(1), 27-33.

Pasut, W. D. (2012). Evaluation of various CFD modelling strategies in predicting airflow and temperature in a naturally ventilated double skin façade. *Applied Thermal Engineering, 37*, 267-274.

Peppes, A., Santamouris, M., & Asimakopoulos, D. (2001). Buoyancy-driven flow through a stairwell. *Building and Environment, 36*(2), 167-180.

Peppes, A., Santamouris, M., & Asimakopoulos, D. (2002). Experimental and numerical study of buoyancy-driven stairwell flow in a three storey building. *Building and Environment, 37*(5), 497-506.

Posner, J. D., Buchanan, C. R., & Dunn-Rankin, D. (2003). Measurement and prediction of indoor air flow in a model room. *Energy and Buildings, 35*, 515-526.

Raji, A., Hasnaoui, M., & Bahlaoui, A. (2008). Numerical study of natural convection dominated heat transfer in a ventilated cavity: Case of forced flow playing simultaneous assisting and opposing roles. *International Journal of Heat and Fluid Flow*, 1174-1181.

Ramponi, R. B. (2012). CFD simulation of cross-ventilation flow for different isolated building configurations: Validation with wind tunnel measurements and analysis of physical and numerical diffusion effects. *Journal of Wind Engineering and Industrial Aerodynamics, 4*, 104–106.

Ravikumar, P., & Prakash, D. (2009). Analysis of thermal comfort in an office room by varying the dimensions of the windows on adjacent walls using CFD: A case study based on numerical simulation. *Building Simulation, 2*(3), 187-196.

Restivo, A. (1979). *Turbulent Flow in Ventilated Room.* London: Ph.D. Thesis, University of London.

Riffat, S., & Kohal, J. (1994). Experimental study of interzonal natural convection through an aperture. *Applied Energy, 48*(8), 305-313.

Riffat, S., & Shao, L. (1995). Characteristics of buoyancy-driven interzonal airflow via horizontal openings. *Building Services Engineering Research and Technology, 16*(3), 149-152.

Roache, P. J. (1994). Perspective: A Method for Uniform Reporting of Grid Refinement Studies. *Journal of Fluids Engineering, 116*(3), 405-413.

Rohdin, P., & Moshfegh, B. (2011). Numerical modelling of industrial indoor environments: A comparison between different turbulence models and supply systems supported by field measurements. *Building and Environment, 46*, 2365-2374.

Rundle, C. A., & Lighstone, M. F. (2007). Validation of turbulent natural convection in square cavity for application of CFD modelling to heat transfer and fluid flow in atria geometries. *2nd Canadian Solar Building Conference.* Calgary, Canada.

Rundle, C., Lightstone, M., Oosthuizen, P., Karava, P., & Mouriki, E. (2011). Validation of computational fluid dynamics simulations for atria geometries. *Building and Environment*, 1943-1353.

Saha, S. G. (2012). Experimental and computational investigation of indoor air quality inside several community kitchens in a large campus. *Building and Environment, 52*, 177-190.

Saha, S., Saha, G., Ali, M., & Islam, M. Q. (2006). Combined free and forced convection inside a two-dimensional multiple ventilated rectangular enclosure. *ARPN Journal of Engineering and Applied Sciences, 1*(3), 23-35.

Santamouri, M., Argiriou, A., Asimakopoulos, D., Klitsikas, N., & Dounis, A. (1995). Heat and mass transfer through large openings by natural convection. *Energy and Buildings, 23*(1), 1-8.

Schmeling, D., Westhoff, A., Kühn, M., Bosbach, J., & Wagner, C. (2011). Large-scale flow structures and heat transport of turbulent forced and mixed convection in a closed rectangular cavity. *nternational Journal of Heat and Fluid Flow*(32), 889-900.

Seok-Ki Choi, S.-O. K. (2012). Turbulence modeling of natural convection in enclosures: A review. *Journal of Mechanical Science and Technology, 26*(1), 283-297.

Shih, T., Liou, W., Shabbir, A., Yang, Z., & Zhu, J. (1995). A new k-ε eddy viscosity model for high reynolds number turbulent flows. *Computers & Fluids, 24*, 227–238.

Shur, M., Spalart, P., Strelets, M., & Travin., A. (1999). Detached-eddy simulation of an airfoil at high angle of attack.Engineering turbulence modelling and experiments 4. *Paper read at Proceedings of the 4th International Symposium on Engineering Turbulence Modeling and Experiments*, 669-678.

Siddiqui, M. J. (2012). CFD analysis of dense gas dispersion in indoor environment for risk assessment and risk mitigation. *Journal of Hazardous Materials, 209–210*, 177-185.

Siebers, D. L. (1983). *Experimental mixed convection heat transfer from a large, vertical surface in a horizontal flow.* California : Ph.D., Stanford University.

Sourtiji, E., Hosseinizadeh, S. F., Gorji-Bandpy, M., & M.Khodadadi, J. (2011). Computational Study of Turbulent Forced Convection Flow in a Square Cavity with Ventilation Ports. *Numerical Heat Transfer, Part A: Applications*, 59: 954–969.

Sourtiji, E., Hosseinizadeh, S., Gorji-Bandpy, M., & Ganji, D. (2011). Heat transfer enhancement of mixed convection in a square cavity with inlet and outlet ports due to oscillation of incoming flow. *International Communications in Heat and Mass Transfer*, 806-814.

Srebric, J., & Chen, Q. (2002). An example of verification, validation, and reporting of indoor environment CFD analyses (RP-1133). *ASHRAE Transactions*, 108(2), 185-194.

Stamou, A., & Katsiris, I. (2006). Verification of a CFD model for indoor airflow and heat transfer. *Building and Environment, 41*, 1171-1181.

Steeman, H., A.Janssens, J.Carmeliet, & M.DePaepe. (2009). Modelling indoor air and hygrothermal wall interaction in building simulation: Comparison between CFD and a well-mixed zonal model. *BuildingandEnvironment*, 572-583.

Steeman, M., Paepe, M. D., & Janssens, A. (2010). Impact of whole-building hygrothermal modelling on the assessment of indoor climate in a library building. *Building and Environment*(45), 1641–1652.

Straube, J. (9 de Mayo de 2008). *buildingscience.com.* Recuperado el 26 de Abril de 2013, de http://www.buildingscience.com/documents/digests/bsd-014-air-flow-control-in-buildings

Suárez, M. J., Sanjuan, C., Gutiérrez, A. J., Pistono, J., & Blanco, E. (2012). Energy evaluation of an horizontal open joint ventilated façade. . *Applied Thermal Engineering, 37*, 302-313.

Sumedha M, J. (2008). The sick building syndrome. *Indian J Occup Environ Med, 61*(4).

Sun, Z., & Wang, S. (2010). A CFD-based test method for control of indoor environment and space ventilation. *Building and Environment*, 1441–1447.

Susin, R. M., Lindner, G. A., Mariani, V. C., & Mendonça, K. C. (2009). Evaluating the influence of the width of inlet slot on the prediction of indoor airflow: Comparison with experimental data. *Building and Environment, 44*, 971-986.

Tan, Q., & Jaluria, Y. (2001). Mass flow through a horizontal vent in an enclosure due to pressure and density differences. *International Journal of Heat and Mass Transfer, 44*(8), 1543-1553.

Tanny, J., Haslavsky, V., & Teitel, M. (2008). Airflow and heat flux through the vertical opening of buoyancy-induced naturally ventilated enclosures. *Energy and Buildings, 40*(4), 637-646.

Teodosiu, C., Hohota, R., Rusaouen, G., & Woloszyn, M. (2003). Numerical prediction of indoor air humidity and its effect on indoor environment. *Building and Environmen*(38), 655-664.

Tian, Y., & Karayianni, T. (2000). Low turbulence natural convection in an air filled square: Part I, Part II. *International Journal of Heat and Mass Transfer 43*, 849-866.

Tu, J., Yeoh, G. H., & Liu, C. (2008). Computational fluid dynamics, A practical approach. Oxford: Elsevier Inc.

Tun, J. M., Xamán, J., Álvarez, G., & Noh, F. (2007). Estudio numérico de la transferencia de calor conjugada en cavidades ventiladas con flujo turbulento. *Centro Nacional de Investigación y Desarrollo Tecnológico. CENIDET-DGEST-SEP*, Caos Conciencia 1: 41-54.

Tye-Gingras, M. G. (2012). Comfort and energy consumption of hydronic heating radiant ceilings and walls based on CFD analysis. *Building and Environment, 54*, 1-13.

University of Massachusetts, D. o. (2002). A Comparison of Turbulence Natural Convection Modeling Prediction to Experimental Data for an Air Filled Square Cavity. *Center for Energy Efficiency and Renewable Energy*.

Vera, S. (2009). Interzonal air and moisture transport through large horizontal openings: An integrated experimental and numerical study. *Athesis in the Department of Building, Civil and Environmental Engineering*. Montreal, Canadá: Concordia University.

Vera, S., Fazio, P., & Rao, J. (2010). Interzonal air and moisture transport through large horizontal openings in a full-scale two-story test-hut: Part 1 – Experimental study. *Building and Environment, 45*(5), 1192-1201.

Vera, S., Fazio, P., & Rao, J. (2010). Interzonal air and moisture transport through large horizontal openings in a full-scale two-story test-hut: Part 2 – CFD study. *Building and Environment, 45*(3), 622-631.

Vera, S., Rao, J., Fazio, P., & Campo, A. (2012). Heat transfer induced by mixed convection flows through a horizontal opening in a full-scale two-story test-hut. *5th International Building Physics Conference.* . Kyoto.

Voigt, L. K. (2000). *Comparison of Turbulence Models for Numerical Calculation of Airflow in an annex 20 Room* . International Centre for Indoor Environment and Energy.Department of Energy Engineering.Technical University of Denmark.

Wanga, H., & Zhai, Z. (2012). Application of coarse-grid computational fluid dynamics on indoor environment modeling: Optimizing the trade-off between grid resolution and simulation accuracy. *HVAC&R Research, 18*(5), 915-933.

Wilcox, D. (1988). Reassessment of the scale-determining equation for advanced turbulence models. *AIAA Journal, 26*, 1299–1310.

Woloszyn, M., & Rusaouën, G. (1999). Airflow through large vertical openings in multizone modelling . *Building Simulation, 6*, 465-471.

Wu, W. Z. (2012). Evaluation of methods for determining air exchange rate in a naturally ventilated dairy cattle building with large openings using computational fluid dynamics (CFD) . *Atmospheric Environment, 63*, 179-188.

Yakhot, V., & Orszag, S. (1986). Renormalization group analysis of turbulence. *Journal of Scientific, 1*, 3–51.

Yang Li, P. F. (2012). Numerical investigation of the influence of room factors on HAM transport in a full-scale experimental room. *Building and Environment*, 114-124.

Zhai, Z., Zhang, Z., Zhang, W., & Chen, Q. (2007). Evaluation of Various Turbulence Models in Predicting Airflow and Turbulence in Enclosed Environments by CFD: Part 1— Summary of Prevalent Turbulence Models. *HVAC&R RESEARCH*, 853-870.

Zhang, T., & Chen, Q. (2007). Novel air distribution systems for commercial aircraft cabins. *Building and Environment*, 1675–1684.

Zhang, W., & Chen, Q. (2010). Large Eddy Simulation of Natural and Mixed Convection Airflow Indoors with Two Simple Filtered Dynamic Subgrid Scale Models. *Numerical Heat Transfer, Part A: Applications*, 447-463.

Zhang, Z., Zhang, W., Zhai, Z. J., & Chen, Q. Y. (2007). Evaluation of Various Turbulence Models in Predicting Airflow and Turbulence in Enclosed Environments by CFD: Part 2—Comparison with Experimental Data from Literature. *HVAC&R Research , 13*(6), 871-886.

Zhao, F.-Y., Liu, D., Tang, L., Ding, Y.-L., & Tang, G.-F. (2009). Direct and inverse mixed convections in an enclosure with ventilation ports. *International Journal of Heat and Mass Transfer*, 4400–4412.

Zitzmann, T., & Cook, M. P. (2005). Simulation of steady-state natural convection using CFD. *Building Simulation.* Montréal, Canada.

Zohrabian, A., Mokhtarzadeh-Dehghan, M., Reynolds, A., & Marriott, B. (1989). An experimental study of Buoyancy-driven flow in a half-scale stairwell model. *Building and Environment, 24*(2), 141-148.

Zuo, W., Hu, J., & Chen, Q. (2010). Improvements in FFD Modeling by Using Different Numerical Schemes. *Numerical Heat Transfer, Part B:Fundamentals*, 58:1, 1-16 .